Democratic and Popular republic of Algeria
Ministry of Higher Education
And
Scientific Research
University of Ibn Khaldoun
Department of Electrical Engineering

Master Degree Memory

Field: Science and Technology

Specialty: Automation And Industrial Computing

Submitted By: Dahli Khadidja

Theme

Fault Tolerant Control of Hybrid Wind-Solar Generation System

Supervised by:	*Pr*	*Allaoui Tayeb*	*supervisor*
	Dr	*Selam Karim*	*Co-supervisor*
Members of committee:	*MCA*	*Belkacem. Belabbas*	*President*
	MCB	*Chahrazed Ogab*	*Examiner*
	MCB	*Selmane Kouadria*	*Examiner*

PROMOTION 2019/2020

DEDICATION

I dedicate my thesis and my entire work to my family.

A special feeling of gratitude and appreciation to my loving parents, Dahli Mostefa and Selam Rebiha who have never left my side and never stopped encouraging me and pushing me to be the better version of myself.

I'm also very grateful to my little sister Asoumi and my brothers for their endless love and support; I appreciate and love all of you ,
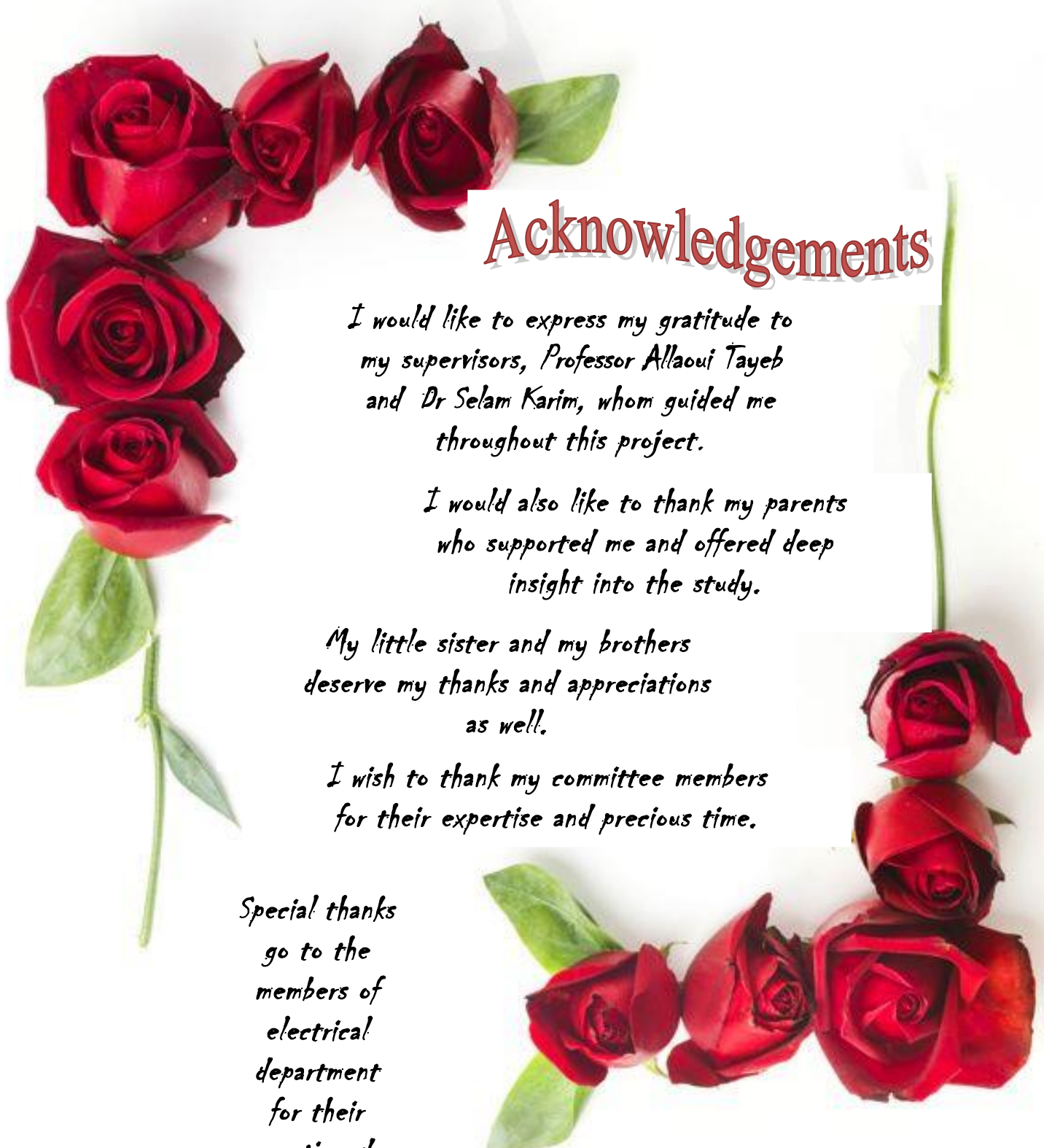
Acknowledgements

I would like to express my gratitude to my supervisors, Professor Allaoui Tayeb and Dr Selam Karim, whom guided me throughout this project.

I would also like to thank my parents who supported me and offered deep insight into the study.

My little sister and my brothers deserve my thanks and appreciations as well.

I wish to thank my committee members for their expertise and precious time.

Special thanks go to the members of electrical department for their continued

TABLE OF CONTENT

Abstract

This work describes a study of the tolerant control of a hybrid wind-solar system. The thesis is divided into three main parts. The first part includes general concepts, definitions and the MPPT control of the solar system, using two types of controllers the perturb and observe (P&O) and the FUZZY logic, where each of these controllers search for the maximum output in the case of the irradiance-changing conditions. The second part includes general concepts, definitions and vector control of the wind power system, using three regulators for the rotor side the proportional-integral (PI), the linear quadratic LQR control based on the LMI approach and the RST regulator, as well as a controller for the grid side and a mechanical torque controller. In the third part, the performance of both models was validated in the event of a failure occurring in the transmission line and the converter. Finally, the results are compared and analyzed using Matlab software. The main objective of this study is to choose the best regulator for optimum performance for both solar and wind systems with or without failure occurring on the system.

Résumé

Ce travail décrit une étude de la commande tolérante aux défauts d'un système hybride éolienne-solaire. La thèse est divisée en trois parties principales. La première partie comprend des concepts généraux, des définitions et la commande MPPT du système solaire, utilisant deux types de contrôleurs le perturbe et observation (P&O) et la logique flue où chacun recherche la sortie maximale dans le cas de changement des conditions de rayonnement. La deuxième partie comprend des concepts généraux, des définitions et la commande vectorielle du système éolienne, utilisant trois régulateurs pour le coté rotor le proportionnel-intégral (PI), la commande linéaire quadratique LQR basé sur l'approche LMI et le régulateur RST, ainsi qu'un contrôleur pour le côté réseaux et un contrôleur du couple mécanique. Dans la troisième partie, les performances des deux modèles ont été validées en cas de panne survenant dans la ligne de transmission et le convertisseur. Enfin, les résultats sont comparés et analysés à l'aide du logiciel Matlab. L'objectif principal de cette étude est de choisir le meilleur régulateur pour des performances optimales pour les systèmes solaires et éoliens avec ou sans panne survenant sur le système.

ملخص

هدا العمل يدرس التحكم في نظام هجين شمسي ورياحي في الحالة العادية و في حالة حدوث عطل أو خلل في النظام. الأطروحة مقسمة إلى ثلاثة أجزاء رئيسية. الجزء الأول يتضمن المفاهيم العامة والتعريفات بالإضافة إلى التحكم في للنظام الشمسي، وذلك باستخدام نوعين من أجهزة التحكم التعطيل والمراقبة, ومنطق التدفق حيث يبحث كل منهما عن الحد الأقصى للأداء في حالة تغير ظروف إشعاع الخلايا الشمسية. الجزء الثاني يتضمن المفاهيم العامة والتعريفات بالإضافة إلى التحكم في نظام طاقة الرياح ، وذلك باستخدام ثلاثة أنواع من أجهزة التحكم للجانب الدوار للمحرك: التكامل النسبي ، والتحكم الخطي التربيعي و المتحكم متعدد الحدود ، وكذلك وحدة تحكم لجانب الشبكات. في الجزء الثالث ، تم التحقق من صحة أداء كلا النموذجين في حالة حدوث عطل في خط النقل والمحول. و في الأخير تمت مقارنة النتائج وتحليلها باستخدام برنامج المحاكاة ماتلاب. الهدف الرئيسي من هذه الدراسة هو اختيار أفضل متحكم للأداء لأنظمة الطاقة الشمسية وطاقة الرياح مع أو بدون حدوث أعطال في النظام.

Table of symbols

Ω	Mechanical speed
Ω_{ref}	Mechanical refrence speed
G	Slip
C_r	Resistant Torque
T_{em}, T_e	Electromagnitical torque
ω_s	Stator Pulsation
ω_r	Rotor Pulsation
θ	Angular phase between stator and rotor
θ_s, θ_r	Stator and rotor angle
v_{sabc}, v_{rabc}	Stator and rotor voltages
i_{sabc}, i_{rabc}	Stator and rotor currents
Φ_{sabc}, Φ_{rabc}	Rotor and stator Fluxes
R_s, R_r	Rotor and stator Resistances
R_f	Fault resistance
T_s, T_r	Rotor and rotor Time gain
l_s, l_r	Propre Inductances of the rotor and stator
m_s, m_r	Inductance mutuelle statorique et rotorique
L_s, L_r	Mutual Inductances of the rotor and stator
M_{sr}	Cyclique Inductance stator and rotor
L_{so}, L_{ro}	Homopolar stator and rotor rotor inductance
M_{sr}	Maximum value of stator rotor mutual inductance coefficients
Cc	short circuit
v_{sd}, v_{sq}	Stator and rotor voltages in the park reference
i_{sd}, i_{rq}	Stator and rotor currents in the park reference
v_{s0}, v_{r0}	Homopolar component of the stator and rotor voltage in the park reference
i_{s0}, i_{r0}	Zero sequence component of the stator and rotor current in the park frame
σ	Coefficient of dispersion
V_p, f_p	frequency Amplitude
$\Phi_{sd\_mes} \ \Phi_{sq\_mes}$	Estimted stator Fluxes
v_{rd}^r, v_{rq}^r	Regulated voltage
K_f	Coefficient of friction
ω_n	Electric pulsation
$K_{pi}, , K_{qi}, , K_{p\Omega}$	Proportional Regulator gains
$K_{ii}, K_{i\Omega}$	Integrator regulator gains radius of the wind turbine rotor (m)
Cp	turbine performance coefficient
V	wind speed.
Λ	the tip speed ratio,
β	the pitch angle of the rotor blades,.

Jr	rotor moment of inertia.
Wt	rotor angular speed.
Br	rotor damping effect.
Ta	applied torque on the rotor.
Tls	low speed shaft torque.
Jls	driver moment of inertia (cancelled).
wls	angular speed of the low speed shaft.
Bls	low speed damping effect.
Kls	stiffness of low speed shaft.
Qt	rotor angular displacement.
Qls	low speed angular displacement
Jls	generator moment of inertia.
wg	angular speed of the high speed shaft.
Bg	high speed damping effect.
Ths	high speed shaft torque.
Tgen	generator electromagnetic torque.
Kgear	gearbox ratio
Vs, Vr	Supplied stator and rotor voltage
Is, Ir	Stator and Rotor current
Es, Er	Induced emf in the stator and rotor
Rs, Rr	Stator and rotor resistance (Ω)
Lm	Mutual inductance (H)
$L\sigma$s	Stator leakage inductance (H)
$L'\sigma$r	Rotor leakage inductance (H)
Ns,Nr	Stator, rotor windings, number of turns per phase
I_{ph}	light generated current
I_S	reverse saturation current
R_S	series resistances of the cell.
R_{sh}	parallel inherent resistances of the cell.
q	the electron charge $1.60217646 \times 10^{-19}$
C	Boltzmann's constant $1.3806503 \times 10^{-23}$ J/K
I_{SC}	Short Circuit current
V_{OC}	Open circuit voltage
Pm	Maximum power point
FF	Fill Factor
η	Efficiency
Eg	Semiconductor band gap energy (Electron Volt)
Eg0	Band gap energy at T = 0 Kelvin (Electron Volt)
I	Cell output current (Ampere)
I0	Dark saturation current (Ampere)
I0,final	Final value of I0 (Ampere)
Id	Diode current (Ampere)
Imp	Current at the maximum-power point (Ampere)
I0,r	Short circuit current
Iph	Photocurrent (Ampere)
Iph,final	Final value of photocurrent (Ampere)

General introduction

our environment is affected by all energy sources .however by most measures, fossil fuels—coal, oil, and natural gas—do markedly more harm than renewable energy sources, including air and water pollution, damage to public health, wildlife and habitat loss, water use, land use, and global warming emissions. Human activity is overloading our atmosphere with carbon dioxide and other global warming emissions. These gases act like a blanket, trapping heat. The result is a web of significant and harmful impacts, from stronger, more frequent storms, to drought, sea level rise, and extinction. In the United States, about 29 percent of global warming emissions come from the electricity sector. Most of those emissions come from fossil fuels like coal and natural gas [73].

In contrast, most renewable energy sources produce little to no global warming emissions.Over the last two decades, the EU's renewable energy share has increased continuously .In China, where air quality remains an important issue, the COVID-19 outbreak has led to lower pollution levels. According to data released by China's Ministry of Ecology and Environment, PM2.5 levels decreased by more than 20 percent during January and April in 337 cities compared to previous months [72]. Experts say decreased industrial activity and reduced vehicular emissions are the major reasons behind the temporarily cleaned air. Hybrid energy systems are the most efficient way for electrical power generation. It solves the issue behind the unpredicted climate and intermittency .By combing two or more power resources each one completes the other's weaknesses. Hybrid wind-solar energy system is the most usable hybrid systems however the performance of the system can be easily interrupted by possible faults and failures .In this context, this work describes a study of a fault tolerant hybrid wind-solar energy control system

The first chapter provides a brief introduction of renewable power systems, wind power system and solar power system and basic definitions and classifications concepts. The second chapter presents a study on the complete model of the hybrid energy system where a basic mathematical model of the Solar Photovoltaic System is developed, that includes modeling the fundamental components such as a solar cell, power inverter and a boost chopper. And a mathematical modeling of a doubly-fed induction generator (DFIG) for a wind turbine is proposed, that includes the aerodynamics, the Electrical system and mechanical system of the wind turbine.

The third chapter presents the synthesis of regulators necessary for the control of the hybrid wind solar system, where the wind turbine system controller is developed, including pitch angle and mechanical torque controller, grid side controller and rotor side controller, three types of regulator are used. The synthesis of a Proportional - Integral regulator is carried out. In order to compare its performance to other regulators, we also synthesize an RST regulator calculated by placing robust poles and an LQR regulator, based on the linear matrix inequality (LMI).Then, the solar turbine system controller is developed, by controlling the boost converter. The synthesis of a MPPT P & O method regulator is carried out. In order to compare its performance to other regulators, we also synthesize an MPPT FUZZY logic controller.

The fourth chapter provides a brief introduction of power system faults, fault tolerant control (FTC) and fault detection and isolation (FDI) and defined basic definitions and classifications concepts. Starting with some definitions and describing different types of faults and failures that can occur in actuators, sensors or transmission line in wind system, and in the boost converter for the solar system.

The fifth chapter consists of simulation results using MATLAB/SIMULINK platform and conclusions,where a comparison of three regulators (PI, RST and LQR) is developed on wind turbine generator. A series of tests are also carried out when the transmission line fault occurs on the wind turbine system. Then the fuzzy logic (FL) based MPPT controller is simulated and compared with the conventional perturbation and observation (P&O) based MPPT controller. A series of tests are also carried out when the open or short circuit fault occurs on the boost converter of the solar system.

Chapter I:

Hybrid wind and solar electric systems

A

I Chapter I: Hybrid wind and solar electric systems

I.1 Introduction

Renewable energy resources are the most efficient, easy, and more importantly constantly replenished method to minimize both global pollution and electricity bills. However, the issue behind its under-use appears in the environment and climate unpredicted and intermittency. Wind power is only generated when it's windy, solar power is only generated when it's sunny To solve this issue there are many options, such as net metering policies to counting on energy storage. One more beneficial new way is through hybrid energy systems: by combing wind and solar systems which we will be deeply getting through out in this chapter.

I.2 Renewable Energy

Renewable energy, often known as clean energy, is a constantly replenished and permanent natural power sources. Although their availability depends on time and weather sunlight keeps shining and wind keeps blowing.

Even thou the uses of renewable energy are boundless such as heating, transportation, lighting, and more, humans constantly turned to coal and gas and many other cheaper, dirtier energy sources over the past 500 years or so. [1]

I.2.1 Types of Renewable Energy Sources

Us we mentioned earlier energy can be extracted from renewable sources such as sun, wind, geothermal, wave—tidal and ocean thermal energy, and water. These power sources are mainly transformed in electricity depending on their geographical location, distance from main networks, and the operating period that usually does not exceed 2,500 h/year. [1]

I.2.1.1 Solar Energy

The solar energy arriving at earth surface can be used for hitting hot water or for producing electricity by using photovoltaic cells. Depending on the latitude, time of day, and atmospheric conditions typical values of the rate of the solar energy are 300–1,000 W/m2. [2]

I.2.1.2 Wind Energy

Wind turbines are blown round by the wind and produce power to generate electricity. Wind energy has been usually used at sites where wind velocities are high and almost steady all the year round. [3]

I.2.1.3   Geothermal Energy

Geothermal energy is the natural heat within the earth's crust. Natural-occurring water from aquifer with a temperature range of 50–150 _C (122–302 _F) can be used for building heating, district heating, agriculture, and spas. [1]

I.2.1.4   Wave, Tidal, and Ocean Thermal Energy

Another way to produce electricity is by using wave motion and tidal power. While wave energy is attached to water height, from hollow to crest, and to the kinetic energy due to the water motion, tidal energy is attached to the exploitation of the oscillatory motion of the water level that occurs periodically and in a predictable way. In order to produce electricity ocean thermal energy conversion uses the heat energy stored in the Earth's ocean. [1]

I.2.1.5   Hydraulic Energy

A hydraulic turbine converts the energy of gravitational energy of water into mechanical energy. A hydroelectric generator converts this mechanical energy into electricity. [4]

I.2.1.6   Energy from Waste

Energy from Waste is generated by converting non-recyclable waste into usable forms of energy such us heat, fuels and electricity. [1]

I.2.2   Energy Storage

Transforming energy from primary into various forms is only possible because of energy storage that comes in different forms [1]

I.2.2.1   Thermal Storage

Thermal energy storage (TES) is generally defined as the temporary storage of energy for heating, cooling applications and power generation. [1]

I.2.2.2   Hydro Storage

The principle of hydro storage is to store energy in the form of water in an upper reservoir, pumped from another reservoir at a lower high. Power is generated by releasing the stored water through turbines in the same manner as a conventional hydropower station. [1]

I.2.2.3   Mechanical Storage

Mechanical energy storage involves a physical connection between a flywheel and the driven wheels. The flywheel is a typical device for the storage of mechanical energy. The

quantity of stored energy depends on the shaft speed, the mass, and the radius of gyration of the flywheel. [1]

I.2.2.4   Electric Storage

Electric energy can be simply stored by using electric batteries, among which the most common type is lead-acid. The use of electric batteries for storage depends on many parameters such as charge and discharge cycle life, energy-mass and power-mass ratios, and of course energy-cost ratio. [1]

I.2.2.5   Fuel Cells

Fuel cells are electrochemical devices in which electric energy is produced by combining hydrogen and oxygen and by releasing water vapor into the atmosphere. Basically, the main components of a fuel cell are the anode, the cathode, and the electrolyte (liquid, solid, membrane) between them. [1]

I.2.3   World Energy Demand

The energy demand is expected to keep extending everywhere the globe because the population is growing as well as its need for goods and luxury.

In its newly released International Energy Outlook 2019 (IEO2019) Reference case, the U.S. Energy Information Administration (EIA) projects that world energy consumption will grow by nearly 50% between 2018 and 2050. Most of this growth comes from countries that are not in the Organization for Economic Cooperation and Development (OECD), and this growth is focused in regions where strong economic growth is driving demand, particularly in Asia. Figure bellow shows Global power consumption by region (2010-2050) [5]
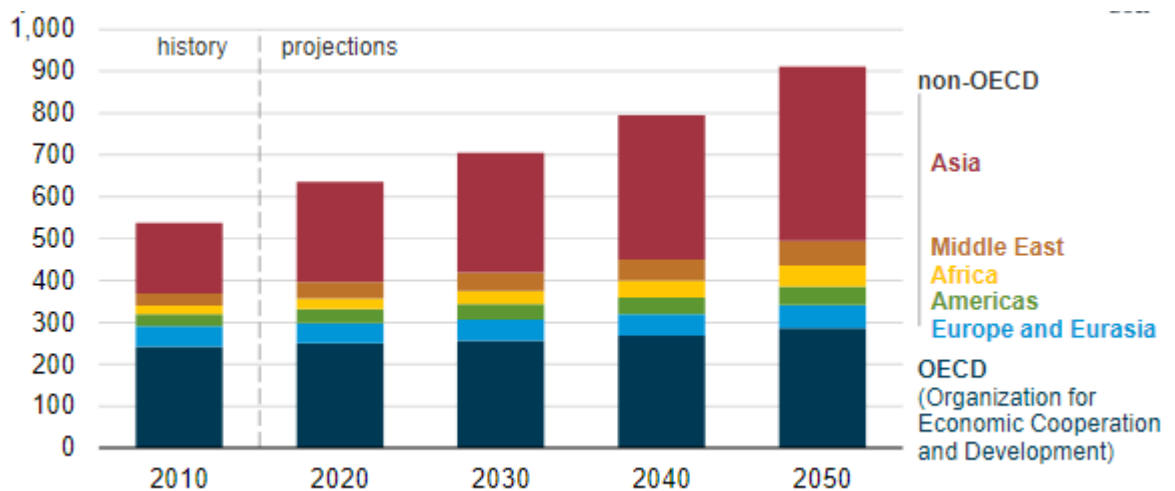
Figure I.1: Global power consumption by region (2010-2050)

I.2.4   Energy Generation by source

The world uses and produces many different types and sources of energy. In 2019, the share of world energy consumption for electricity generation by source was coal at 38%, natural gas at 23.3%, nuclear at 10.2%, renewable energy at 25.1 %(solar, wind, geothermal, biomass, etc.) .Coal and natural gas were the most used energy fuels and hydro was the most used renewable energy for generating electricity; Figure bellow shows global energy generation scenarios for the year 2019. [5]
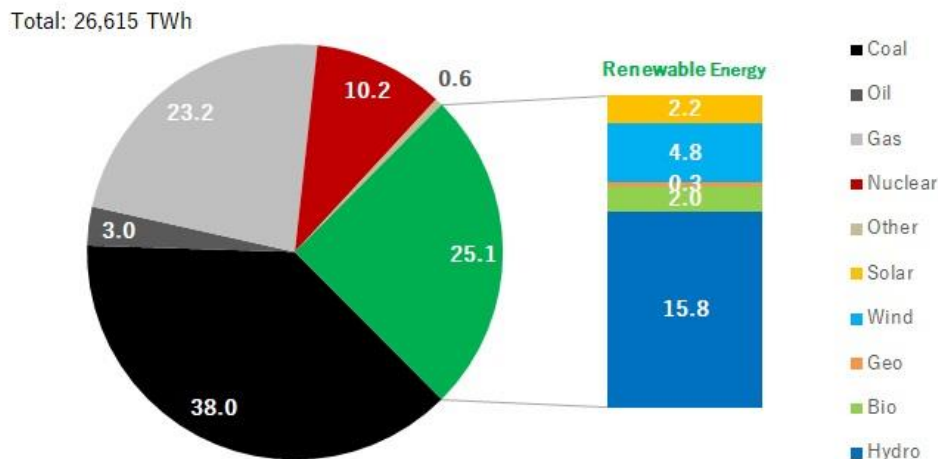
Figure I.2: Global energy generation scenarios 2019

I.2.5   Environmental Pollution: Global Warming Problem

Unfortunately, consuming energy leads to environmental pollution .Most of our energy comes from fossil fuels, and burning these fuels generates gases (SO2, CO, NOX, HC and CO2) that cause environmental pollution. The most principal effects are climate change or global warming problems, which is mainly caused by CO2 and other gases – called greenhouse gases (GHG). NASA satellite images (shown in the figure bellow) show a dramatic fall in pollution over China that is "partly related" to the economic slowdown due to the corona virus outbreak. Maps comparing NO2 concentrations showed a marked decline between January 1-20, before a sweeping quarantine was imposed on Wuhan and other cities, and February 10-25. [5]
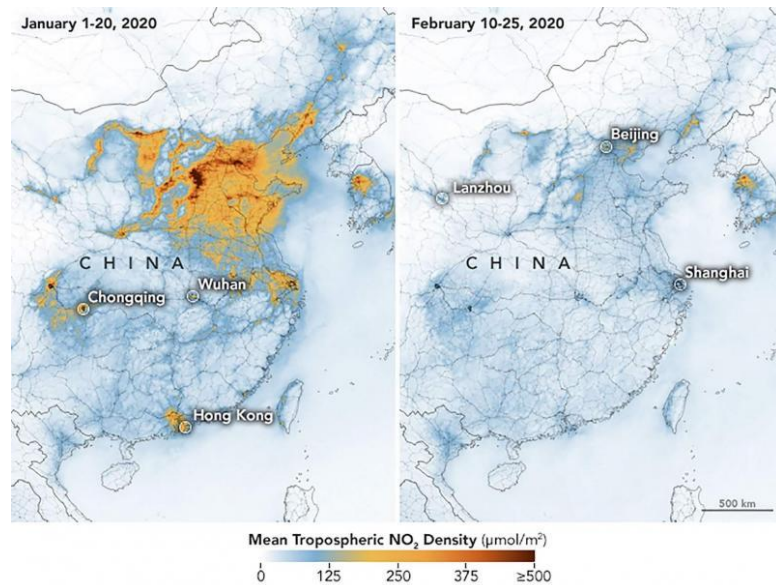
Figure I.3: A handout photo by nasa and earth observatory of china before and after coronavirus outbreak

I.2.6   The problem with renewable energy

I.2.6.1   Intermittency

The biggest problem with mainstream renewable energy is intermittency. Wind power is only generated when it's windy, solar power is only generated when it's sunny. [6]

I.2.6.2   Space and efficiently

Renewable energy resources are horribly inefficient. For example we need huge solar farms and hundreds of wind turbines to produce a normal amount of electricity. [6]

I.2.6.3   Cost

One of the great things about renewable energy is that the sun, the wind, and water currents are all free. That means that, theoretically, these kinds of technologies are one-time costs. In reality, the initial outlay can be huge and the continued costs can be far more than you might expect. [6]

I.2.6.4   Environment and climate change

By far the biggest argument for switching to renewable energy is the unpredicted climate change. [6]

I.3   SOLAR ENERGY

Solar energy is radiant light and heat from the Sun .It is an essential and bountiful source of renewable energy. It has a lot of capabilities like producing heat, causing chemical reactions, or generating electricity. The sun has the potential to satisfy all future energy needs it provides about 120,000 terawatts to Earth's surface, which is 6000 times more than the present rate of the world's energy consumption; therefore, it is expected to become increasingly appealing as a renewable energy source . Solar energy is picked up in a variety

of ways, the most common of which is with solar cells that produce direct current electricity from sunlight. [7]

I.3.1   A brief history of solar power

Solar energy had been captured and converted into usable energy through various methods in ancient history but it only begin to become a viable source of electricity to power devices after 1954.In 1954, Bell Labs developed the first silicon photovoltaic cell. The first solar cells converted solar radiation to electricity at efficiency of 4 percent - for reference; however now a day's many widely available solar panels can convert sunlight to solar power at above 20 percent efficiency, a number continually on the growth. [8]

I.3.2   Solar panel system components

- Solar PV systems are constituted of four main components [10]:
- Solar photovoltaic panels ("solar panels")
- Inverters
- Racking and mounting system
- Performance monitoring systems

I.3.2.1   Solar panels

A solar panel cell (solar module) consists of a layer of silicon cells, a metal frame, a glass casing unit, and wiring to transfer electric current from the silicon. It is a panel designed to absorb the sun's rays as a source of energy for heating and generating electricity that is estimated 34% conversion efficiency, however, only about 24% has been achieved in the majority of panels so far. This means that 70%–76% of solar energy is lost as heat. Solar cells are mostly made of silicon. That is the chemical element of atomic number 14, a non-metal with semiconducting properties, used in making electronic circuits. [11] The photovoltaic process steps:

- The silicon photovoltaic solar cell absorbs solar radiation.
- When the sun's rays interact with the silicon cell, electrons begin to move, creating a flow of electric current.

- Wires capture and feed this direct current (DC) electricity to a solar inverter to be converted to alternating current (AC) electricity. Figure bellow clarifies the effect of combination of photon and electron
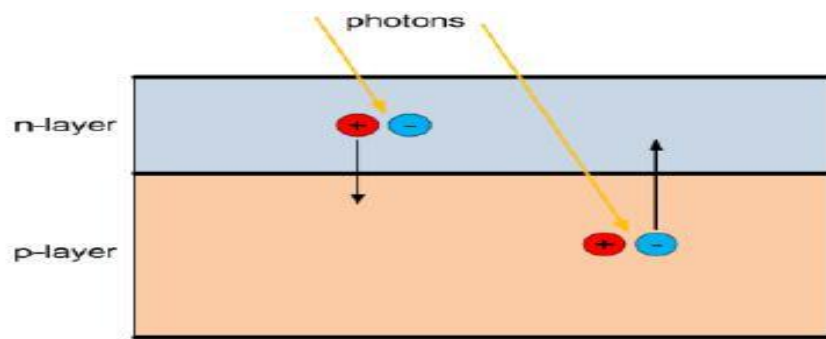
Figure I.5:   Effect of combination of photon and electron

I.3.2.2   Inverters

The cells in solar panels collect the sun's energy and turn it into direct current (DC) electricity. A solar inverter takes the DC electricity from the solar array and uses it to create AC electricity [10].

I.3.2.3   Performance monitoring systems

Performance monitoring systems provide detailed information about the performance of solar panel system. They are used to track trends in a single photovoltaic (PV) system, to identify faults in or damage to solar panels, to compare the performance of a system to design specifications. [10]

I.3.3   Installing solar panels in series vs. parallel
I.3.3.1   Wiring solar panels in series

Wiring solar panels in a series (as shown in the figure bellow) means that each panel is connected to the next in a "string." The total voltage of each solar panel is summed together, but the amps of electrical current stay the same, only one wire needed for each string of solar panels. [12]
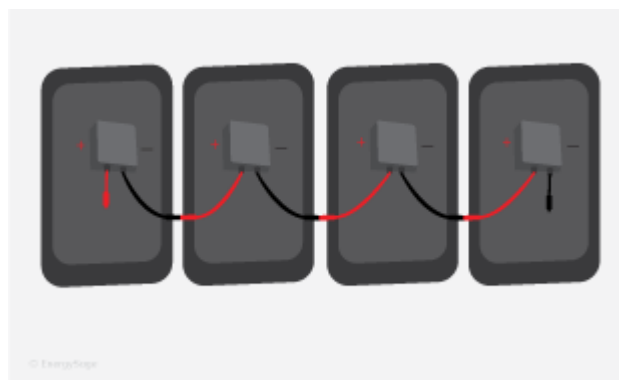
Figure I.5: Solar panels installation in series

I.3.3.2   Wiring solar panels in parallel

Wiring solar panels in parallel (as shown in the figure bellow) means that each panel's wires are connected to a centralized wire leading from the roof. The amps of

electrical current for each solar panel are summed together, but the system voltage stays the same. More wires are needed. [12]
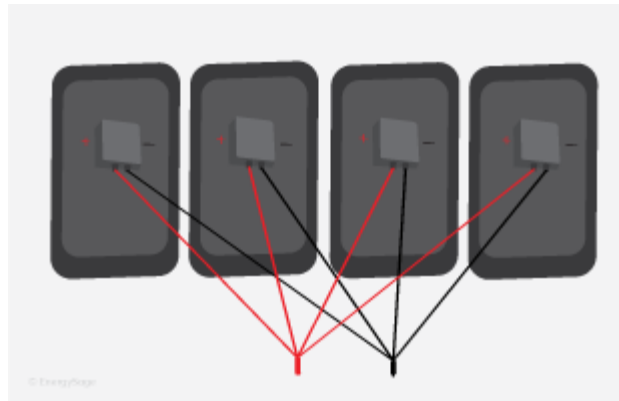
Figure I.6: Solar panels installation in parallel

I.3.4   Types of solar panels

According to the differences in appearance between each type of solar panels, they are classified to three major types: monocrystalline, polycrystalline, and thin-film. Each type is deferent then another by appearance, performance, costs, and the installations .they each has their own unique advantages and disadvantages. [13]

I.3.4.1   Monocrystalline solar panels

Monocrystalline panel(as shown in the figure bellow) is a solar panel with black cells. These cells appear black because of how light interacts with the pure silicon crystal. [13]
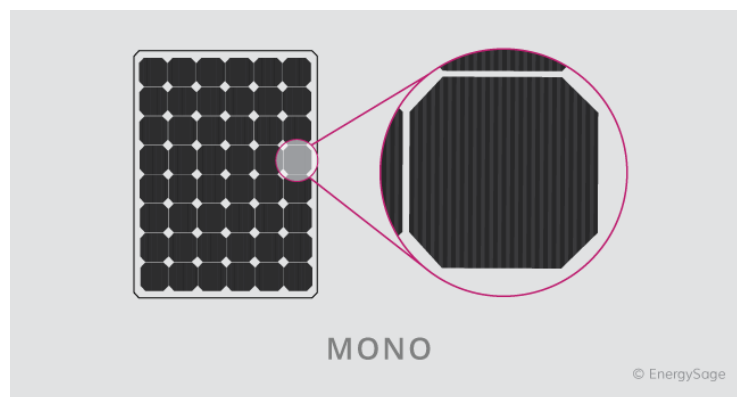
Figure I.7: Monocrystalline solar panels

I.3.4.2   Polycrystalline solar panels

Polycrystalline panel(as shown in the figure bellow) is a solar panel with bluish hue to them that appears because of how the light reflecting off the silicon fragments in the cell. [13]
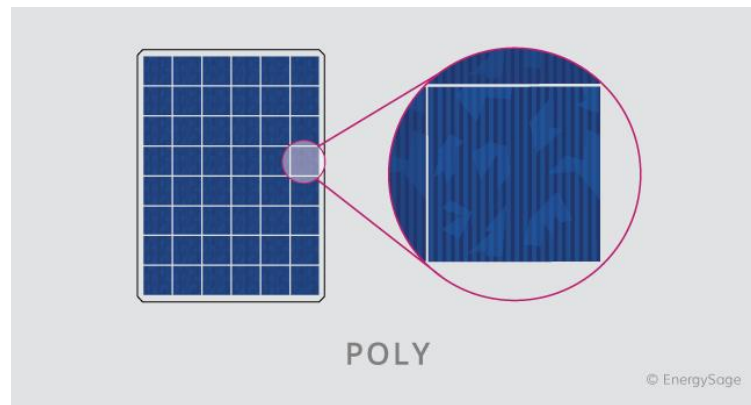
Figure I.8: Polycrystalline solar panels

I.3.4.3   Thin-film solar panels

As their name suggests, thin-film panels(as shown in the figure bellow) are often thin and slim. They are roughly 350 times thinner than other panel types. [13]
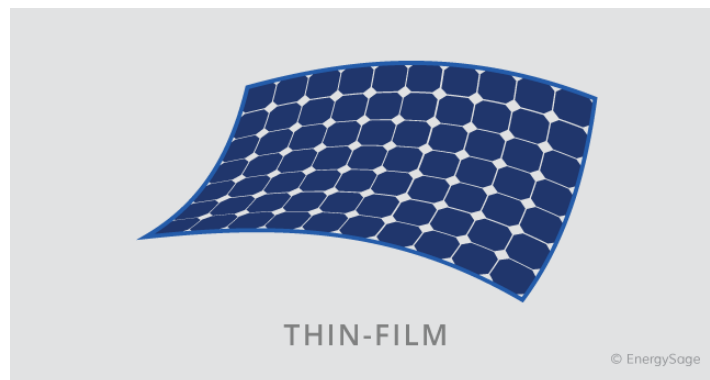
Figure I.9: Thin-film solar panels

I.3.5   Types of photovoltaic power systems

According to their application, photovoltaic power systems are classified into two types grid connected as well as off grid. They can be designed to produce DC and/or AC voltage, can function independent of grid or with grid. [11]

I.3.5.1   Grid connected PV system:

A grid-interactive photovoltaic (PV) system (as shown in the figure bellow) uses solar energy to generate renewable power that charges batteries for use during power failures and feeds power into the electricity grid. As inverter convert DC power to AC power, only

AC power is fed into grid [11].

Figure I.10: Grid connected PV system

I.3.5.2   Stand-Alone Photovoltaic Systems:

Stand-alone PV systems (as shown in the figure bellow) are designed to operate independent of the electric utility grid they are generally used to supply certain DC and/or AC electrical loads. Electrical energy storing devices (batteries) are required to operate the load during sunlight hours as well as night hours fed by PV power. [11]
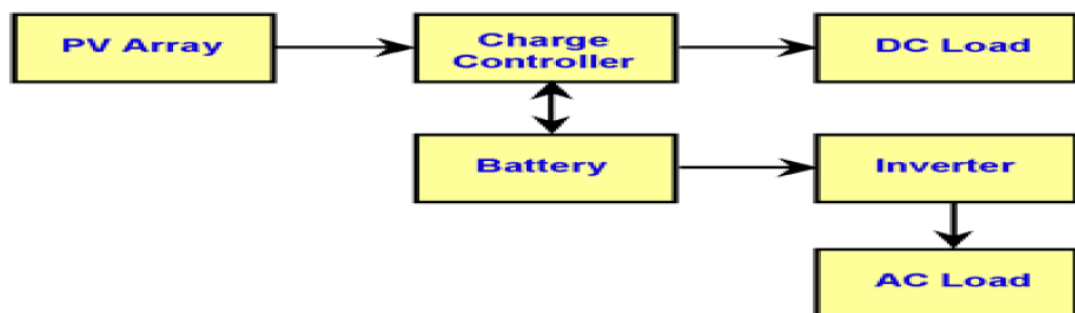
Figure I.11: Standalone PV system

I.3.6   Advantages [17]

- Solar energy is a clean source of energy.
- Solar energy will not be exhausted for a long time it is renewable for life.
- Solar energy protects the environment .As solar energy does not cause any air pollution.
- Solar energy systems are almost maintenance free and it need no cleaning what's or ever.
- If we don't consider the costs of building and other equipment, solar energy is almost cost free.
- solar energy devices can charge low power–consuming devices .

I.3.7   Disadvantages [17]

- Solar energy depends on regional, seasonal, and daily fluctuations, as tt can be used only on sunny days
- Solar energy require a large number of solar panels that use more space and are quite expensive.
- Solar energy for sure needs batteries at night. These batteries are larger in
- Size and heavy, so a space for storage is required, and these must be periodically replaced.
- Nowadays, power generation from solar energy is quite expensive.

I.4   Wind power

Wind is the movement of the air in the form of a current of air blowing from a particular direction, caused by the uneven heating of the atmosphere by the sun, the differences of the earth's surface and the rotation of the earth. Wind can be used to provide the mechanical power through wind turbines to turn on electric generators which produce electricity.

I.4.1   A Brief History of Windmills

The only source of power that human had controlled was wind even before the discovery of electricity. For the first time in history. A Greek engineer, Heron of Alexandria, creates a wind-driven wheel that is used to power a machine, in the 1st century AD.By 7th to 9th century, in the Sistan region of Iran, near Afghanistan. Windmills wind wheels are used for practical uses such as grinding corn and flour, and pumping water.Windmills were used to make salt in China and Sicily,in the 1000 AD. In 1180s, Vertical windmills were used in Northwestern Europe for grinding flour.The first known wind turbine used to produce electricity is built in Scotland in 1887.Wind turbines kept developing ever since and the rest is history. [3]Figure bellow shows the first windmill from Hero of Alexandria.
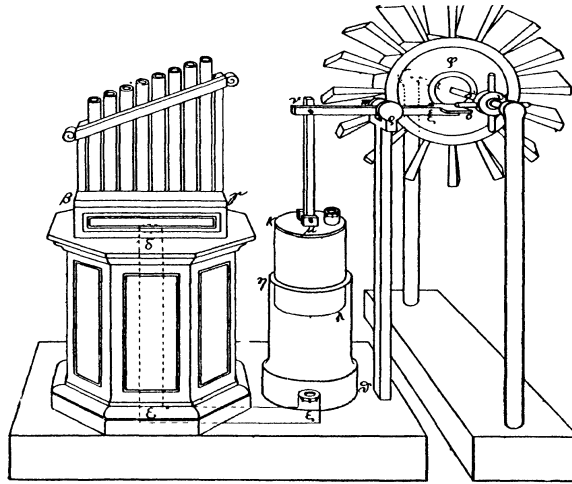
Figure I.12: The first windmill from Hero of Alexandria

I.4.2   Wind Turbines

A wind turbine is a large tall structure with blades that are blown around by the wind. It is a machine which converts the power in the wind into electricity; it is simply the opposite of a fan(as shown in the figure bellow). Instead of using electricity to create wind, it uses wind to create electricity. Wind turbines are connected to some electrical network. These networks include battery-charging circuits, residential scale power systems, isolated or island networks, and large utility grids. [3]

I.4.3   The principal components of a wind turbine

Wind turbines are placed on a tower in order to grab the energy from the wind. The higher the blades are, the better they can capture the wind. A simple wind turbine consists of (as shown in the figure bellow):

- The rotor, which consist of the blades and the supporting hub.
- The drive train, which includes the rotating parts of the wind turbine that are shafts, gearbox, coupling, a mechanical brake, and the generator.
- The nacelle and main frame, which includes wind turbine housing, bedplate, and the yaw system.
- The tower and the foundation.
- The machine controls.
- The balance of the electrical system, which includes cables, switchgear, transformers, and possibly electronic power converters. [3]
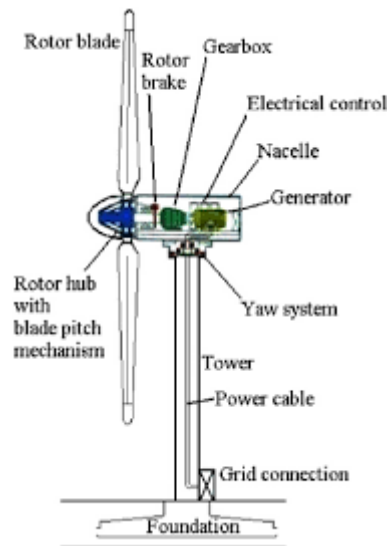
Figure I.13: Major components of a horizontal axis wind turbine

I.4.4   Types of wind turbine
I.4.4.1   HAWT Wind Turbine

Horizontal axe wind turbines (HAWT) are known with their parallel axis of rotation to the ground. They could be classified according to the rotor orientation (upwind or downwind of the tower), hub design (rigid or teetering), rotor control (pitch vs. stall), number of blades (usually two or three blades), and how they are aligned with the wind (free yaw or active yaw). Horizontal axis wind turbines currently have an average life span of 1.5 years. [3]The figure bellow shows the difference between upwind HAWT and downwind .
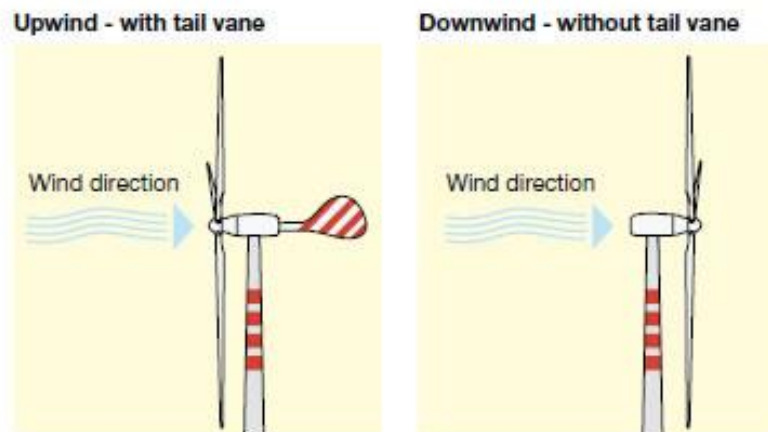
Figure I.14: upwind or downwind

I.4.4.2   VAWT wind turbine

Vertical axe wind turbines (VAWT) (as shown in the figure bellow) are known with their perpendicular axis of rotation to the ground. They are classified into two types: a Darrieus vertical-axis wind turbine that require manual push and has two vertically oriented

blades revolving around a vertical shaft. And a Savonius vertical-axis wind turbines which are a slow rotating, high torque machines with two or more scoops and are used in high-reliability low-efficiency power turbines. [3]
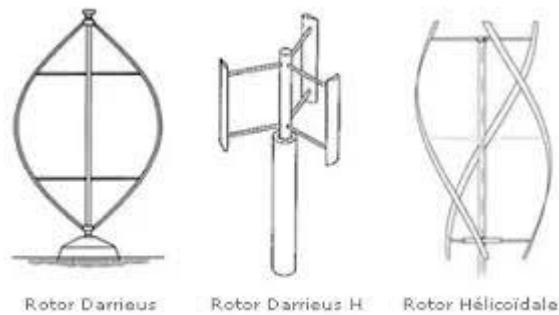
Figure I.15: VAWT wind turbine

I.4.5   Advantages of Wind Energy

- Clean & Environment friendly Fuel source [3]

- Renewable & Sustainable [3]

- Cost Effective [3]

- Industrial and Domestic Installation [3]

- Job Creation [3]

I.4.6   Disadvantages of Wind Energy

- Fluctuation of Wind and Good wind sites [3]

- Noise and aesthetic pollution [3]

- Not a profitable use of land [3]

- Threat to wildlife [3]

I.5   Hybrid energy systems

Hybrid energy systems are all kind of energy sources that are paired together to improve the weaknesses of electricity generation. Hybrid energy systems can take the form of solar panels paired with fossil fuel power plants the reason why is because fossil fuel plants require electricity to start off their generator and if the power goes out solar panels would make a great back up plan. Hybrid energy systems can also take the form of a wind turbine combined with solar panels, solar and wind make a natural pairing because they are basically the opposite(solar shines at morning while wind blows at night) which mains a better and more efficient electricity production during the year. [21]

I.6   Wind-solar systems

Wind & solar paired together are used for power generation and know as wind solar hybrid system. This system is designed combining the solar panels and wind turbines generators for generating electricity. There are four types of wind-solar systems such as [22]:

- Wind-solar grid supply
- Wind-solar building
- Wind-solar lighting
- Solar panels on turbines
- Solar and wind combination advantage

The times when solar and wind energy are at their best are the exact opposite of each other. Solar is best during daylight hours in the summer. Meanwhile, wind turbines tend to produce the most electricity during nighttime hours in the winter ,and that is the main reason why they work both very well together , output from both solar and wind energy systems is highly predictable and follows recognizable patterns, making it easy to plan for times when output decrease from solar panels or wind turbines. Each resource balances the other's weaknesses [22].

I.7   Conclusion

Hybrid energy systems are the most efficient way for electrical power generation. It solves the issue behind the unpredicted climate and intermittency .By combing two or more power resources each one completes the other's weaknesses.

Hybrid wind-solar energy system are the most usable hybrid systems, because they are both highly predictable and follow recognizable patterns which make it easy to control power output ;when they are combined together they provide more electricity during more hours, as well as ensure production during both summer and winter hours of peak electricity usage.

Chapter II:

Modeling of a hybrid system (Wind-photovoltaic)

II Chapter II: modeling of a hybrid system (Wind-photovoltaic)

II.1   Introduction

In the aim of being capable of controlling the hybrid wind solar systems, optimizing their performances and studying their impact. It is necessary to provide the basic concepts of the wind solar energy generation system .therefore a complete model of the hybrid energy system have been developed in this chapter. First a basic mathematical model of the Solar Photovoltaic System has been developed, that includes modeling the fundamental components such as a solar cell, power inverter and a boost chopper. Then a mathematical modeling of a doubly-fed induction generator (DFIG) for a wind turbine has been proposed, that includes the aerodynamics, the Electrical system and mechanical system of the wind turbine.

II.2   Solar system Modeling

Solar energy is expected to become increasingly important as a renewable energy source .A solar electric system produces electricity from the sun energy arriving at earth surface. The four main components of a solar energy system are the panels, inverter(s), and racking and solar battery storage unit [23]. First the panels, which converts sunlight into DC electricity that is fed to the battery through a solar regulator which makes sure that the charging of the battery is proper and not flawed. DC loads can be connected directly to the battery, but AC loads needs an inverter to convert the DC into AC power.
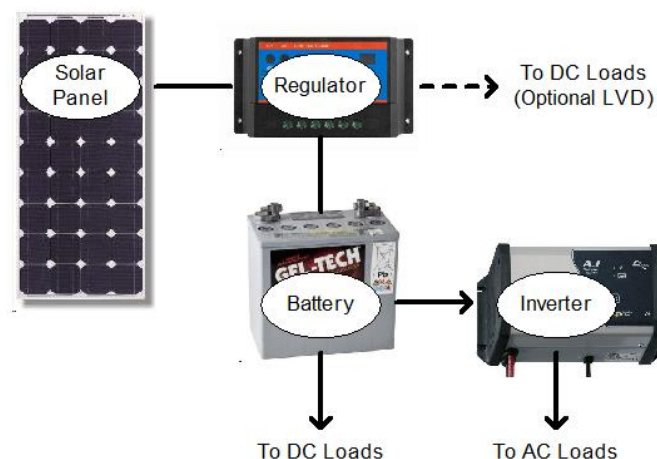
Figure II.1: Components of a basic solar power system

II.2.1   Solar System Mathematical Model

Mathematical models are used to estimate behavior of the system which makes it easier to control it. A basic mathematical model of the Solar Photovoltaic System is a set of mathematical equations that includes modeling the fundamental components such as a solar cell, power inverter and a boost chopper [23].

II.2.1.1 Solar Cell Model

A basic solar cell can be modeled by using a current source, a diode and two resistors.A circuit equivalent model of a solar panel can be constructed using a resistance Rs that is connected in series with a parallel combination of a Current source consisting of single diode (or more) with a shunt resistance structure RSH [24],as it is shown in the figure below.
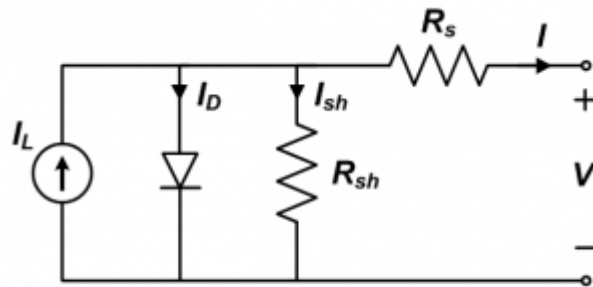
Figure II.2: single diode solar cell model

By Kirchhoff law from the current produced by the solar cell is given as

$$Il = Iph.\,Np - Id - Ish \tag{II.1}$$

By Shockley's equation diode current is given as:

$$Id = Np.\,Is\left[e^{(V/Ns)+(IRs/Ns)/N.V.C} - 1\right] \tag{II. 2}$$

By Ohm's Law, the current through the shunt resistor is given as

$$Ish = \frac{Vj}{Rsh} \tag{II. 3}$$

While

$$Ish = \frac{(V + IRs)}{Rsh} \tag{II. 4}$$

By substituting these equations in one equation load current is given as [30]

$$Il = Iph.Np - Np.Is\left[e^{(V/_{NS})+(IRS/_{NS})/N.V.C} - 1\right] - \frac{(V + IRs)}{Rsh} \qquad \text{(II. 5)}$$

II.2.1.1.1 Parameters of Solar cell

The efficiency of converting sunlight to electricity is determined by the parameters of solar cells. The major parameters that have an impact on the performance of solar cells are the peak power Pmax, the short-circuit current density Isc, the open circuit voltage Voc, and the fill factor FF. [26]

II.2.1.1.1.1 Short Circuit current (ISC):

Short Circuit Current is is the maximum current from a solar cell .It is calculated by considering voltage equals to zero (at V=0) [27]

II.2.1.1.1.2 Open circuit voltage (VOC):

Open Circuit voltage is the maximum voltage from a solar cell .It is calculated by considering current equals to zero(at I=0)the equation for Voc become: [27]

$$Voc = \frac{nkT}{q} ln\left(\frac{Il}{I0} + 1\right) \qquad \text{(II. 6)}$$

II.2.1.1.1.3 Maximum power point (Pm):

Maximum power point can be calculated by multiplying the maximum voltage with the maximum current. [27]

$$Pm = VmIm \qquad \text{(II.7)}$$

II.2.1.1.1.4 Fill Factor (FF):

The fill factor determines the maximum power from a solar cell. It is the ratio of maximum power to the theoretical power available at its output terminal. [27]

$$FF = \frac{Pmax}{VocIsc} \qquad \text{(II.8)}$$

II.2.1.1.1.5 Efficiency (η):

It is the ratio of maximum power to the incident light power. [27]

$$\eta = \frac{Pmax}{Pin} \qquad \text{(II.9)}$$

II.2.1.1.2 Solar cells characterization

A solar cell is characterized with two curves called PV and IV characteristics. Knowing the electrical I-V or P_V characteristics (more importantly Pmax) of a solar cell, or panel is critical in determining the device's output performance and solar efficiency. The performance of a solar panel changes depending on environmental parameters (temperature and irradiance) and cell parameters (parasitic resistance and ideality factor).

II.2.1.1.2.1   PV Curve of Solar cell

A power (P) versus Voltage (V) Curve of a PV Solar Module shows the possible combinations of its power and voltage outputs which is shown in the figure bellow.The power produced will vary depending on the operating voltage the voltage at any point on the graph can still be calculated using the following equation [32]

$$P = I.V.Pmax \qquad (II.10)$$
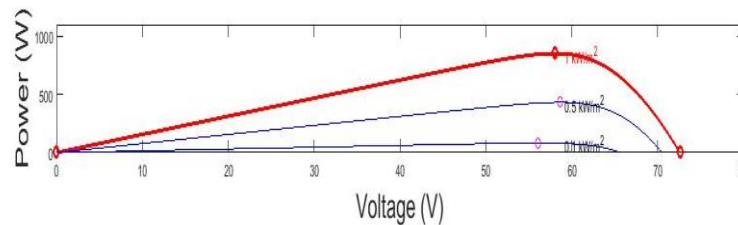
Figure II.3: PV Curve of Solar cell

II.2.1.1.2.2   IV Curve of Solar cell

Solar Cell I-V Characteristics Curves are basically a graphical representation of the possible combinations of the current and voltage outputs which is shown in the figure bellow. The characteristic equation can be given as [32]

$$V = \frac{kT}{q} ln \left(\frac{I}{I0} + 1\right) \qquad (II.11)$$

Array type: 1Soltech 1STH-215-P;
2 series modules; 2 parallel strings
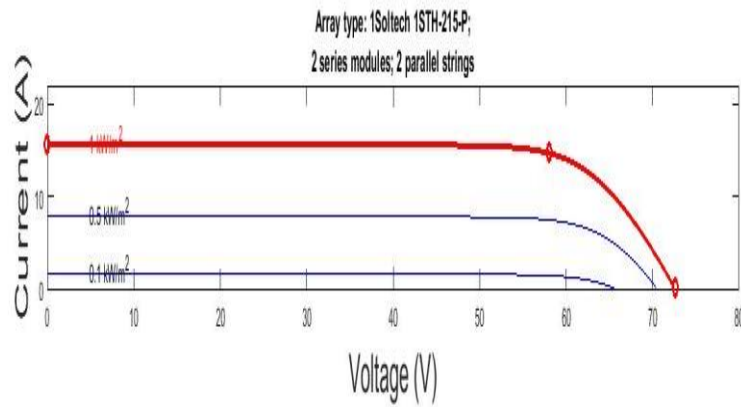
Figure II.4: I-V curve of a solar panel

II.2.1.1.2.2.1   Influence of Light on the Characteristic I(V)

Solar cells are sensitive to sun light. Changing the light intensity changes all solar cell parameters. The light intensity on a solar cell is called the number of suns, where 1 sun corresponds to standard 1 kW/m^2. The open-circuit voltage is directly proportional to the number of suns. The voltage variation is very small and usually ignored. The impact of increasing light intensity is shown in the figure below. [32]
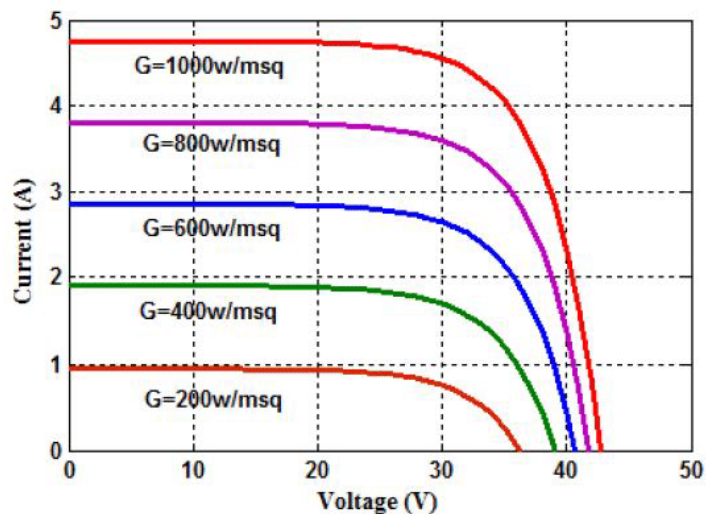
Figure II.5: Influence of light on IV curve characteristics

II.2.1.1.2.2.2   Influence Temperature on the Characteristic I(V)

Solar cells are sensitive to temperature. Changing the temperature changes all solar cell parameters. the parameter most affected by an increase in temperature is the open-circuit voltage. The impact of increasing temperature is shown in the figure below. [32]
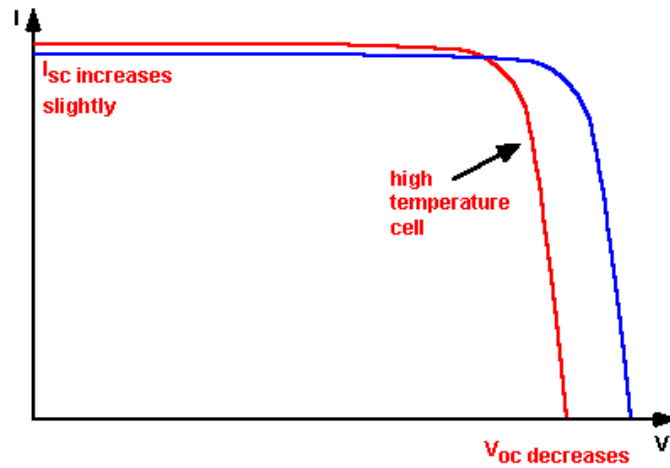
Figure II.6: The effect of temperature on the IV characteristics of a solar cell.

II.2.1.1.2.2.3 Influence of Ideality factor on the Characteristic I(V)

The efficiency of the solar cell performance changes with the change of the ideality factor. The more the ideality factor increases the closer the I-V shape to a rectangle. The impact of increasing the ideality factor is shown in the figure below. [32]
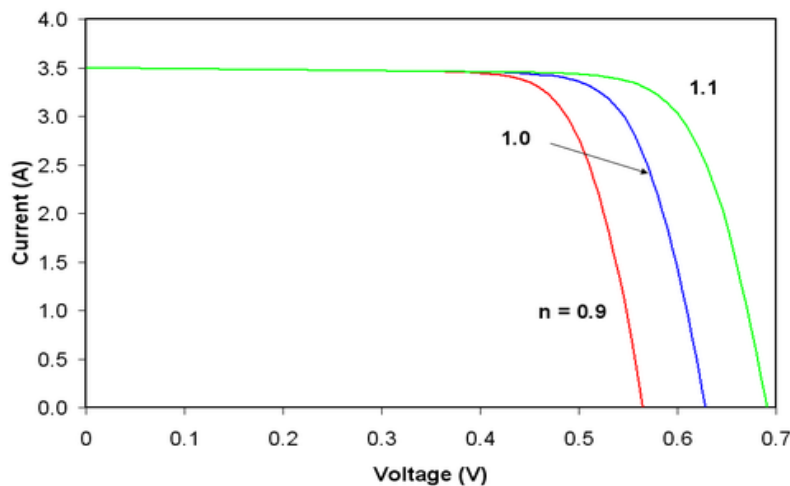
Figure II.7: The effect of the fill factor on the IV characteristics of a solar cell.

II.2.1.2 DC-DC BOOST CONVERTER

A boost converter is a switch mode converter. It is used to boost or step up the DC input voltage by adjusting the duty ratio of the switch. The duty ration should be more than 0.5 so the output voltage is more than the input voltage. The boost converter circuit as shown in the figure bellow consists of a inductor, a switching device, a diode and a capacitor. Also a voltage source and a load is necessary [**53**]
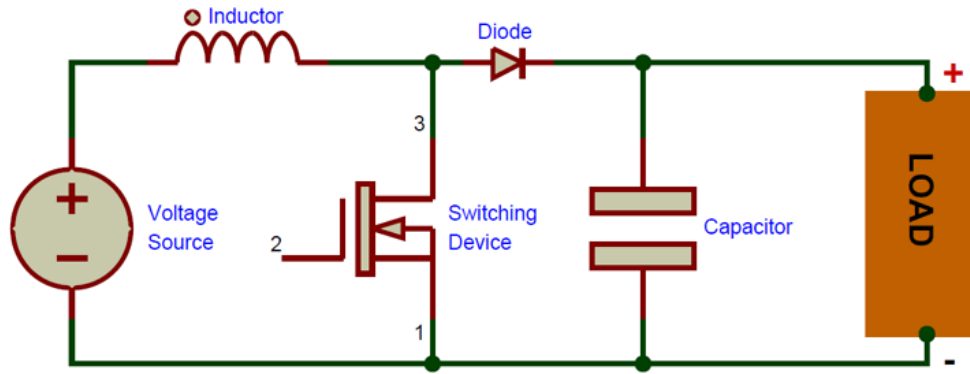
Figure II.8: DC-DC boost converter

The operation of the boost converter goes through these following steps:

- Step one the switch is turned ON which means the diode is not conducting. This step is accomplished during the following interval:

$$0 < t < DT_S \tag{II.12}$$

In this stage the following equations are given :

$$V_{in} = L\frac{di_L}{dt} \tag{II.13}$$

$$i_L = t\frac{V_{in}}{L} + c \tag{II.14}$$

$$\Delta i_L(ON) = \frac{V_{in}}{L}DT \tag{II.15}$$

- Step two the switch is turned OFF which means the diode is conducting. This step is accomplished during the following interval:

$$DT_S < t < T_S \tag{II.16}$$

In this stage the following equations are given :

$$V_{in-}V_{out} = L\frac{di_L}{dt} \tag{II.17}$$

$$i_L = t\frac{V_{in-}V_{out}}{L} + c \tag{II.18}$$

$$\Delta i_L(OFF) = \frac{V_{in} - V_{out}}{L}(1 - D)T \tag{II.19}$$

By making the sum of the On and Off current equal to 0 the following equation is obtained:

$$\Delta i_L(ON) + \Delta i_L(OFF) = 0 \tag{II.20}$$

$$\frac{V_{in}}{L}DT + \frac{V_{in} - V_{out}}{L}(1 - D)T = 0 \tag{II.21}$$

Where the duty cycle (D) is given as:

$$D = \frac{T_{on}}{T_{off}} \tag{II.22}$$

From the previous equations we obtain the following equality:

$$v_{out} = \frac{1}{1 - D}v_{in} \tag{II.23}$$

II.3 Wind system modeling

A wind turbine is device that generates electrical power from the wind. It works on a simple principle .Turbines catch the wind's energy with their blades, which spins the rotor then turns a shaft inside the nacelle, which goes into a gearbox. The gearbox increases the rotational speed so it fits the generator .the generator then uses magnetic fields to convert the mechanical energy into electricity. [33] A basic wind energy system is constructed with the following components: [34]

- Turbine rotor and blade assembly (prime mover);
- Shaft and gearbox unit (drive train and speed changer);
- Induction generator;
- Control system.
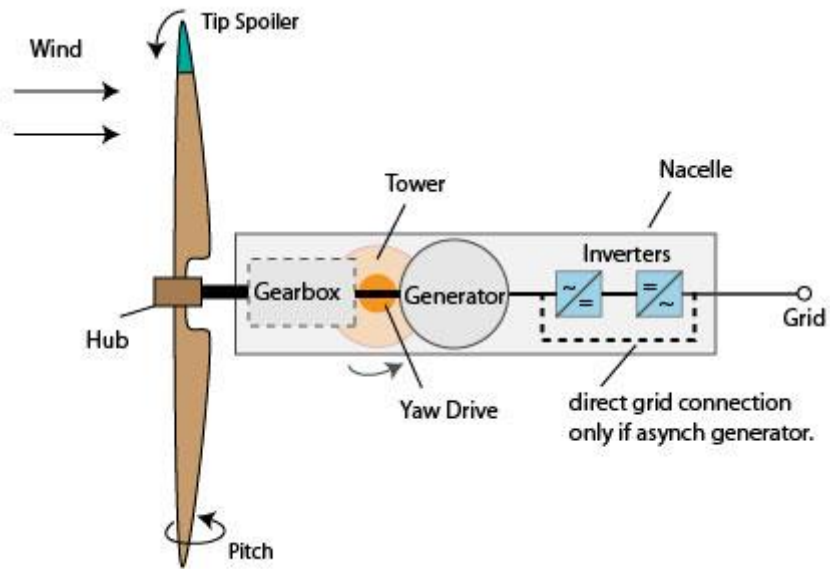
Figure II.9: Wind energy systems

II.3.1   The aerodynamics of wind turbines

Aerodynamics of wind turbines are the forces that act on a turbine blade. As wind moves around the blade, two aerodynamic forces are created: drag and lift. Lift force acts perpendicular to the direction of wind flow; and drag force acts parallel to the direction of wind flow. So clearly drag and lift forces act perpendicularly to each other. The aerodynamic of the wind turbine consists of three major parameters: tip-speed ratio, rotor power coefficient (CP), and aerodynamic torque. The figure below shows lift and drag forces directions. [35]
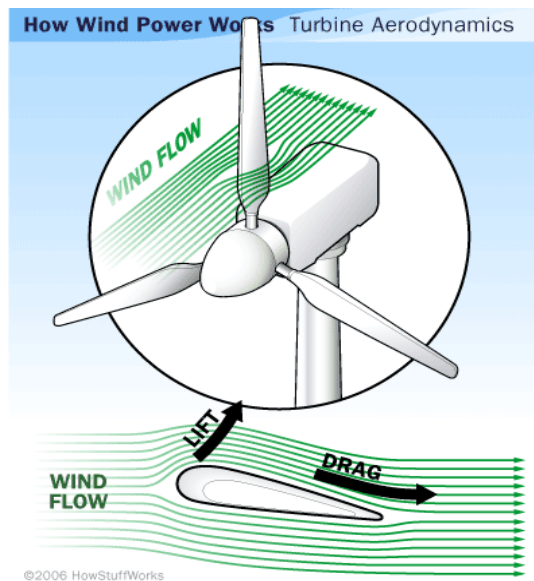
Figure II.10: Wind Turbine Aerodynamics

Wind energy is the kinetic energy of the moving air. The kinetic energy of of an air mass moving at a wind speed is given by

$$E = \frac{1}{2} m V wind^2 \tag{II.24}$$

Where mass flow through an area A is given by

$$m = \rho A V wind \tag{II.25}$$

Wind power (P_{wind}) is the power available in the wind that provides the mechanical power through wind turbines to turn electric generators [39].It is given by:

$$P wind = \frac{1}{2} \rho A V wind^3 \tag{II.26}$$

And the rotor power (P_{rotor}) is the power produced from the rotation of the rotor due to the interaction between the windings and magnetic fields [39] .it is given as:

$$P rotor = \frac{1}{2} \rho C p A V wind^3 \tag{II.27}$$

The aerodynamic torque is defined as the torque produced by the rotor blades it is calculated by [39]:

$$\Gamma rotot = \frac{P rotor}{\omega rotor} \tag{II.28}$$

It could be also given as:

$$\Gamma rotot = \frac{1}{2} \rho A C p V / \lambda \tag{II.29}$$

II.3.2   The Electrical system of the wind turbine

The main components of the electrical system of wind turbine (as shown in the figure bellow) [41] are:

- Double Fed Induction Generator: It is an electrical generator in which both the field magnet windings and armature windings are separately connected to equipment outside the machine.
- Grid Side Converter: It is an AC-DC converter circuit which is used to supply a regulated DC voltage to the inverter.
- Rotor Side Converter: It is a DC-AC converter which is used to supply regulated AC voltage to the rotor

.
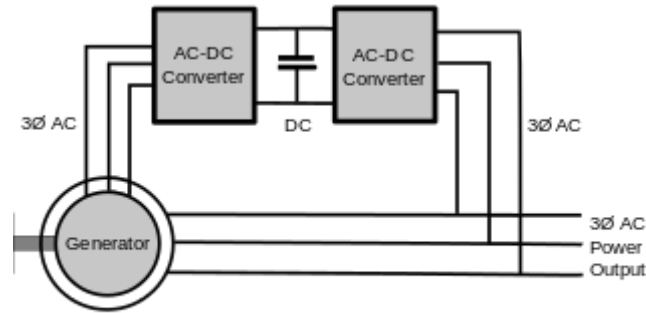
Figure II.11: Electrical system of wind turbine components

II.3.2.1 Reasons of using DFIG for wind systems

The reasons why doubly fed induction machines (DFIG) are preferably used in wind energy systems are [42]:

- Constant frequency output signal whatever the rotor speed is.
- Low power rating required for the power electronic devices
- Power factor is controlled.
- Electric power generation at low wind speed. These properties make the cost of DFIG lower and the power losses less than the other types of generators.

II.3.2.2 Modeling of DFIG

A Doubly Fed Induction generator It is an electrical generator in which both the rotor and stator windings are fed with 3 phase AC signal. Also, the field magnet windings and armature windings are separately connected to equipment outside the machine [42]. The DFIG electric circuit can be presented by only one phase of the stator and because of the symmetry in the machine, the other two phases are modeled as essentially equal as shown below
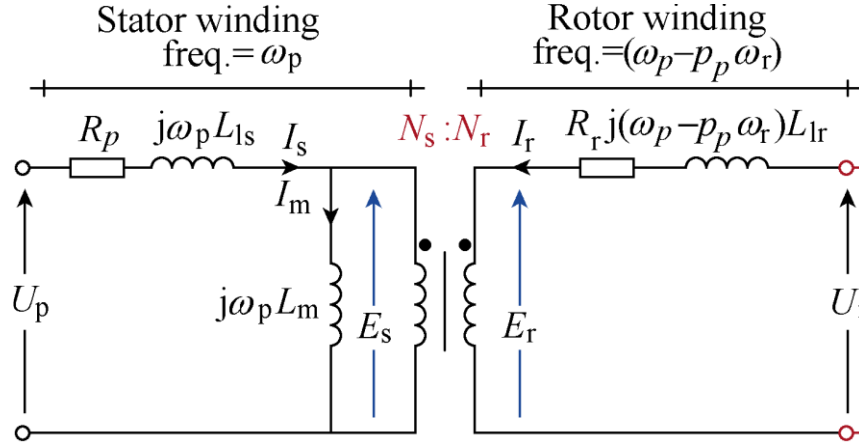
Figure II.12: One-phase steady-state equivalent electric circuit of the DFIM

The DFIG is described in the Park d–q frame can be given by the following set of equations [5]

The stator dq voltage equations are given as bellow

$$v_{ds} = R_s i_{ds} + \frac{d\varphi_{ds}}{dt} - \omega_s \varphi_{qs} \qquad (\text{II.30})$$

$$v_{qs} = R_s i_{qs} + \frac{d\varphi_{qs}}{dt} + \omega_s \varphi_{ds} \qquad (\text{II.31})$$

The rotor dq voltage equations are given as bellow

$$v_{dr} = R_r i_{dr} + \frac{d\varphi_{dr}}{dt} - \omega_r \varphi_{qr} \qquad (\text{II.32})$$

$$v_{qr} = R_r i_{qr} + \frac{d\varphi_{qr}}{dt} + \omega_r \varphi_{dr} \qquad (\text{II.33})$$

The stator dq flux equations are given as bellow

$$\varphi_{ds} = L_s i_{ds} + L_m i_{dr} \qquad (\text{II.34})$$

$$\varphi_{qs} = L_s i_{qs} + L_m i_{qr} \qquad (\text{II.35})$$

The rotor dq flux equations are given as bellow

$$\varphi_{dr} = L_m i_{ds} + L_r i_{dr} \qquad (\text{II.36})$$

$$\varphi_{qr} = L_m i_{qs} + L_r i_{qr} \qquad (\text{II.37})$$

The mechanical power in the shaft P$_m$ minus the cupper losses in the stator and rotor is equal to the sum of the stator active power P$_s$ and the rotor active power P$_{r \text{ as follows}}$

$$Ps + Pr = Pm + Pcu\_r + Pcu\_s \qquad (II.38)$$

While

$$Pcu_s = 3Rs|Is|^2 \qquad (II.39)$$

And

$$Pcu_r = 3Rr|Ir|^2 \qquad (II.40)$$

The efficiency of the machine particular to motor or generator operation can be given as:

$$\eta = \frac{Pm}{Ps + Pr} \qquad , Pm > 0 \qquad (II.41)$$

$$\eta = \frac{Ps + Pr}{Pm} \qquad , Pm < 0 \qquad (II.42)$$

By neglecting the power losses in the stator and rotor resistances the stator active and reactive powers can be given as follows:

$$Ps = \frac{3}{2}(VdsIds + VqsIqs) \qquad (II.43)$$

$$Qs = \frac{3}{2}(VqsIds + VdsIqs) \qquad (II.44)$$

The rotor active and reactive powers can be given as follows:

$$Pr = \frac{3}{2}(VdrIdr + VqrIqr) \qquad (II.45)$$

$$Qr = \frac{3}{2}(VqrIdr + VdrIqr) \qquad (II.46)$$

II.3.3   The mechanical system of the wind turbine

The mechanical system of the wind turbines mainly consists of wind turbine gear box which contains two main shafts, the low speed shaft which is basically connected with the

wind turbine blades, and the high speed shaft which connected directly to the generator [35] as it is shown in the figure bellow
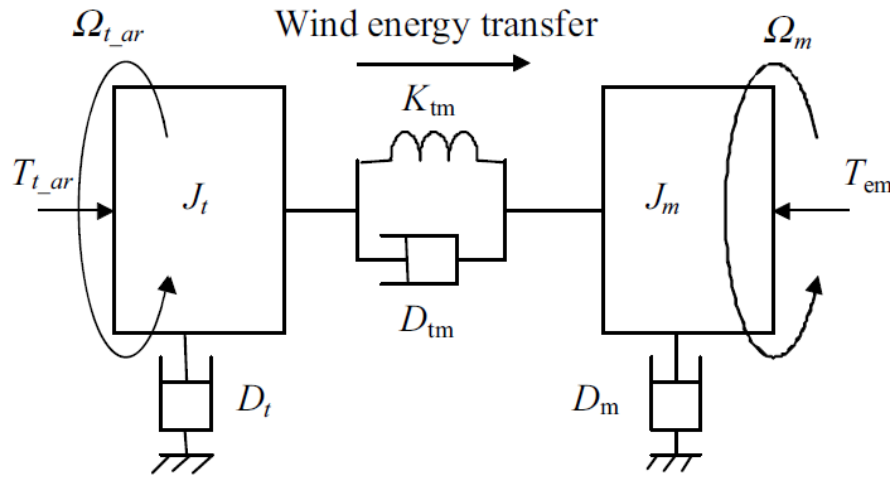
The turbine rotational speed in the fast shaft is given by

$$\Omega t_{ar} = N\Omega t \tag{II.47}$$

The driving torque in the fast shaft is given by

$$Tt_{ar} = \frac{Tt}{N} \tag{II.48}$$

The mechanical speed evolution equation in the fast shaft is given by

$$Jt\frac{d\Omega t\_ar}{dt} = Tt_{ar} - Dt\Omega t_{ar} - Tem \tag{II.49}$$

The mechanical speed evolution equation in the low speed shaft is given by

$$Jm\frac{d\Omega m}{dt} = Tem - Dm\Omega m - Tt\_ar \tag{II.50}$$

The driving torque in the low speed shaft evolution equation Is given by

$$\frac{dTem}{dt} = Ktm(\Omega t_{ar} - \Omega m) + Dtm\left(\frac{d\Omega t\_ar}{dt} - \frac{d\Omega m}{dt}\right) \tag{II.51}$$

by neglecting the damping coefficients (D_t, D_m, and D_{tm}).The resulting transfer function relating the generator torque and speed presents a pole at w_{01} pulsation and a zero w_{02} pulsation as follows :

$$\omega 01 = \sqrt{Ktm\frac{Jt + Jm}{JtJm}} \qquad (II.52)$$

$$\omega 02 = \sqrt{\frac{Ktm}{Jt}} \qquad (II.53)$$

II.4 Conclusion

This chapter presented a detailed modeling of a hybrid system based on PV and Wind energy. The chapter systematically outlined an electrical characteristic modeling of a DFIG unit for wind turbine designing. And an electrical characteristic of a solar cell for Solar Photovoltaic System design. The models described in this chapter will be employed next in the next chapter in order to simplify the control methods.

Chapter III:

Control of a hybrid system

(Wind-photovoltaic)

III Chapter III: control of a hybrid system (Wind-photovoltaic)

III.1 Introduction

The equations of the hybrid wind solar system necessary for voltage control were represented in the previous chapter. In this chapter, the synthesis of regulators necessary for the realization of this command has been developed.First, the wind turbine system controller is developed, including pitch angle and mechanical torque controller, grid side controller and rotor side controller, three types of regulator are used. The synthesis of a Proportional - Integral regulator is carried out. In order to compare its performance to other regulators, we also synthesize an RST regulator calculated by placing robust poles and an LQR regulator, based on the linear matrix inequality (LMI).Then, the solar turbine system controller is developed, by controlling the boost converter. The synthesis of a MPPT P & O method regulator is carried out. In order to compare its performance to other regulators, we also synthesize an MPPT FUZZY logic controller. The figure below presents a hybrid wind solar system control strategy.
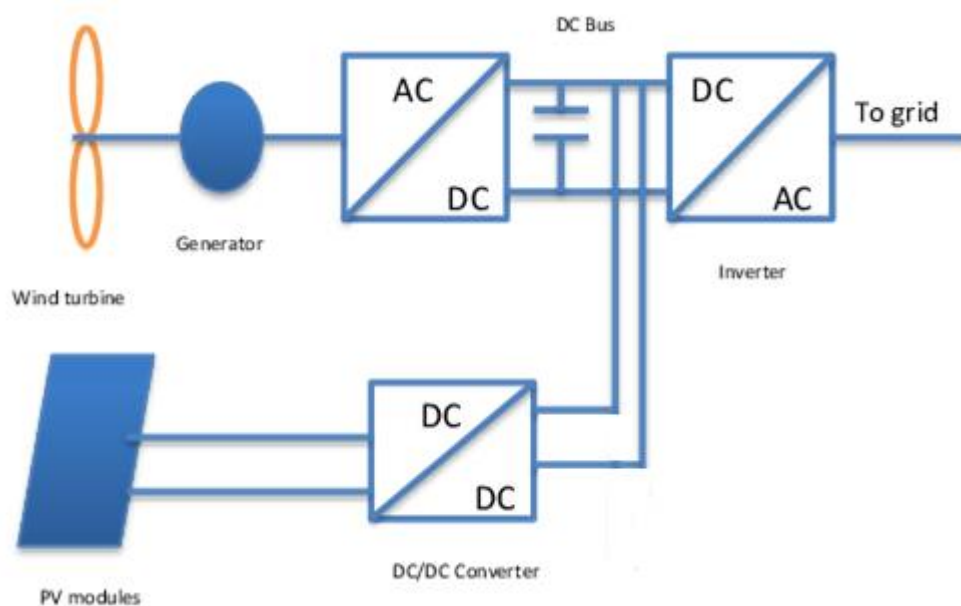
Figure III.1: hybrid wind solar control strategy.

III.2 Wind system control

This part covers the fundamental control methods of wind turbine control system. In order to optimize power output and ensure long efficient performance in a low wind speed the pitch of the blade and speed of the DFIG controlling is necessary. Controlling the synchronous DFIG speed can be achieved by the control of the electrical subsystem using

power electronics or electronic converters that are coupled to the generator. The two types of DFIG control are stator side and rotor side control. In our case we controlled the rotor side of the DFIG to change the synchronous speed. [44]The Figure 1 shown bellow presents wind energy control system, which uses DFIG. The two main components of the system which will be separately controlled are the wind turbine and the DFIG.
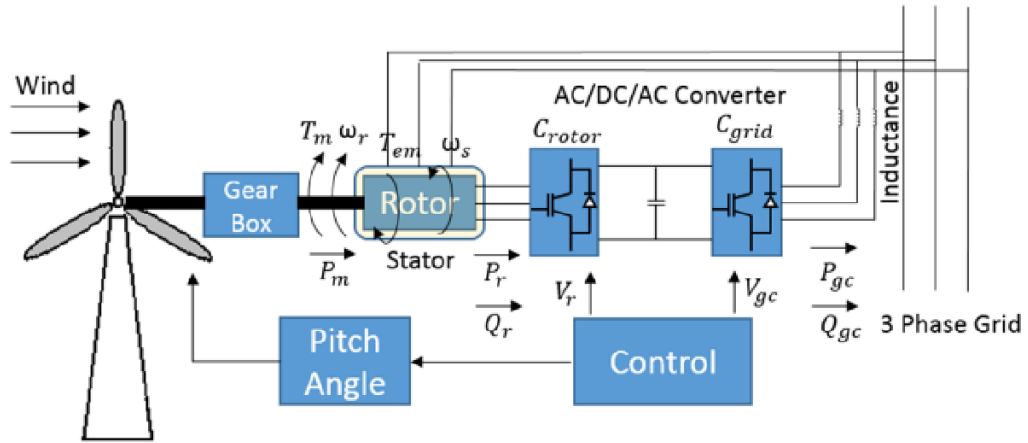
Figure III.2: wind energy control system

III.2.1 Variable pitch wind turbine control

As we have seen in chapter 1 wind turbines produce electricity from the wind through an electrical generator. A turning power is generated when wind passes over the blades. in order to optimize turbine performance in low wind speeds and limit it in the strong ones, the pitch angle of the blades can be adjusted using an electric pitch servos .Therefore the blade control strategy considered in this section is all about sending the error between the generator rotor speed and its set point to the controller to produce a reference value for the pitch angle.

III.2.1.1 Mechanical torque control

The Mechanical torque control model is based on the steady-state power characteristics of the turbine, the power output of the wind turbine can be optimized by controlling the torque which is given as [45]:

$$T_e(ref) = \frac{P_{m(max)}}{\omega_m} \qquad \text{(III.1)}$$

From the power equation (mentioned in chapter 2), $T_e(ref)$ can be written as:

$$T_e(ref) = \frac{c_p(max)R^2\rho 0.5\pi \left(\frac{R\omega_{mf}}{\lambda_{opt}}\right)^3}{\omega_m} \tag{III.2}$$

Knowing the steady-state power characteristics of the turbine gives us the following equality:

$$\omega_m = ng\omega_{mf} \tag{III.3}$$

Which give us the optimal gain, written by:

$$K_{opt} = \frac{c_p(max)R^2\rho 0.5\pi}{\lambda_{opt}^3 n_g^3} \tag{III.4}$$

Thus, the control law can be given as:

$$T_e(ref) = K_{opt}\omega_m^2 \tag{III.5}$$

III.2.1.2 PITICH CONTROL

The blades are turned by the pitch actuator which describes the dynamic behavior between a demand pitch angle from the controller and the measured one □. The change in the pitch angle is given as [45]:

$$\frac{d\beta}{dt} = \frac{\beta_d - \beta}{\tau_\beta} \tag{III.6}$$

Applying Laplace transform, the transfer function for the actuator becomes:

$$\frac{\beta}{\beta_d} = \frac{1}{\tau_\beta s + 1} \tag{III.7}$$

The PI controller and desired pitch angle can be given as:

$$\beta_d = K_p e + K_i \int e \, dt \tag{III.8}$$

Considering the variation range of e is very small for an adjustable-slip asynchronous generator, Kp is far greater than Ki .Therefore the equation above can be simplified as follows.

$$K_p = \frac{d\beta_d}{de}$$

(III.9)

$$K_i = 0$$

(III.10)

III.2.2 Control of the DFIG

The control strategy of the DFIM used in this part is designed to capture optimum power from the wind at its low speed through closed loop current and rotor speed control of the machine. Firstly a vector control of the DFIM is introduced. Then active and reactive power decoupling control is adopted from the principle of stator oriented field control. Finally mathematical model of DFIG with current speed control loop using PI, RST and LMI controller is designed to optimize the power captured from the wind. The results shown are obtained from simulation in Matlab/Simulink platform which shows the effectiveness of the strategy proposed.

III.2.2.1 Structure and Configuration of the DFIM

The typical configuration of the DFIM When it is connected to the grid shown in the figure bellow is established in these three main steps. The first step is the synchronization of the stator voltages with the grid voltages, which are the reference in our case. The second step is the stator is connected to the grid and the rotor is connected to the converter via a back-to-back converter. The third step is the power electronic interface controls the rotor current to capture optimum power from the wind [46]. The power electronics only process the rotor power, typically less than 25% of the overall output power. Thus the DFIG offers the advantage of speed control with low cost and optimum power.
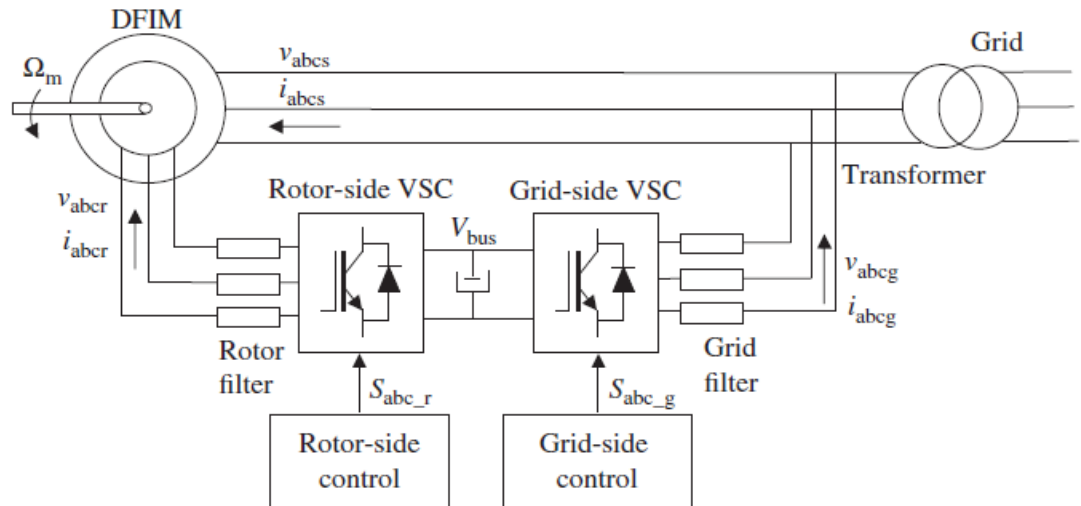
Figure III.3: typical supply configuration of DFIM

III.2.2.1.1 A back-to-back converter

In this part, we will study the back-to-back converter which is a two IGBT-based three-phase two-level voltage source converters connected in series with the opposite polarity that are both operated through a controlled pulse width modulation. The back-to-back converter connects the DFIG to the grid. Generator-side and grid-side converters as shown in the figure bellow. [47]
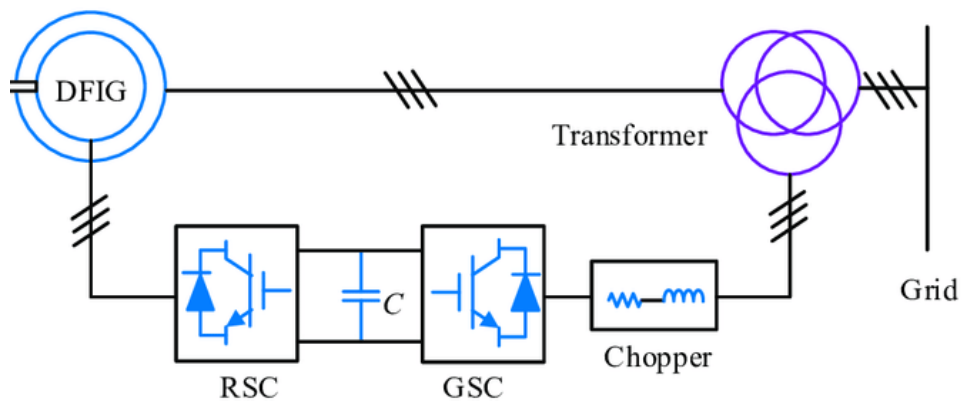
Figure III.4: Back-to-back converter-based DFIG power system configuration

The main components of the back-to-back converter are as follows:

DC-link Voltage

Both of the generator-side and grid-side converters has to produce an AC voltage at least equal

to the AC-side nominal voltage in order to properly control the injected AC-side current. The AC-side line-to-line output is given as:

$$V_{LL} = \frac{\sqrt{3}}{2\sqrt{3}} m v_{dc}$$

(III.11)

DC-link Capacitor

The selection of the DC-link capacitor of a back-to-back converter is given as:

$$C = \frac{S}{4\pi f_{min} v_{dc} \Delta v_{dc}}$$

(III.12)

Line Reactor and Step-up Transformer

The line reactor is used as protection and filter. In our case we used LC filters to reduce the harmonic content.

III.2.2.1.2 Vector Control of DFIM

This part presents vector control of grid-connected wind turbines with doubly-fed induction generators (DFIG) in which only the rotor-side converter control is studied .the vector control of the DFIM is performed in a synchronously rotating dq frame, in which the d-axis is aligned, in this case, with the stator flux space vector, as illustrated in Figure below. [5]
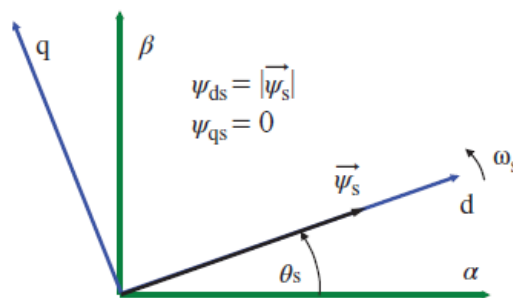
Figure III.5: synchronous rotating dq reference frame aligned with the stator flux space vector

III.2.2.1.3 Rotor side Control of the DFIM

III.2.2.1.3.1 Rotor Current Control Loops

by substituting the stator dq flux equations and the rotor dq flux equations into the rotor voltage equation we obtain the rotor voltage as a function of the rotor currents and stator flux [**5**]

$$V_{dr} = \sigma L_r \frac{di_{dr}}{dt} + R_r i_{dr} - \sigma L_r \omega_r i_{qr} + \frac{L_m}{L_s} \frac{d\varphi_{ds}}{dt} \qquad \text{(III.13)}$$

$$V_{qr} = \sigma L_r \frac{di_{qr}}{dt} + R_r i_{qr} + \sigma L_r \omega_r i_{dr} + \frac{L_m}{L_s} \omega_r . \varphi_s \qquad \text{(III.14)}$$

Note that

$$\varphi s = \varphi ds \; \rightarrow \varphi qs = 0 \qquad \text{(III.15)}$$

$$V_{qs} = V_s = \omega_s . \varPhi_s \rightarrow V_{ds} = 0 \qquad \text{(III.16)}$$

While

The stator dq flux equations are given as

$$\varphi_{ds} = L_s i_{ds} + L_m i_{dr} \qquad \text{(III.17)}$$

$$\varphi_{qs} = L_s i_{qs} + L_m i_{qr} \qquad \text{(III.18)}$$

The rotor dq flux equations are given as

$$\varphi_{dr} = L_m i_{ds} + L_r i_{dr} \qquad \text{(III.19)}$$

$$\varphi_{qr} = L_m i_{qs} + L_r i_{qr} \qquad \text{(III.20)}$$

The rotor dq voltage equations are given as

$$v_{dr} = R_r i_{dr} + \frac{d\varphi_{dr}}{dt} - \omega_r \varphi_{qr}$$

$$v_{qr} = R_r i_{qr} + \frac{d\varphi_{qr}}{dt} + \omega_r \varphi_{dr}$$

<div align="right">(III.22)</div>

With the crosses coupling terms between the d and q axis given as:

$$-\sigma L_r \omega_r i_{qr}$$

<div align="right">(III.23)</div>

$$\sigma L_r \omega_r i_{dr} + \frac{L_m}{L_s} \omega_r . \varphi_s$$

<div align="right">(III.24)</div>

The equation of the rotor voltage above is used to rewrite the rotor currents as:

$$i_{dr} = \left(v_{dr} + \omega_r \sigma L_r i_{qr}\right)\left(\frac{1}{\sigma L_r s + R_r}\right)$$

<div align="right">(III.25)</div>

$$i_{qr} = \left(v_{qr} - \omega_r \sigma L_r i_{dr} - \frac{L_m}{L_s} \omega_r . \varphi_s\right)\left(\frac{1}{\sigma L_r s + R_r}\right)$$

<div align="right">(III.26)</div>

We can then represent the closed-loop current control as shown in the figure bellow:
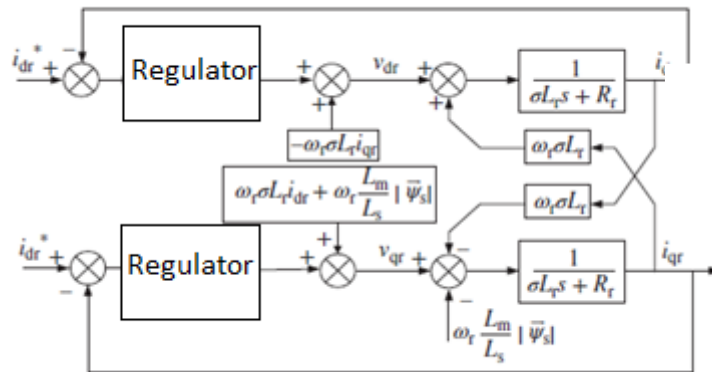
Figure III.6: closed-loop current control

III.2.2.1.3.2   Power and Speed Control Loops

The torque expression in the dq frame is given as (mentioned in chapter 2): [5]

$$T_{em} = \frac{3}{2} p \frac{L_m}{L_s} \left(\varphi_{qs} i_{dr} - \varphi_{ds} i_{qr}\right) \quad \rightarrow \quad T_{em} = -\frac{3}{2} p \frac{L_m}{L_s} \left(\varphi_s i_{qr}\right)$$

<div align="right">(III.27)</div>

While

$$-\frac{3}{2}p\frac{L_m}{L_s}(\varphi_s) = cst$$

(III.28)

This means that the q rotor current component is proportional to the torque which can be then simplified as follows:

$$T_{em} = K_T i_{qr}$$

(III.29)

consequently, the speed of the machine can be written as:

$$\omega_m = p\Omega m = p\left(\frac{1}{Js}\right)[T_{em} - T_{load}]$$

(III.30)

Supposedly that

$$T_{load} = 0$$

(III.31)

We can then represent the closed-loop speed control as shown in the figure bellow:
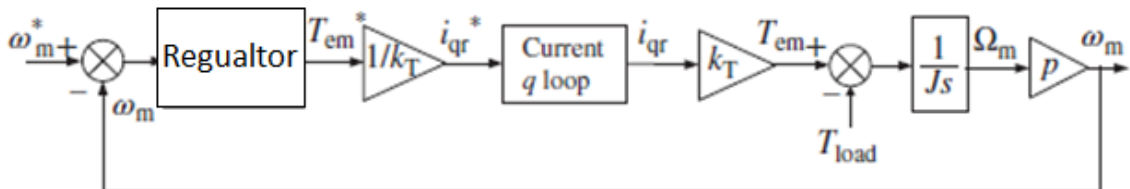
Figure III.7: closed_loop speed control

In a similar way, by developing the stator reactive power expression in the dq frame, we obtain the following expression:

$$Q_s = \frac{3}{2}(V_{qs}i_{ds} - V_{ds}i_{qs})$$

(III.32)

$$\rightarrow Q_s = -\frac{3}{2}\omega_s\frac{L_m}{L_s}\varphi_s\left(i_{dr} - \frac{\varphi_s}{L_m}\right)$$

(III.33)

$$\rightarrow Q_s = K_Q \left(i_{dr} - \frac{\varphi_s}{L_m} \right)$$

(III.34)

We can then represent the closed-loop stator reactive power expression control as shown in the figure bellow:
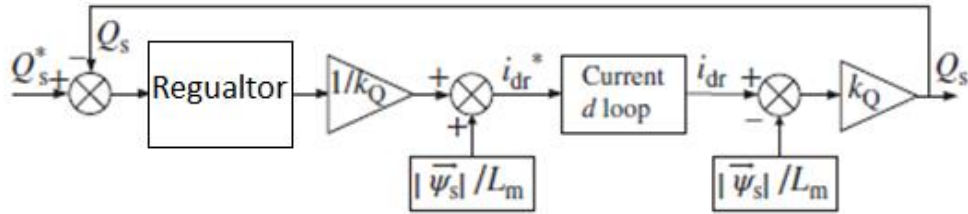
Figure III.8: closed-loop stator reactive power expression control

III.2.2.1.3.3 Synthesis of the Proportional regulator – integral

This part presents a proportional-integral controller (PI controller) that is a control loop feedback controller commonly used in the industry. PI controller calculates the error between a measured grander and a desired set point

III.2.2.1.3.3.1 Current control with PI regulators

The current control strategy described above is been studied in the case of PI regulators (integral proportional). The Figure bellow shows the closed loop system regulated by a PI regulator. [48]
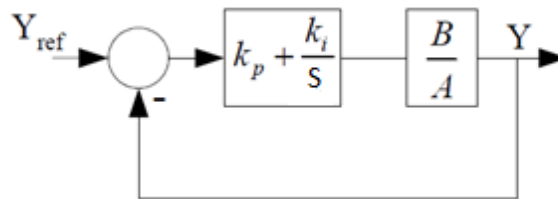
Figure III.9: Functional diagram of an PI regulator.

In our case the regulator's values of A and B are:

$$A = \sigma L_r s + R_r$$

(III.35)

$$B = 1$$

(III.36)

The opened loop transfer function is given as

$$FTBO = \left(k_p + \frac{k_i}{s}\right)\left(\frac{1}{\sigma L_r s + R_r}\right)$$

(III.37)

The closed loop transfer function is then expressed by

$$FTBF = \frac{k_p + \frac{k_i}{s}\left(\frac{1}{\sigma L_r s + R_r}\right)}{1 + \left(k_p + \frac{k_i}{s}\left(\frac{1}{\sigma L_r s + R_r}\right)\right)}$$

$$= \frac{sk_p + k_i}{\sigma L_r s^2 + \left(R_r + k_p\right)s + k_i}$$

(III.38)

The figure below shows an equivalent second-order system of closed-loop current control with PI regulators:
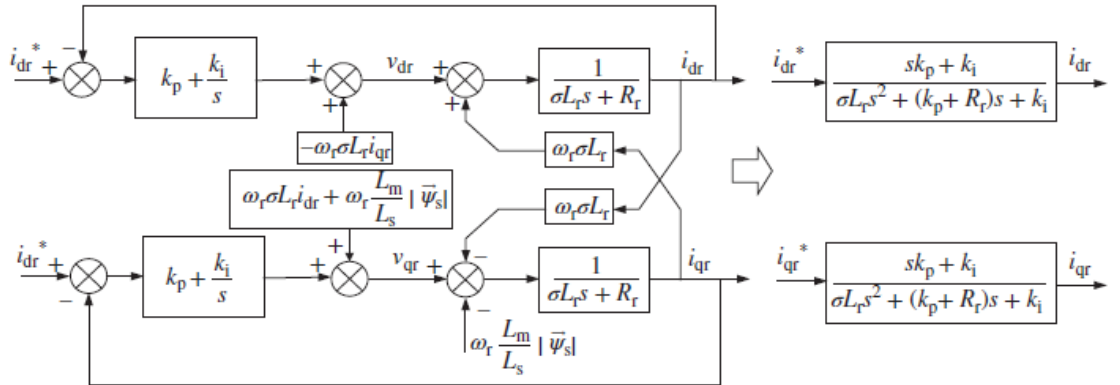
Figure III. 10: Equivalent second-order system of closed-loop current control with PI regulators

We have chosen to set the response time of the system to this value

$$\tau = \frac{\sigma L_r}{R_r} = 0.059$$

(III.39)

Which means that

$$\omega_n = \frac{100}{\tau}$$

(III.40)

Which leads us to the following results:

$$Kp_{id} = Kp_{iq} = 2\omega_n \sigma L_r - R_r$$

(III.41)

$$Ki_{id} = Ki_{iq} = \omega_n^2 \sigma L_r - R_r$$

(III.42)

III.2.2.1.3.3.2 Power and Speed Control Loops

The power and speed control strategy described above is been studied in the case of PI regulators (integral proportional). In this case the regulator's values of A and B are:

$$A = Js$$

(III.43)

$$B = P$$

(III.44)

The opened loop transfer function is given as

$$FTBO = \left(k_p + \frac{k_i}{s}\right)\left(\frac{P}{Js}\right)$$

(III.45)

The closed loop transfer function is then expressed as follows:

$$FTBF = \frac{k_p + \frac{k_i}{s}\left(\frac{P}{Js}\right)}{1 + \left(k_p + \frac{k_i}{s}\left(\frac{P}{Js}\right)\right)} = \frac{sk_p + k_i}{\frac{J}{P}s^2 + k_p s + k_i}$$

(III.46)

The figure below shows an equivalent second-order system of closed-loop speed control and a first order system of closed-loop reactive power control with PI regulators:
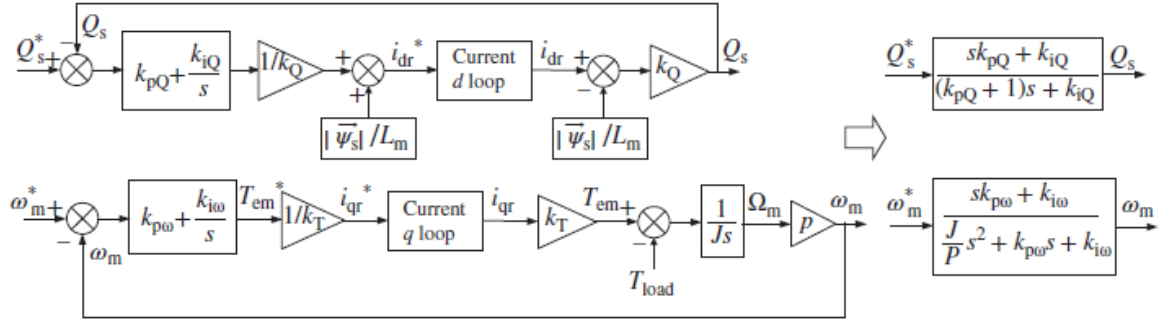
Figure III.11: Equivalent closed loop system of Q_s and ω_m loops control with PI regulators

We have chosen to set the response time of the system to this value

$$\tau = 0.05$$

(III.47)

Which means that

$$\omega_n = \frac{1}{\tau}$$

(III.48)

Which leads us to the following results:

$$Kp_N = \frac{2\omega_n J}{P}$$

(III.49)

$$Ki_N = \frac{\omega_n{}^2 J}{P}$$

(III.50)

III.2.2.1.3.4 RST CONTROL OF A DFIM

In this part we introduce the control of DFIM systems with an RST type regulator.

This regulation technique is carried out in order to improve the performance of the control. An RST type regulator is a polynomial regulator which presents itself as an interesting alternative to PID type regulators . It is also called regulator with two degrees of freedom, because in addition to choosing the poles in closed loop the zeros are also selected. The principle is based on the resolution of the Diophantine equation which leads to the identification of the polynomials R, S and T, thus making it possible to largely limit the

problems of the regulation and to achieve excellent performance of compensation with a very good robustness. [49]

The RST structure is based on decomposition according to three polynomials R, S and T, the degree of which is fixed according to the degree of the transfer, tracking and regulation functions in open loop. They are calculated from a pole placement strategy for stable or unstable systems. The regulation loop representing this regulator can be described by the figure bellow. [49]
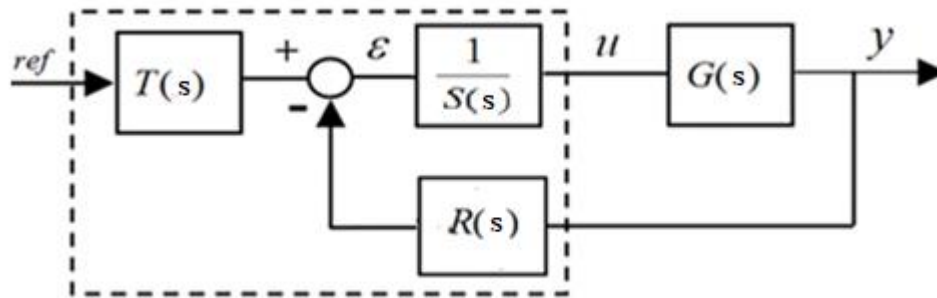
Figure III.12: Structure of the RST regulator.

G (s) in our case is the opened loop rotor current control function given as:

$$G(s) = \frac{B(s)}{A(s)} = \frac{1}{\sigma L_r \, s \, + \, R_r} \tag{III.51}$$

While A and B can be also written by:

B(s) = b0

$$\tag{III.52}$$

A(s) = a0+ a1*s

$$\tag{III.53}$$

The control signal is given by the following expression:

$$u(s) = \frac{T(s)}{S(s)} ref(s) - \frac{R(s)}{S(s)} y(s) \tag{III.54}$$

In general, the purpose of the command is to impose a desired closed loop transfer function between y (s) and ref (s).

$$y(s) = \frac{Bd(s)}{Ad(s)} ref(s) \tag{III.55}$$

In our case given as:

$$Bd(s) = B(s) = 1 \tag{III.56}$$

$$Ad(s) = 1 + s \tag{III.57}$$

While

$$Pa_d = exp(-pa * Te) \tag{III.58}$$

$$Te = 5.0000exp - 06 \tag{III.59}$$

from the above equations ,the following equality is obtained :

$$\frac{y(s)}{ref(s)} = \frac{B(s)T(s)}{A(s)S(s) + B(s)R(s)} \tag{III.60}$$

This gives as these equations:

$$A(s)S(s) + B(s)R(s) = Ad(s) \tag{III.61}$$

$$B(s)T(s) = Bd(s) \tag{III.62}$$

After multiplying and dividing the expression of the closed-loop transfer function by B (s), we obtain:

$$A(s)S(s) + B(s)R(s) = B(s)A_d(s)$$

(III.63)

And

$$T(s) = Bd(s)$$

(III.64)

To determine R (s) and S (s), we must solve the previous Diophantine equation given as:

$$A(s)S(s) + B(s)R(s) = B(s)Ad(s)$$

(III.65)

This can be written as:

$$A(s)S(s) + B(s)R(s) = C(s)$$

(III.66)

The polynomials R (s) and S (s) must verify the following conditions:

$$deg\ R(s) < degA(s) \rightarrow deg\ R(s) = degA(s) - 1$$

$$deg\ S(s) = degA(s) \rightarrow deg\ S(s) = degR(s) + 1$$

$$deg\ C(s) = deg\ S(s) + deg\ R(s)$$

One way to solve the Diophantine equation is to write the Diaphontine equation in a matrix form called the Sylvester matrix which is a square matrix defined as follows:

$$\begin{bmatrix} b_0 & a_1 & 0 \\ 0 & a_0 & a_1 \\ 0 & 0 & a_0 \end{bmatrix} \begin{bmatrix} r_0 \\ s_1 \\ s_0 \end{bmatrix} = \begin{bmatrix} c_1 \\ c_0 \\ 0 \end{bmatrix}$$

(III.67)

It is noted that the zeros of the system to be adjusted G (s) are stable.

The model to be pursued is generally very simple, low order, generally guaranteeing the desired characteristics in closed loop given as:

$$y(s) = \frac{Bd(s)}{Ad(s)} \qquad \text{(III.68)}$$

The arbitrary polynomial C (s) is specified by the pole placement method.

As following:

$$C(s) = c_2 s^2 + c_1 s = (Pa_d - a_1 + a_0)s^2 + a_1 s \qquad \text{(III.69)}$$

Which leads us to the following results:

$$R = 0.9972 \qquad \text{(III.70)}$$

$$S = 1s + 0 \qquad \text{(III.71)}$$

$$T = 1 \qquad \text{(III.72)}$$

III.2.2.1.3.5 The LMI-Based-LQR control

This part presents LQR control based on the LMI calculation method of grid-connected wind turbines with doubly-fed induction generators (DFIG) in which only the rotor-side converter control is considered.

The structure of the LQR based on LMI control system is shown in the figure bellow.
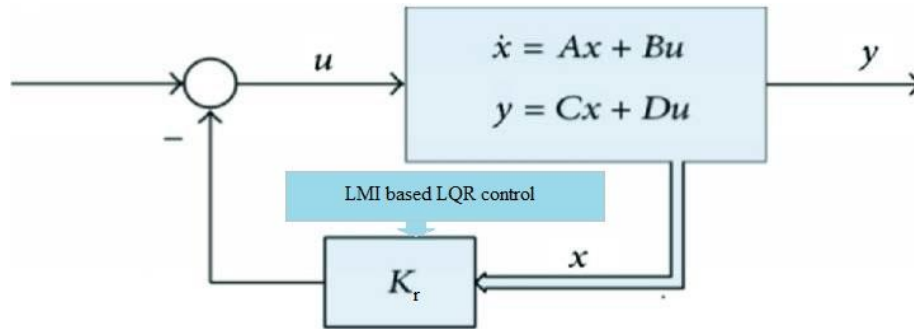
Figure III.13: the LMI based LQR control system

In our case the state space system's values of A, B, C and D are:

$A = -16.95$

$B = 64$

$C = 91.33$

$D = 0$

III.2.2.1.3.5.1 LQR control

The linear–quadratic regulator (LQR) is a highly used feedback controller which, controls and optimizes the feedback gains in order to ensure a stable closed-loop system and an optimum performance. [50]

the state-feedback law equality for a continuous time system is given as

$$u = -Kx$$

(III.73)

Where k is given by:

$$K = R^{-1}(B^T S + N^T).$$

(III.74)

The quadratic cost function minimized by the state-feedback law is written as

$$J(u) = \int_0^\infty (x^T Q x + u^T R u + 2x^T N u)\, dt$$

(III.75)

Where the system is defined as

$$\dot{x} = Ax + Bu$$

(III.76)

In addition to that the S solution is found by solving the continuous time algebraic Riccati equation given as:

$$A^T S + SA - (SB + N)R^{-1}(B^T S + N^T) + Q = 0$$

(III.77)

While

$$Q = Q - NR^{-1}N^T$$

(III.78)

And

$$A = A - BR^{-1}N^T$$

(III.79)

III.2.2.1.3.5.2 The LMI control

The Linear matrix inequalities (LMI) are defined as a set of matrix linear variables Used to solve a convex optimization problem with LMI constraints. The LMIs are used in several application such as robust stability, optimal LQG control, estimation, and many others, in our case we will be using it to calculate the gain Kr of the LQR controller. The LMI expression has the following form: [51]

$$F(x) = F_0 + x_1 F_1 + \cdots + x_n F_n = F_0 + \sum_{i=0}^{n} x_i F_i > 0$$

(III.80)

In the case of nonlinear matrix inequalities a change of variables can be used to transform these nonlinear inequalities into suitable LMI forms. As it is the case in the

State feedback LQR controller

The objective is to determine a matrix F and a positive definite matrix P that solve the following equation:

$$(A + BF)^T P + P(A + BF) < 0,$$

(III.81)

Or

$$A^T P + PA + F^T B^T P + PBF < 0$$

(III.82)

By multiplying either side of the above equation by $Q = P^{-1}$ we obtain:

$$QA^T + AQ + QF^T B^T + BFQ < 0.$$

(III.83)

In order to do the linearization the above equation, we define a second new variable $L = FQ$ which gives us

$$QA^T + AQ + L^T B^T + BL < 0.$$

(III.84)

By solving this LMI, the F and P matrix can be given from the following equation

$$F = LQ^{-1}$$

(III.85)

$$P = Q^{-1}$$

(III.86)

. In our case and after all calculation we obtained the following results:

$$Q = \begin{bmatrix} 1.0e + 07 & * 1.5408 \\ 0 & \end{bmatrix}$$

(III.87)

$$P = 1.0e + 08 * [0.0206 \quad 2.0738]$$

(III.88)

$$R = 4.4348e + 08$$

$$(\text{III.89})$$

The LQR control gain can be calculated as follows:

$$K_r = B' * P * inv(R)$$

$$(\text{III.90})$$

This leads us to the following result:

$$K_r = 0.2969$$

$$(\text{III.91})$$

III.2.2.1.4 Grid side converter control

This part presents a PI controller of a Grid side converter that is defined as an IGBT- based three-phase two-level voltage source converter which operates through a controlled pulse width modulation in the aim of maintaining a constant DC link voltage [52]

The dynamic model of the grid side converter in dq-reference frame is written as:

$$L_g \frac{di_{dg}}{dt} = V_{dg} - R_g i_{dg} - V_{dc} + \omega_g L_g V_{qg}$$

$$(\text{III.92})$$

$$L_g \frac{di_{qg}}{dt} = V_{qg} - R_g i_{qg} - V_{dc} - \omega_g L_g i_{qg}$$

$$(\text{III.93})$$

The active and reactive power associated with the grid side converter in the dq-reference frame, are given as:

$$P_g = \frac{3}{2} \left(V_{dg} * i_{dg} + V_{qg} * i_{qg} \right)$$

$$(\text{III.94})$$

$$Q_g = \frac{3}{2} \left(V_{qg} * i_{dg} - V_{dg} * i_{qg} \right)$$

$$(\text{III.95})$$

To control the grid side converter we use vector control scheme. In which the rotating reference frame dq-axis will be rotated along the grid voltage which gives:

$$V_{dg} = V_g$$

(III.96)

$$V_{qg} = 0$$

(III.97)

The power equations become as follows:

$$P_g = \frac{3}{2}\left(V_{dg} * i_{dg}\right)$$

(III.98)

$$Q_g = -\frac{3}{2}\left(V_{dg} * i_{qg}\right)$$

(III.99)

The grid converter control controls the dq currents loops and the DC voltage loops as shown in the figure bellow:
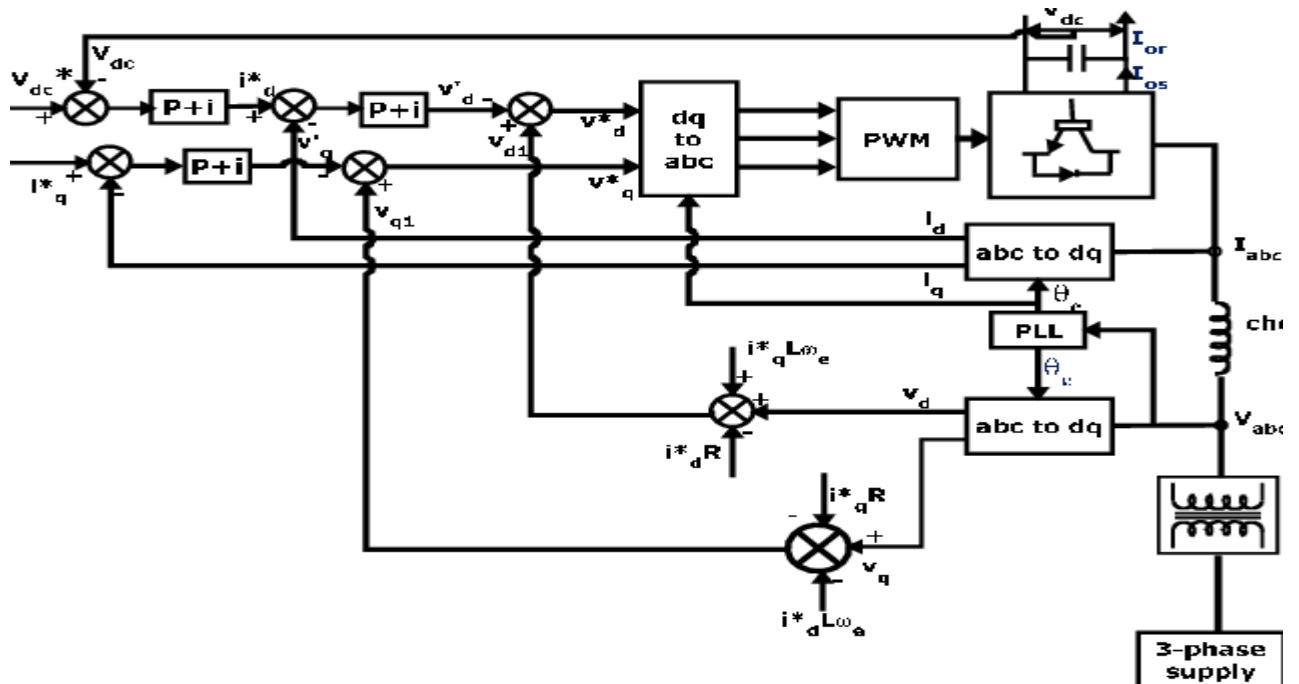
Figure III.14: Grid Converter Control Scheme

The grid dq voltage equations are given as :

$$V_{dg}(ref) = V_{dg} + R_r i_{dr} - (\omega - \omega_r)[i_{qr}L_r + i_{qs}L_m]$$

(III.100)

$$V_{qg}(ref) = V_{qg} + R_r i_{qr} + (\omega - \omega_r)[i_{dr}L_r + i_{ds}L_m]$$

(III.101)

Where V_{dg}, V_{qg} , Q and P are found from the current errors through standard PI controllers and the reference current i_{dr} can be found from the reference torque as follows:

$$i_{dr} = \frac{T_e L_s}{\varphi_s L_m}$$

(III.102)

With the crosses coupling terms between the d axis and q axis given as:

$$(\omega - \omega_r)[i_{qr}L_r + i_{qs}L_m]$$

(III.103)

$$(\omega - \omega_r)[i_{dr}L_r + i_{ds}L_m]$$

(III.104)

We can then represent the closed-loop DC voltage control as shown in the figure bellow:

Figure III.15: the closed-loop DC voltage control

For the DC voltage control we used pi tune matlab tool and we obtained the following results:

$kp\_v = -1000$

$ki\_v = -300000$

And the closed-loop reactive power control as shown in the figure bellow:

In our case we have chosen to set the response time of the system to this value

$$\tau = \frac{L_g}{R_g} = 20$$

(III.105)

Which means that

$$\omega_{ng} = 60 * 2 * pi = 376.9911$$

(III.106)

Which leads us to the following results:

$$Kp_{id} = Kp_{iq} = 2\omega_{ng}\sigma L_g - R_g = 56.8489$$

(III.107)

$$Ki_{id} = Ki_{iq} = \omega_g{}^2\sigma L_g = 56.8489$$

(III.108)

III.3 Solar system control

because of its characteristics; solar panel systems are controllable using power electronics and advanced control strategies such as P&O and Fuzzy logic based MPPT control, the control strategy is based on adjusting the duty ratio of the boost converter, the system to be controlled in this part includes a solar array, DC/DC converter, resistive load and a control unit as it is shown in the figure bellow:
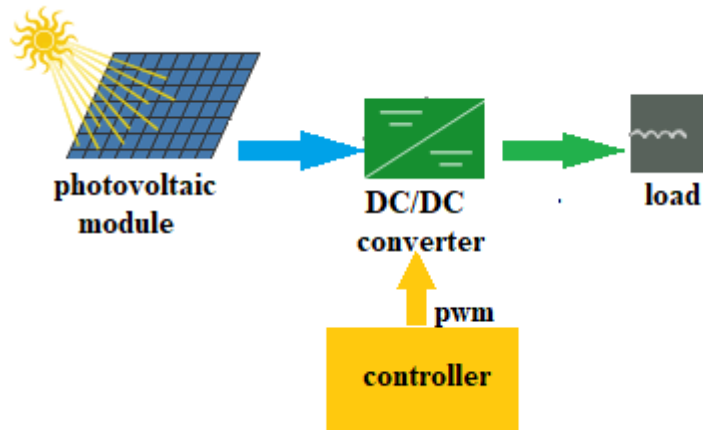
Figure III.17: the considered stand-alone PV system

III.3.1 MPPT in PV systems

As we have seen in chapter 2 the PV system is characterized by its V-P curve(shown in the figure bellow) in which the solar module operates with the maximum efficiency and produces the maximum power output at a maximum point that is called the maximum power point (MPP). A MPPT controller is designed to obtain an operating point close to this MPP where a tracking algorithms is used that checks the compares the output to the previous values and chooses the best power that PV module can produce to supply it to the load. [**54**]
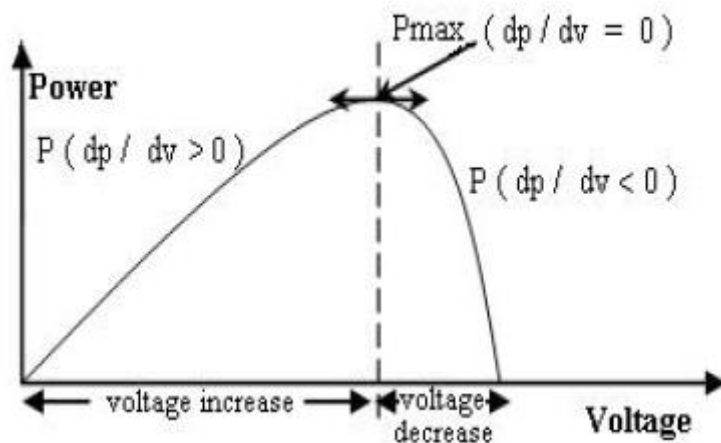
Figure III.18: Power-voltage characteristic of a PV module

III.3.1.1 Perturb-and-observe (p&O method)

Perturb-and-observe (P&O) method is one of the common MPPT control methods as its name indicates the principle of this controller is to provoke perturbation by increasing or decreasing the PWM duty cycle and observing the effect on the output PV power.

Where the present values of PV voltage V(k) and current I(k) are measured ,the present power P(k) is calculated then Compared with the previous power P(k-1). If the power increases, keep the next voltage change in the same direction as the previous change. Otherwise, change the voltage in the opposite direction as the previous one. this can be detailed as follows [54]:

- When $\frac{dv}{dp} > 0$, the voltage is increased, this is done through $D(k) = D(k-1) + C$

(C : incrementation step),

- When $\frac{dv}{dp} < 0$, the voltage is decreased through $D(k) = D(k-1) - C$

. The figure bellow shows the flow chart of the P&O method.
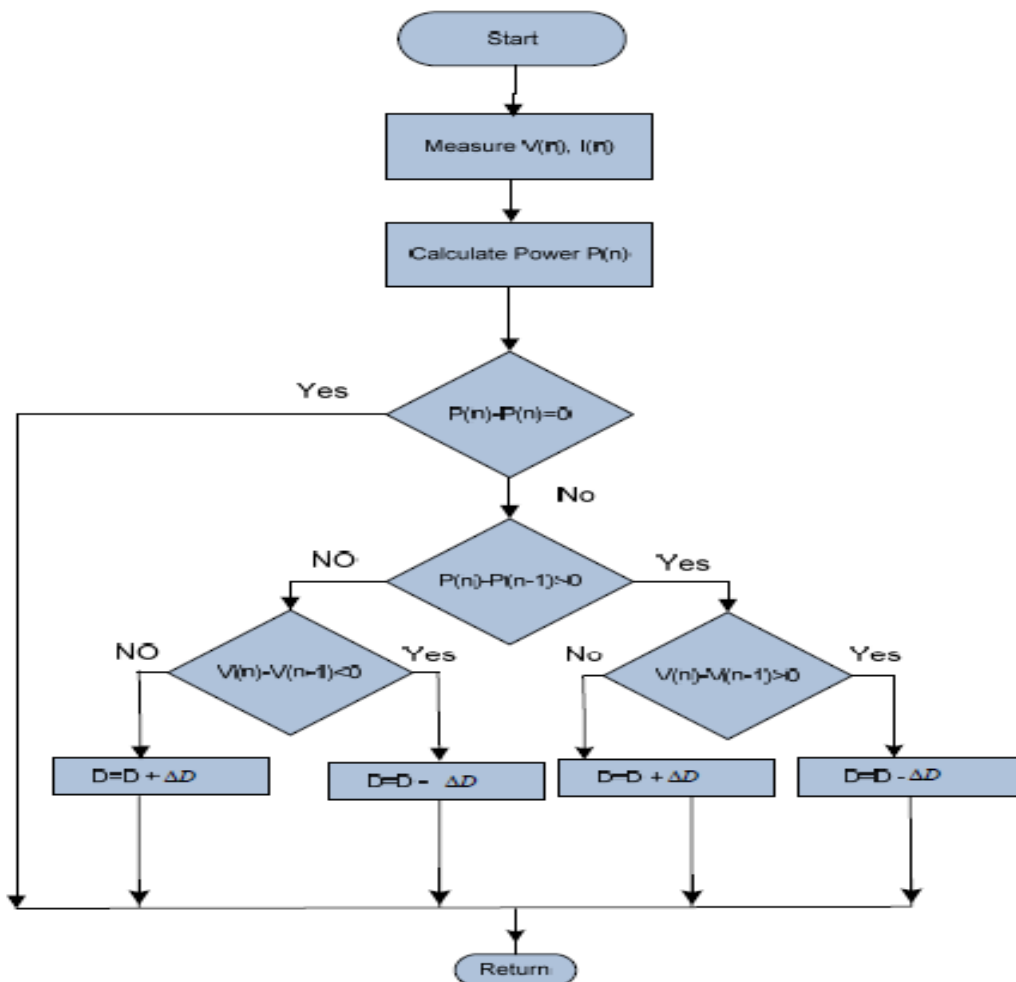
Figure III.19: the flow chart of the P&O method

III.3.1.2 MPPT by the fuzzy logic approach

A fuzzy control system is a non-linear control method based on fuzzy logic. It consists of the input variables that are in general mapped by sets of membership functions (fuzzification), a processing stage(Fuzzy inference), and an output stage which is smooth despite a wide range of input variations (defuzzication) nonmembership is smooth as it is shown in the figure bellow [55]:
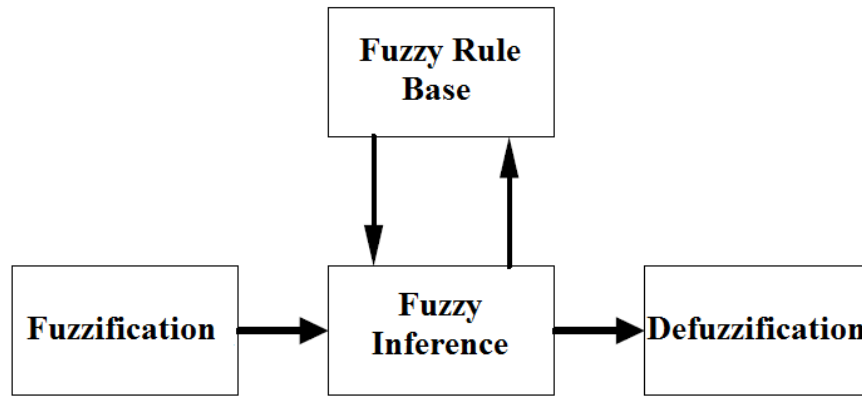
The output variable is the pulse width modulation (PWM) signal called D, which is transmitted to the boost DC/DC converter to drive the load. After the rules have been applied, the center of area as the defuzzication method is used to find the actual value of (D) as a crisp output [56].

The range of the power is and their linguistic variables are considered as negative big (NB), negative s mall (NS), zero (ZE), positive s mall (PS) and positive big (PB) where aschange of voltage range is and its linguistic variables are selected as negative big (NB), negative small (NS), zero (ZE), positive small (PS) and positive big (PB). The output variable is the PWM signal driver whose range is and its linguistic variables are chosen as negative big (NB), negative small (NS), zero (ZE), positive small (PS) and positive big (PB).

the fuzzy input variables chosen are the variations of the solar cell power output (ΔP_{PV}) ,where their linguistic variables are selected as negative big (NB), negative medium (NM), negative small (NS), zero (ZE), positive small (PS) , positive medium (PM) and positive big (PB). And variations of voltage (ΔV_{PV}),where their linguistic variables are selected as negative big (NB), negative small (NS), zero (ZE), positive small (PS) and positive big (PB).The output variable is the PWM signal where its linguistic variables are given as negative big (NB), negative medium (NM), negative

small (NS), zero (ZE), positive small (PS) , positive medium (PM) and positive big (PB).The table bellow shows the fuzzy rules of our algorithm.

$\Delta P(k) \big/ \Delta V(k)$	NB	NM	NS	ZE	PS	PM	PB
NB	PB	PB	PM	NM	NM	NB	NB
NS	PB	PM	PS	NS	NS	NM	NB
ZE	NB	NM	NS	ZE	PS	PM	PB
PS	NB	NM	NS	PS	PS	PM	PB
PB	NB	NB	NM	PM	PM	PB	PB

Figure III.21: Fuzzy rules

Figure below shows the membership of the inputs and outputs.
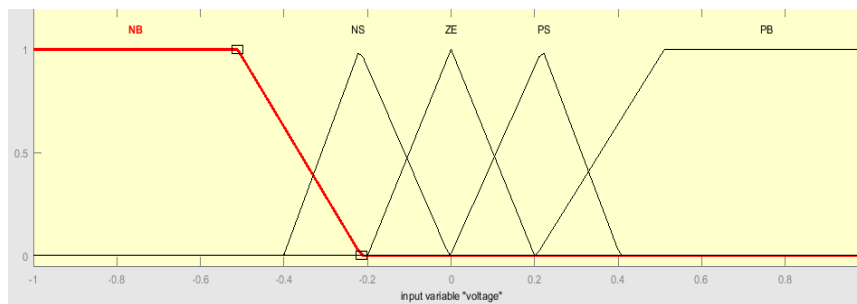
(a)
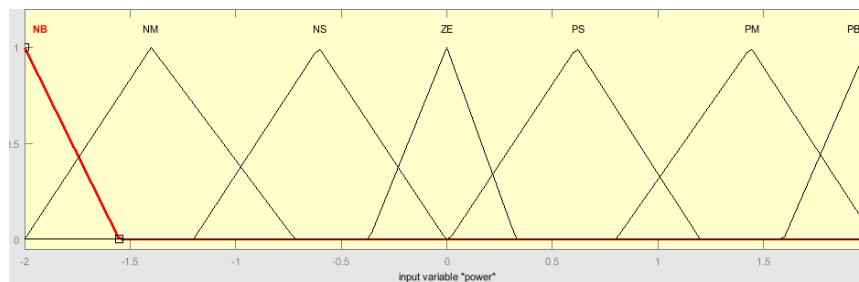
(b)
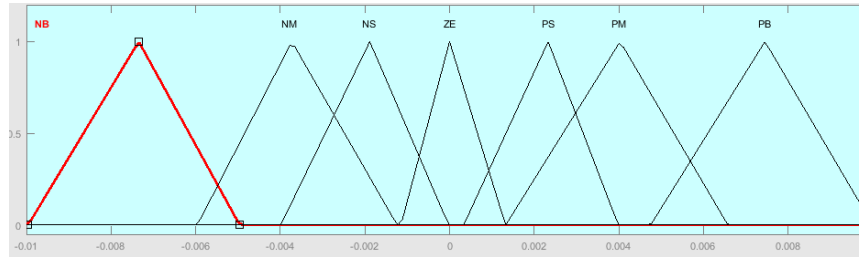
(c)

Figure III.22: Membership functions: (a) Membership function for changes of voltage; (b) Membership function for changes of power; (c) Membership function for increment of duty ratio command

III.4   Conclusion

This chapter has allowed us to develop the hybrid wind solar system controller .first the synthesis of three linear regulators for the control of the DFIM has been studied. A Proportional-Integral regulator which served as a reference for comparison, a polynomial RST regulator based on the theory of robust pole placement and an LQR regulator based on the LMI method. The purpose of these regulators is to control the exchange of active and reactive power between the stator of the machine and the network by modifying the amplitude and the frequency of the rotor voltages. We used the indirect control method where the rotor currents are measured and used to estimate the powers compared to the references.

Then two controllers are developed for the MPP tracking and minimizing the error between the operating power and the reference maximum power which is variable according to the load and of the weather conditions. An intelligent method of maximum power point tracking (MPPT) using fuzzy logic control for stand-alone was used then a conventional perturbation and observation (P&O) technique.

Chapter IV:

Fault tolerant control

IV Chapter IV: fault tolerant control

IV.1 Introduction

The performance of the system can be easily interrupted by possible faults and failures occurring because there is no fault-free system. Therefore, looking for fault-tolerant controller designs with early fault detection, isolation and successful controller reconfiguration would be very beneficial the system control. This chapter provides a brief introduction of power system faults, fault tolerant control (FTC) and fault detection and isolation (FDI) and defined basic definitions and classifications concepts. Starting with some definitions and describing different types of faults and failures that can occur in actuators, sensors or transmission line in wind system, and in the boost converter for the solar system.

IV.2 FAULT-TOLERANT CONTROL

In this part we will be seeing a brief review of fault-tolerant concepts including basic definitions, classifications, causes and consequences. The main objective of the FAULT-TOLERANT CONTROL is to maintain the control aiming even when an occasional fault occurs. the FAULT-TOLERANT CONTROL are essentials and necessary in any system regulation because there is no fault-free system and all types of dynamic systems can be undergone to various faults which could be caused by actuators, sensor or component failures. A fault tolerant control system scheme is shown in the figure bellow
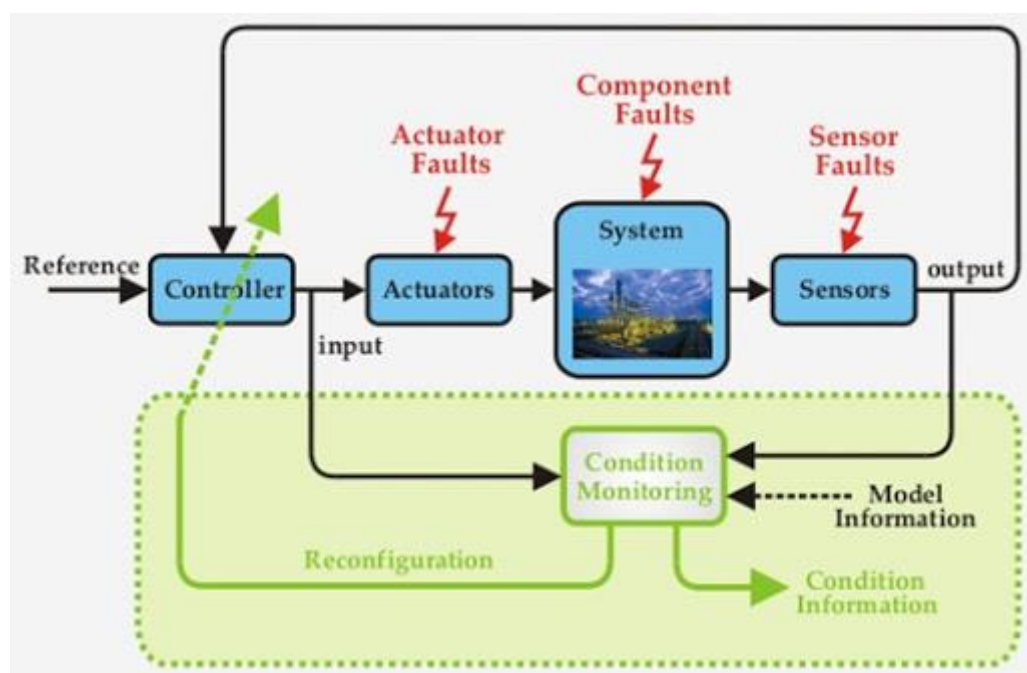
Figure IV.1: Fault tolerant control system scheme

IV.3 Types of Faults in Electrical Power Systems

Electrical power system faults occur because of the failure of the circuit equipment, insulation and conducting path which results short circuit and open circuit of conductors. The electrical fault conditions can be classified into open and short circuit faults which can be symmetrical or unsymmetrical faults. [57]

IV.3.1 Symmetrical faults

Symmetrical short circuit faults also called as balanced fault are defined as the fault that occurs in symmetrical fault currents. Where all the three-phase faults are short circuited with or without involving the ground .These faults rarely occur in practice in the range of 2 to 5% of the total system faults. But they can cause high damage to the equipments but the system remains in balanced condition.

IV.3.2 unsymmetrical faults

Unsymmetrical short circuit faults also called unbalanced faults defined as the fault that occurs in unsymmetrical fault currents in the system. Where only one or two of the three phases get short-circuited with or without involving the ground .it is necessary to analyze these kind of faults in order to determine the size of a circuit breaker for largest short circuit current. In comparaison to symmetrical faults, unsymmetrical faults are more difficult to analyze [57]

IV.3.3 Short Circuit Faults

short circuit fault is defined as an unusual connection of very low impedance between two points of different potential that happens either between two phases of wires or between a phase of wire and ground. The bigger short circuit is, the more heat is produced and burns are caused. It can also cause failure of one or more components of the circuit for instance generators, Transformers, converters others that operate at given voltage level. [58]

IV.3.3.1 Causes OF SHORT CIRCUITS

Short circuit faults can occur either because of breakdown of transmission lines or equipment, aging of insulation, deterioration of insulation in generator, transformer and other electrical equipments, improper installations and inadequate design, which can be classified as Internal effects .or overloading of equipments, insulation failure due to lighting surges and mechanical damage by public, which can be classified as external effects [59].

IV.3.3.2 Effects OF SHORT CIRCUITS

- It can lead to fire and explosion
- It can lead to overheat equipments

- It can lead to the restriction of the power flow
- It also present a great risk to human life and the economy.As was the case on 28 September 2016 where almost the entire state of South Australia suffered a widespread outage that plunged 1.7 million people into darkness for several days. Or on 4 January 2018, a short circuit caused by faulty wiring triggered an arc flash and ignited a fire that gutted a shopping mall in the southern province of Davao in the Philippines, killing 38 people.

In order to keep the grid safe and operating a short circuit fault analysis must be provided in which the amount of short circuit current from a system in calculated, then compared with the interrupting rate of the devices that protect sections of the grid. [60]

IV.3.4   Open circuit:

Open circuit fault also called as series faults is defined as a break or interruption in the current flow path in a circuit.

It occurs because of the failure of one or more conductors, cables , lines, or circuit breaking .it can also occurs because of the fuse or conductor melting in one or more phases. [61]

IV.3.4.1 Causes of the Open Circuit Faults

- Broken conductor that occurs when one or more phases of conductor break. [62]
- Malfunctioning of circuit breaker or isolators in one or more phases. [62]
- unbalanced current flows [62]

IV.3.4.2 Effects of the Open Circuit Faults

single and two phase open conditions can produce the unbalance of the power system voltages and currents that causes great damage to the equipments, which can interrupt the operation of the system, that could become a danger to the persons, animals and environment .Although open circuit faults can be tolerated for longer periods they needs be removed as soon as possible to avoid big damage. [62]

IV.3.5   Transmission Line fault

A transmission line is the most important part of power. Therefore it is necessary to protect transmission lines, that are defined as a system of conductors that transfers electrical signals from one place to another . transmission line can be expose for failure. Some of

which, are because of short circuit and open circuit faults. This can happen in one phase, two or three phases.The figure bellow shows the single transmission line fault diagram. [63]
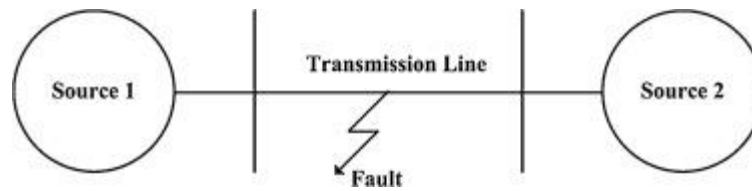
Figure IV. 2: transmission line fault

IV.3.6   BOOST CONVERTER FAULT

The boost converters are defined as an electronic device that increase and boost the input voltage.

For an optimum performance converters must have zero lossless .But that is impossible, boost converters can be expose for failure. Some of which, are because of short circuit and open circuit faults. This can happen in the switch, diode, inductor, capacitor or load.

IV.3.7   Different Type of Faults

Fault tolerance as it was defined earlier is the continuous operation of the system even if its components fail. The three basic notions for fail are fault, failure, and error where [65]:

IV.3.7.1 Failure

It is defined as an irrecoverable event, where the system is unable to do the service required. Note that a failure in a sub-system can be considered as a fault in the global system. Failures are classified by their domain as failures on values and/or timing failures; by their perception by the user; and by their consequences on the environment.

IV.3.7.2 Fault

it is defined as a recoverable event, where a component of the system gets defected which leads to a deviation of parameters from the nominal situation. Faults could be latent then effective then cause failure. In a general aspect there are three different types of faults as shown in Figure bellow.
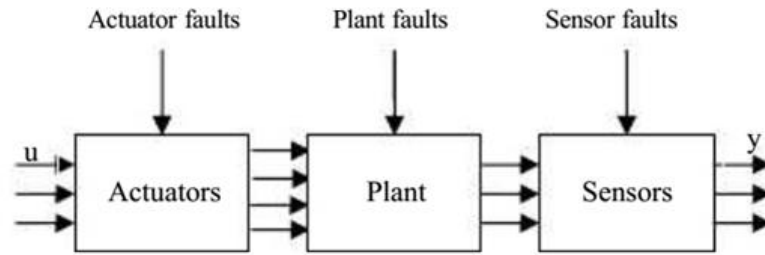
IV.3.7.2.1 Sensor faults

They are defined as substantial faults that occur on sensor readings, but don't impact the system properties.

IV.3.7.2.2 Actuator faults

They are substantial faults that occur on actuator, but don't impact the system properties. It only affects the controller performance.

IV.3.7.2.3 Plant (system) faults

They are substantial faults that occur on the system, which impact its properties.

Faults can be also classified by their nature as: accidental or intentional. By their origin as: physical, human, internal, external, conception, operational. And by their persistence as: transient or permanent.

IV.3.7.3 Error

Is an   action that shows when a fault occurs in order to treat errors. redundancy is necessary to be used in which two main forms exist physical and analytical redundancies.

IV.3.7.3.1 Physical redundancy:

Also known as hardware redundancy is defined as a technique that consists on disposing in parallel of identical subsystems or components to diminish the probability of their overall failure. Redundant actuators will allow continuing to act on a process while redundant sensors will allow detecting the failure of one of them and adopting the correct signal. [43]

IV.3.7.3.2 Analytical redundancy:

Also known as software redundancy is defined as the use of a mathematical model of the controlled system to displays analytical relationships between different physical parameters. It is mainly used for fault detection and identification. A software system is

considered redundant when it performs the same functionality through the execution of different elements. [*43*]

IV.3.8 Structure of Fault Tolerant Control

Fault Tolerant Control system consists of fault detection and identification module, a reconfigurable control module designed to activate fault free redundant components and a flight control law reconfiguration module to adapt the control law to the new control situation, as shown in the figure bellow. [43]
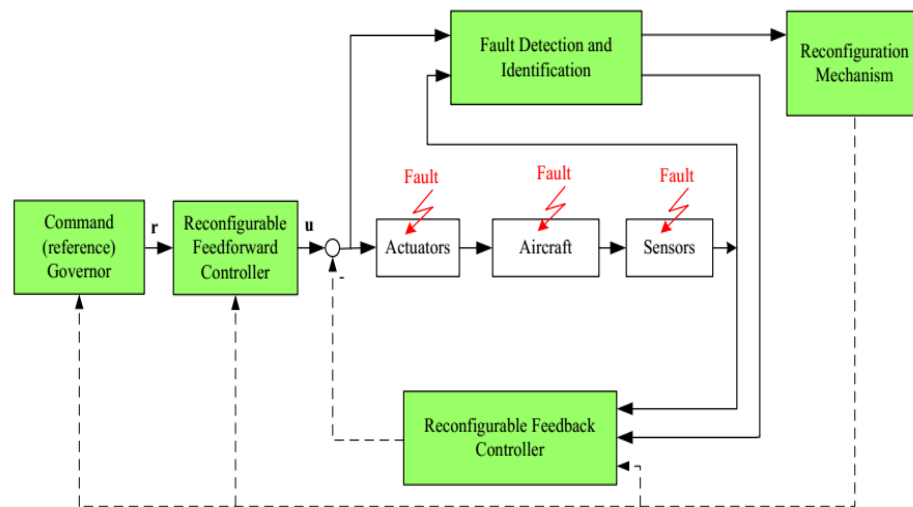
Figure IV.4: Structure of Fault Tolerant Control

IV.3.9 Fault Detection and Identification

Fault Detection and Identification is defined as detecting the fault and allowing the activation of automatic protections and reconfiguration mechanisms resulting in fault tolerance in the objective of keeping the system safe. It is composed of three main activities: [*43*]

IV.3.9.1 Detection

A fault is detected in the system when a nominal model of the fault free system exists, a fault will be characterized by comparing the nominal system with the actual system.

IV.3.9.2 Location

A fault is located in the system when the origin of the fault is traced. In general an original fault may generate a sequence of failures in a system and these cascading failures may mask their real cause.

IV.3.9.3 Identification

A fault is identified ed in the system when the time of the fault occurring, the duration and the amplitude is determined

IV.3.10 Fault tolerant performance

The main technical performance criteria for fault detection and identification are detectability , insolability, sensibility and robustness.

IV.3.10.1 The detectability

It is defined as the ability to detect the presence of a failure in the process. It is closely related to the notion of fault indicators (residuals).

IV.3.10.2 The isolability

It is defined as the ability to directly trace back the origin of the fault.The degree of fault isolation is related to the structure of the generated residuals and to the detection technique.

IV.3.10.3 The sensitivity

It is defined as the ability to detect faults of certain amplitude. It depends not only on the structure of the residuals but also of the relationship between the measuring noise and the fault.

IV.3.10.4 The robustness

It is defined as the ability to detect faults regardless of modeling errors. It relies on analytical redundancy which allows probabilistic tests to decide about the presence of a fault or not.

IV.3.11 Building in Fault Tolerance

Building in Fault Tolerance have the meaning of creating fault tolerance that keeps the system going when a fault occurs and eliminate as possible the failure of the system.

IV.3.11.1 Redundancy

The redundancy is a concept of equipping the system with extra components which are redundant in the aim of not being required to power the system when one of the primary components is functioning abnormally.

Unfortunately in practice this is usually too expensive. For that reason only the most important component of the system and the less expensive one will be made redundant.

IV.3.11.2 Diversity

The diversity is the concept of getting an electricity supply from another source entirely – most likely a backup electricity generator which kicks in automatically in case of a main power failure. it is used when it is not be possible to provide redundancy .note that the

diverse option may not be as efficient as the primary option, which means it can be used temporary until the primary option can be restored.

IV.3.11.3Replication

Replication is the concept of running multiple identical versions of a system or subsystem, and checking that their functioning always results in identical results. If results differ then some procedure is called up to decide which system is faulty.

IV.3.12 Elements of Fault Tolerant Systems

Fault-tolerant systems use backup components that automatically take the place of failed components, ensuring no loss or break in the service. These include: [67]

IV.3.12.1Hardware systems

Hardware systems are defined as systems that are backed up by identical or equivalent systems. By eliminating single points of failure, hardware fault tolerance in the form of redundancy can make any component or system far safer and more reliable.

To provide fault tolerance, the fault tolerant computer system or fault tolerant data storage system may use various elements. This includes replication for the CPU, redundancy for the PSU and RAM, hard drives configured in some form of RAID array which involves both redundancy and replication, and diversity of power supply with the provision of a backup generator.

Fault tolerant networking may be provided by redundant network interface cards (NICs), and/or a variety of diverse networking options such as a wired LAN NIC and a wireless LAN adapter.

IV.3.12.2Software systems

Software systems are defined as systems that are backed up by other software instances. It can be designed to be fault tolerant so that it can continue to operate even when it encounters an error, exception, or invalid input as long as it has been designed to handle such errors rather than defaulting to reporting an error and halting.

In particular, networking protocols such as TCP/IP have been developed expressly to enable the creation of fault tolerant networks. TCP/IP can continue to function in an environment where individual network links or nodes may become unavailable unexpectedly. It can adapt to the varying conditions in order to get packets to their destinations via whatever routes are available whenever possible.

Software systems can also use replication to provide fault tolerance: a critically important database can be continuously replicated to another server, so that if the server hosting the primary database goes down then operations can instantly be redirected to the replica database.

Alternatively, some services, notably web servers, can be placed behind a load balancer so that multiple servers all provide the same service. If one server develops a fault then the load balancer simply sends all web requests to the other ones until the faulty one is repaired.

IV.3.12.3 Power sources

Power sources are defined as systems that are made fault tolerant using alternative sources. As mentioned earlier, many fault tolerant systems include multiple PSUs to provide redundancy in case of a PSU failure. And since it is usually not possible to obtain redundant main power supplies, most organizations rely in diversity in the form of power from an alternative source. This is typically a generator that starts up automatically in the event of a main power failure to ensure that hardware, storage, HVAC and other systems have the power they require. Redundant power sources can help avoid a system fault if alternative sources can take over automatically during power failures, ensuring no loss of service.

IV.3.13 Factors to Consider in Fault Tolerance
IV.3.13.1 Cost

Fault tolerance control systems are considered to be very costly, the reason why is that it requires multiple versions of the same components, extra equipment such as generators and the hardware parts.

IV.3.13.2 Quality Degradation

Due to the high cost of fault tolerance, lower cost and inferior quality redundant components are much used. This can lead to an increase in support and maintenance costs.

IV.3.13.3 Testing and Fault Detection Difficulties

Testing fault and detecting is not that easy, in fact it is considered to be hard to spot faults because it could be latent which doesn't lead to the failure of the system.That means that more resources is often required to test and monitor the health of a system built for fault tolerance. [68]

IV.3.14 Conclusion

This chapter has presented a brief introduction to the fields of the fault tolerant control. It has included basic definitions and classifications of terms mostly used in fault tolerant control such as faults and failures. This chapter also briefly discussed the possible types of faults and failures of the transmission line and the boost chopper that can occur in the hybrid wind solar systems, also redundancy and its importance to the fault tolerant control has been discussed.

Chapter V:

Simulation Results and Conclusion

V Chapter V: Simulation Results and Conclusion

V.1   Introduction

In order to obtain the closest possible results of the experimental device, simulations are used in this chapter using MATLAB/SIMULINK platform. First for the wind system part, a comparison of three regulators (PI, RST and LQR) is developed in terms of pursuit of trajectory, sensitivity to disturbances and robustness with respect to parameter variations, taking into consideration rotor side and grid side converter control. A series of tests are also carried out when the transmission line fault occurs on the wind turbine system.

Then for the solar system part, the fuzzy logic (FL) based MPPT controller is simulated and compared with the conventional perturbation and observation (P&O) based MPPT controller. A series of tests are also carried out when the open or short circuit fault occurs on the boost converter of the solar system.

V.2   Wind turbine system control

In this part a complete control model of a wind turbine system has been developed and implemented in MATLAB/SIMULINK platform. This model includes the mechanical control system part, consisting of pitch angle and mechanical torque controllers. And the electrical control system part, consisting of a DFIM rotor side controller and a grid side controller which are connected with each other via a back to back converter, an output low-pass filter (RC) to interface with the grid is also implanted. The performance of the model and its dynamic response has been then evaluated. Figure below shows the complete model implemented in SIMULINK. It is connected to a programmable voltage source that in our case represents the grid through a step-up transformer.

WIND SYSTEM CONTROL
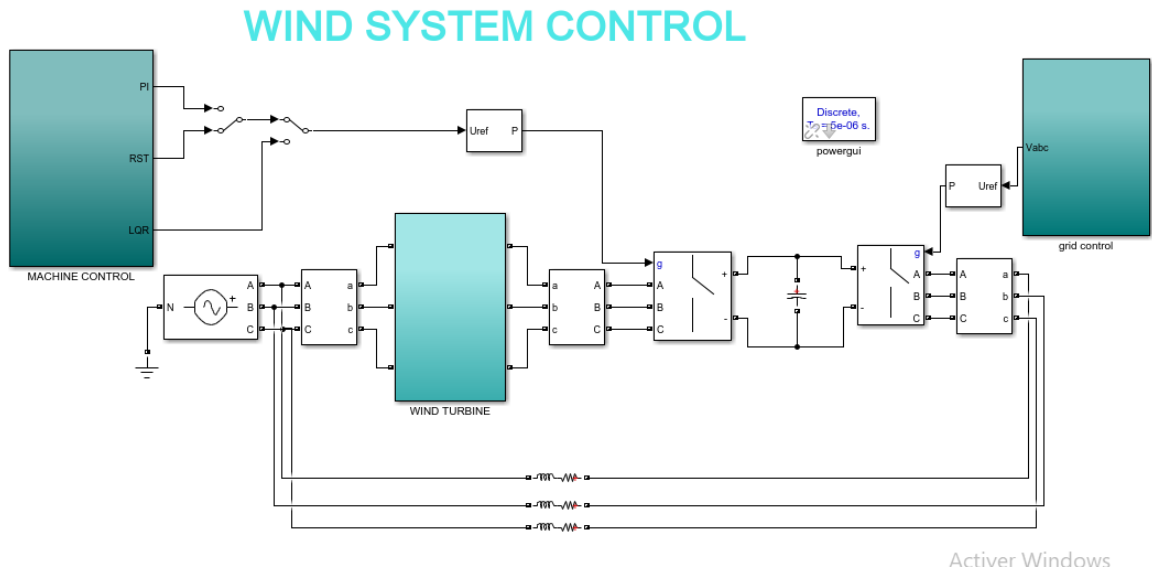
Figure V.1: SIMULINK complete control model of a wind turbine system

V.2.1 Mechanical torque control

The output of the turbine is the mechanical torque which it is applied to the generator to produce an electrical power .Thus the Simulink model used in this part is based on the steady-state power characteristics of the turbine. The three inputs are the generator speed, the pitch angle in degrees and the wind speed in m/s. The Simulink block of the turbine shown bellow is found in the Simscape library
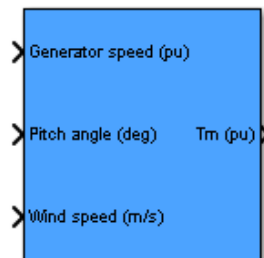
Figure V.57: Simscape Wind turbine block

By looking under the mask the model is illustrated in the following figure.
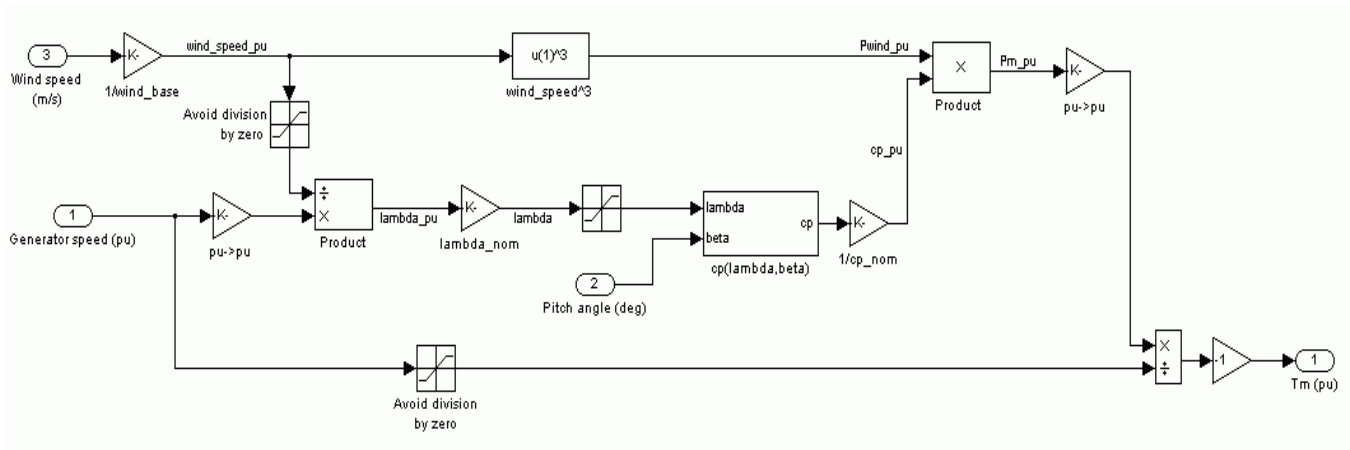
Figure V.3: Simulink control model of mechanical torque of the wind turbine

V.2.2   Pitch angle control

Adjusting the pitch angle of the blades provides an effective means of limiting turbine performance in strong wind speeds. The actuator model that consists of a mechanical and a hydraulic system describes the dynamic behavior between a pitch demand from the pitch controller and the measurement of a pitch angle $\square$.The dynamics of the blades are non-linear with saturation limits on both pitch angle and pitch rate. The error between the generator rotor speed and its set point is sent to the controller to produce a reference value for the pitch angle. Simulink model of the pitch angle control is shown bellow
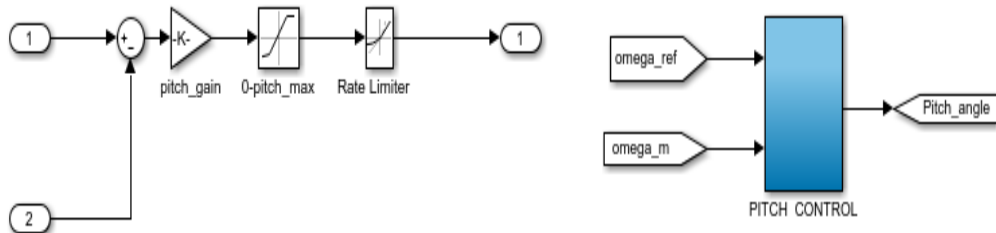
Figure V.4: Simulink model of the pitch angle control

V.2.3   DFIM control

The model of the DFIM control used in this part is designed to capture optimum power from the wind at its low speed through a rotor side and a grid side control. Firstly a vector speed and current control of the DFIG using PI, RST and LMI controllers. The results shown are obtained from simulation in Matlab/Simulink platform which shows the effectiveness of the strategy proposed.

V.2.3.1   Grid side control

The figure bellow shows the grid voltage oriented vector control simulation results. The DC link voltage used is around 900 Volts.
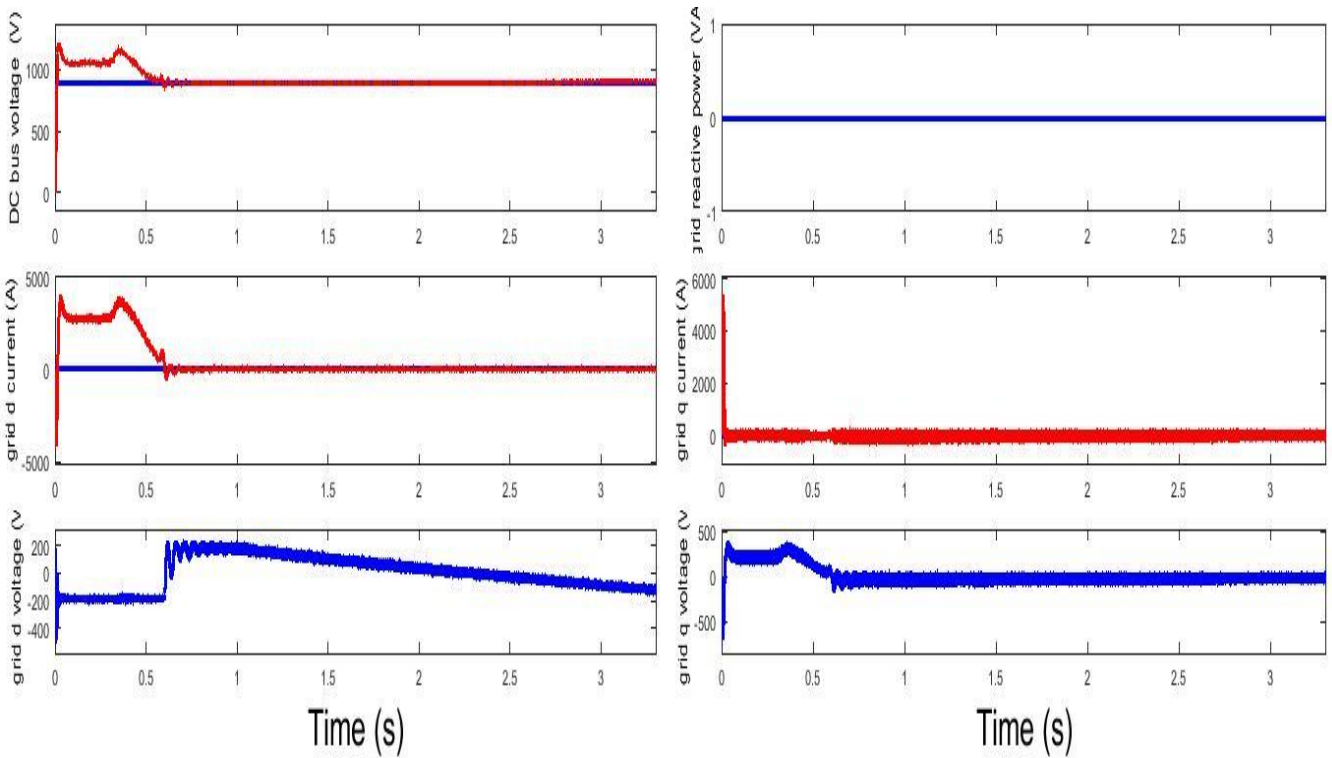
Figure V.5: Grid side control simulation results

The figures above shows the DC link voltage when implementing the grid voltage oriented vector control scheme. Here the by proper control of converter the oscillations are very low and measurement follows the set point.

V.2.3.2   Rotor side control

In this part we represented the closed-loop current and speed control model and simulation with three types of controllers: PI, RST and LMI.

V.2.3.2.1   Pi controller

The figure bellow shows the Pi vector control simulation results. Generator speed reference used is around 141.4269 (wm).
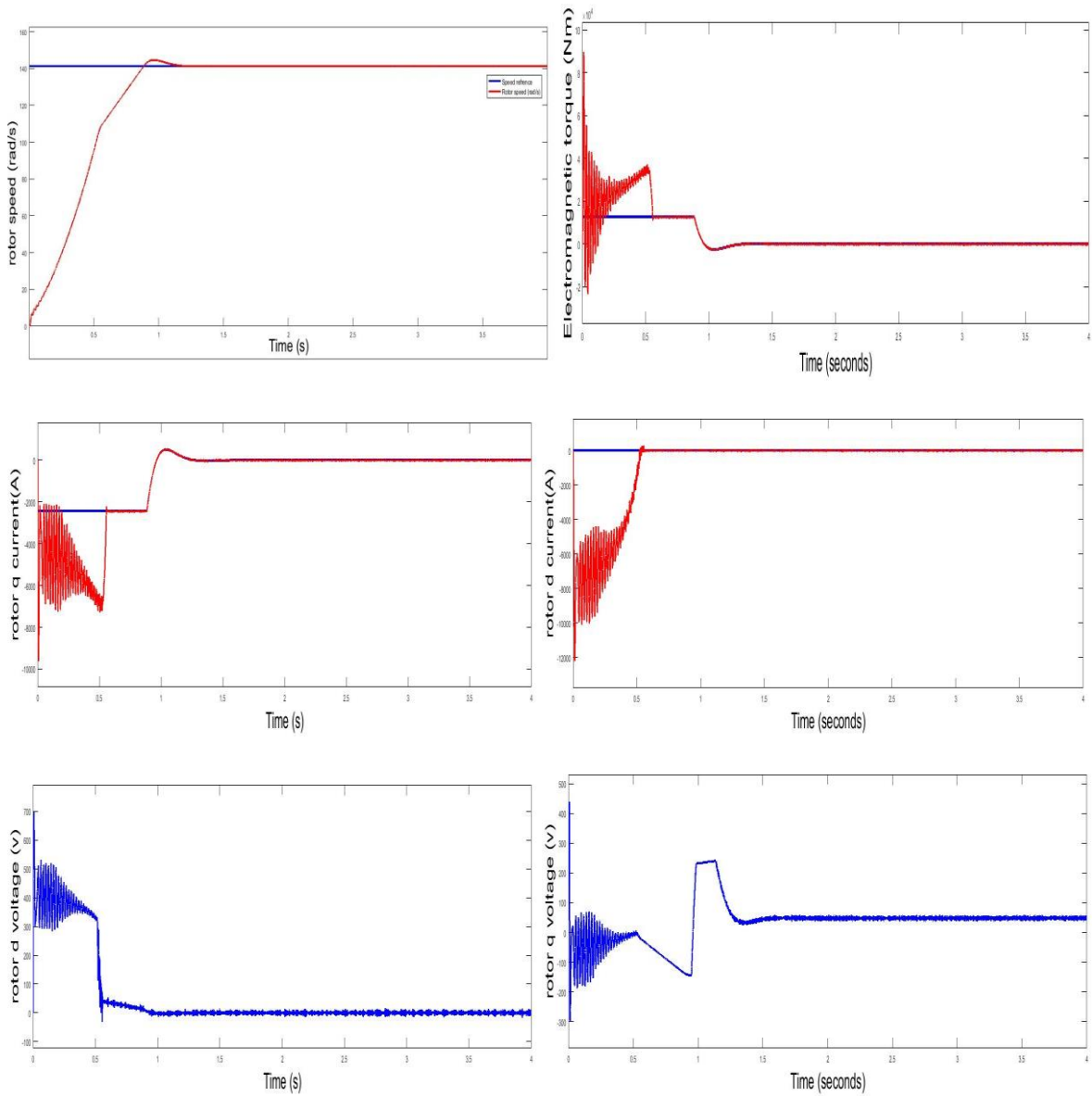
Figure V.6: Rotor side PI control simulation results

V.2.3.2.2   Rst controller

The figure bellow shows the RST vector control simulation results. Generator speed reference used is around 141.4269 (wm).
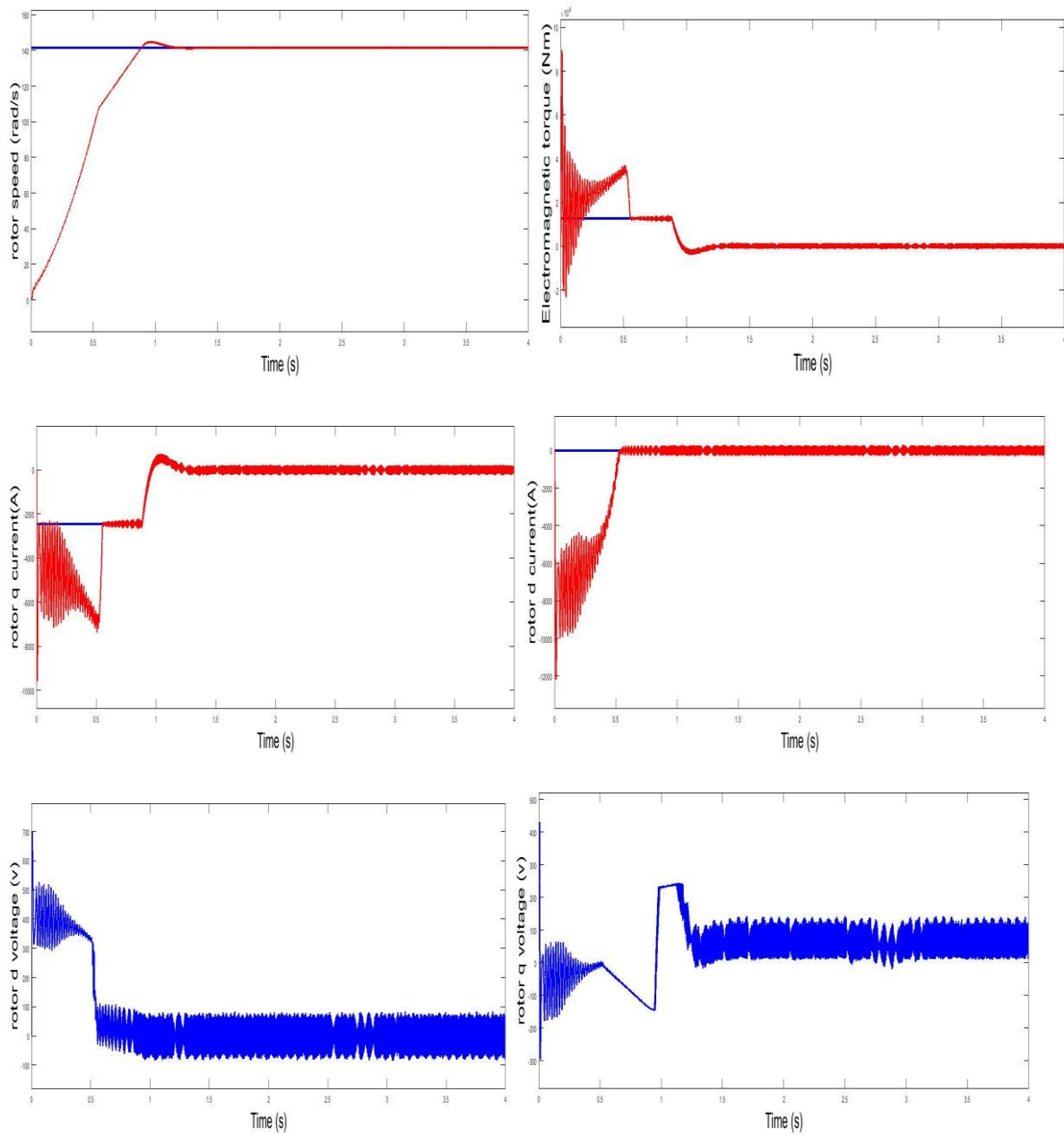
Figure V.7: Rotor side RST control simulation results

V.2.3.2.3 LMI based LQR controller

The figure bellow shows the LMI based LQR vector control simulation results. Generator speed reference used is around 141.4269 (wm).
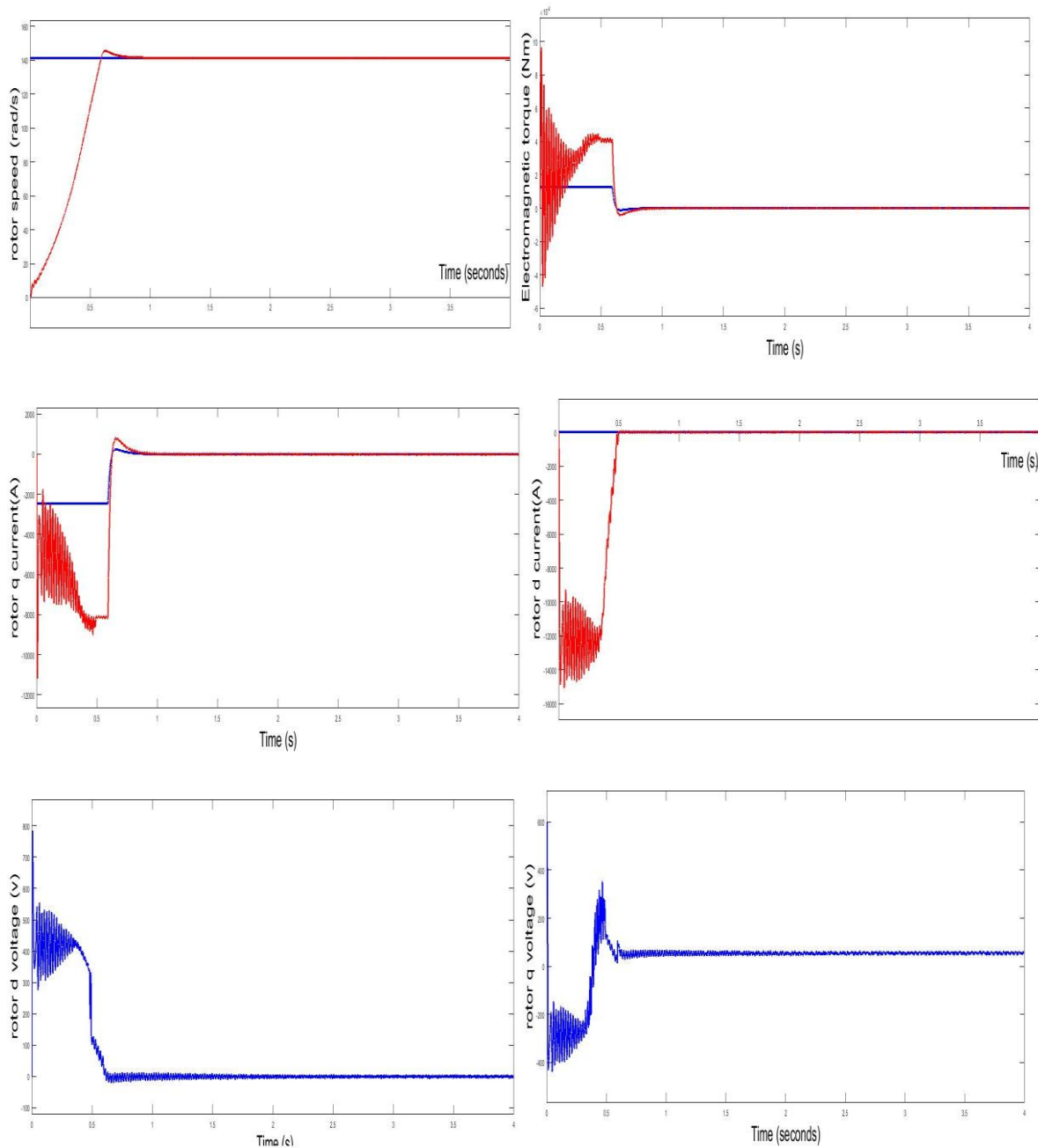
Figure V.8: Rotor side LQR control simulation results

V.2.3.2.4   Comparison

Figures above show the superiority and the good regularity of power signals of the LQR regulator which minimizes the amplitude of the oscillations. Note, however, that the RST and PI regulators are very sensitive to even small variations in the adjustment. This is why, in the context of this test, the performance of these regulators can be considered equivalent.

V.3   Solar system control

In this part a complete control model of a solar system has been developed and implemented in MATLAB/SIMULINK platform. This model includes a P&O and Fuzzy logic based MPPT control, the control strategy is based on adjusting the duty ratio of the boost converter, the system to be controlled in this part includes a solar array, DC/DC converter, resistive load and a control unit.
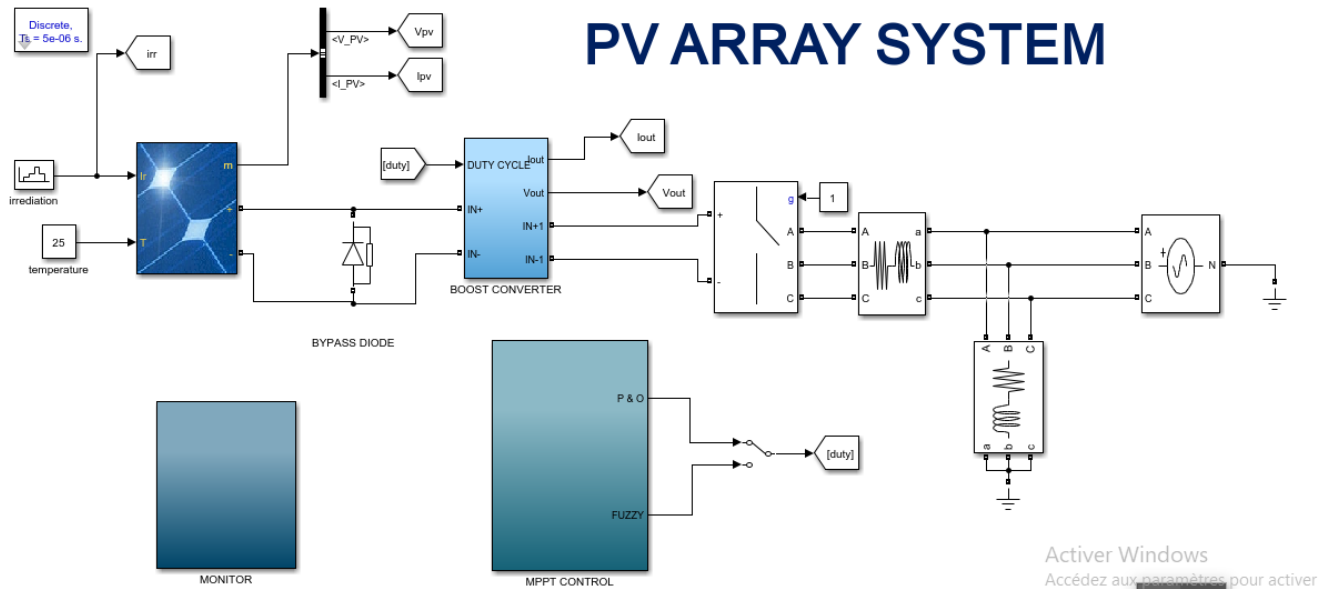
Figure V.9: SIMULINK complete control model of a solar system

V.3.1   P&O MPPT CONTROLLER

Figure bellow shows the simulation results of PV output power, voltage and current for the MPPT P&O control. This control tracks the maximum power point with a variable irradiation and a fixed temperature around 25 degrees.
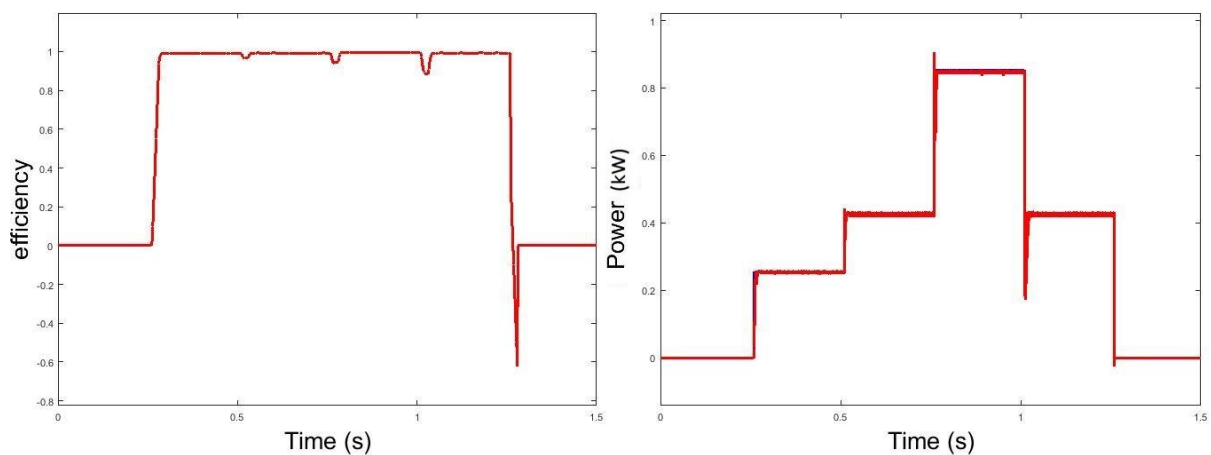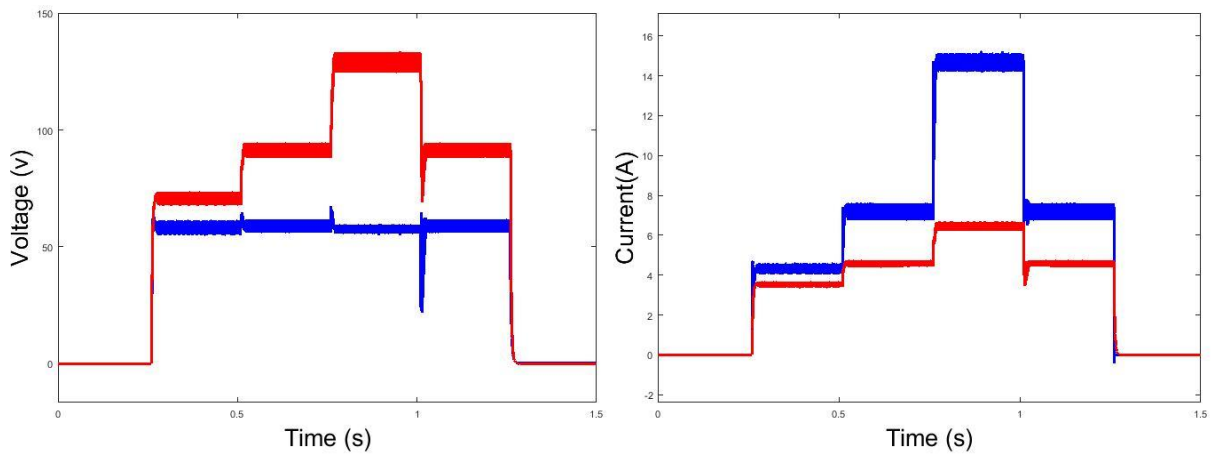
Figure V.10: the simulation results of PV output power P&O control

V.3.2   FUZZY LOGIC CONTROLLER

Figure bellow shows the simulation results of PV output power, voltage and current for the MPPT FUZZY logic control. This control tracks the maximum power point with a variable irradiation and a fixed temperature around 25 degrees.
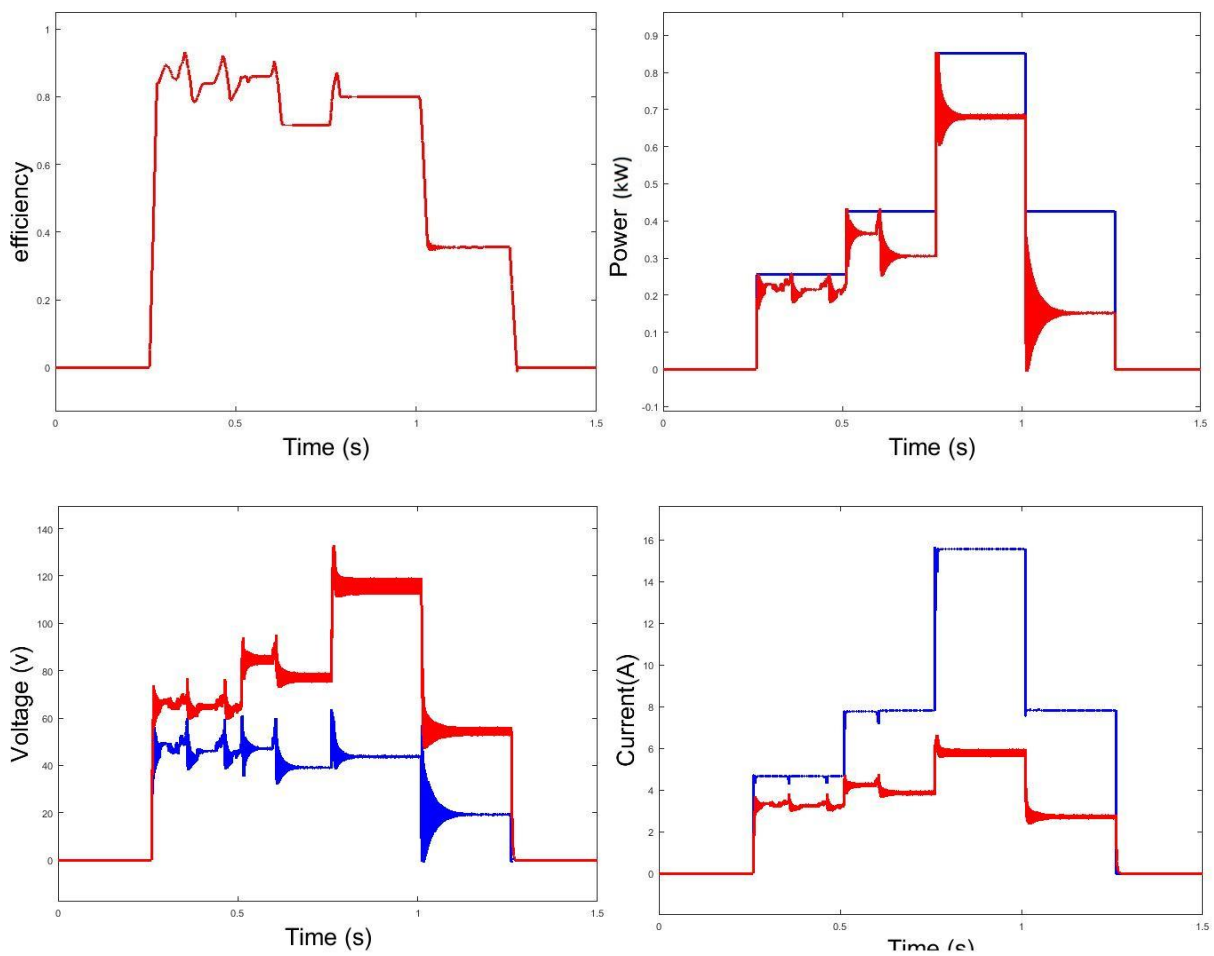
Figure V.11: the simulation results of PV output power FUUZY logic control

V.3.3   Comparison

Figures above show the simulation results of the PV generator output power, operating voltage, operating current, and the efficiency using a boost converter. By comparing Fuzzy Logic based MPPT and conventional P&O MPPT. It has been clearly noticed continues oscillation of operation point for the FL technique. Whereas the oscillation is not observed in P&O based MPPT technique, where signals of power, voltage, current, and efficiency remain almost constant

V.3.4   Fault tolerant control of wind system

This part presents the performance of the wind system model and its dynamic response in the occurring of a fault in the transmission line where the faulty phases are selected. Three selections are studied in this suction, one phase to the ground, two phases to the ground and three phases to the ground. Simulation results are shown for these faults next. All faults are applied between 1.5 to 2 sec in Mat-lab/Simulink and simulation runs for total of 4 sec.
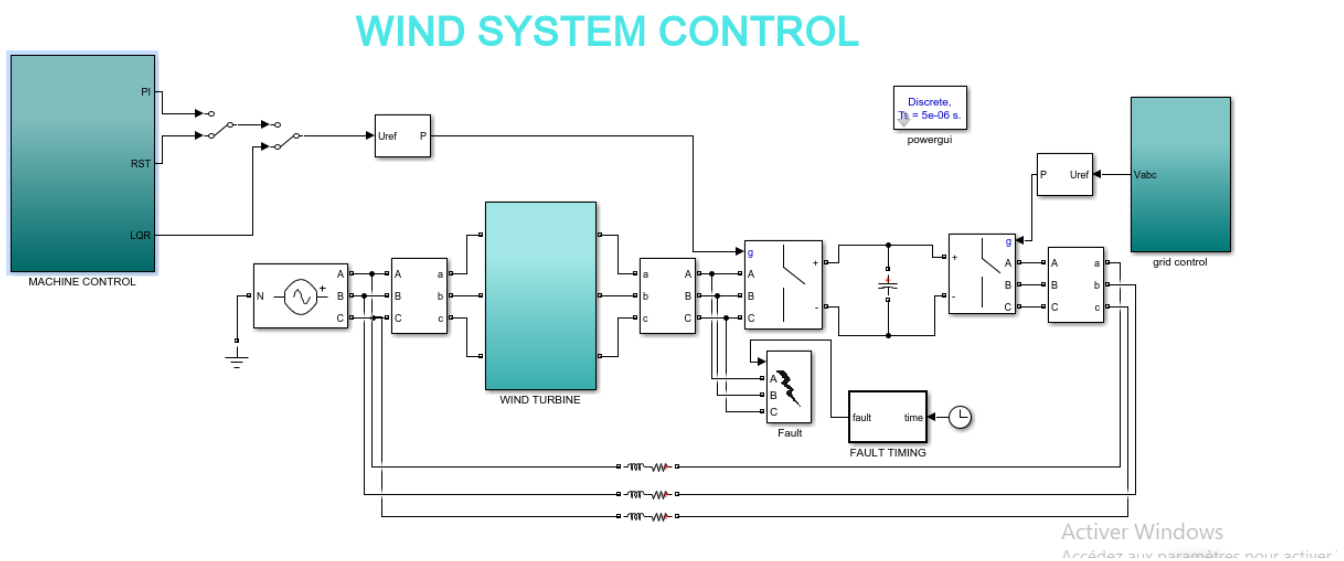
Figure V.12: the wind system model with a fault in the transmission line

V.3.4.1   Single Phase to Ground (L-G) Fault

The faulty phases of the transmission line block parameters, has been selected as phase A to the ground. With a fault resistance of 0.001Ohm,a ground resistance of 0.01Ohm, a snubber resistance of 1e6Ohm and an infinite snubber capacitance.

V.3.4.1.1   Pi controller

The figure bellow shows the Pi vector control simulation results with a one phase to the ground transmission line fault.
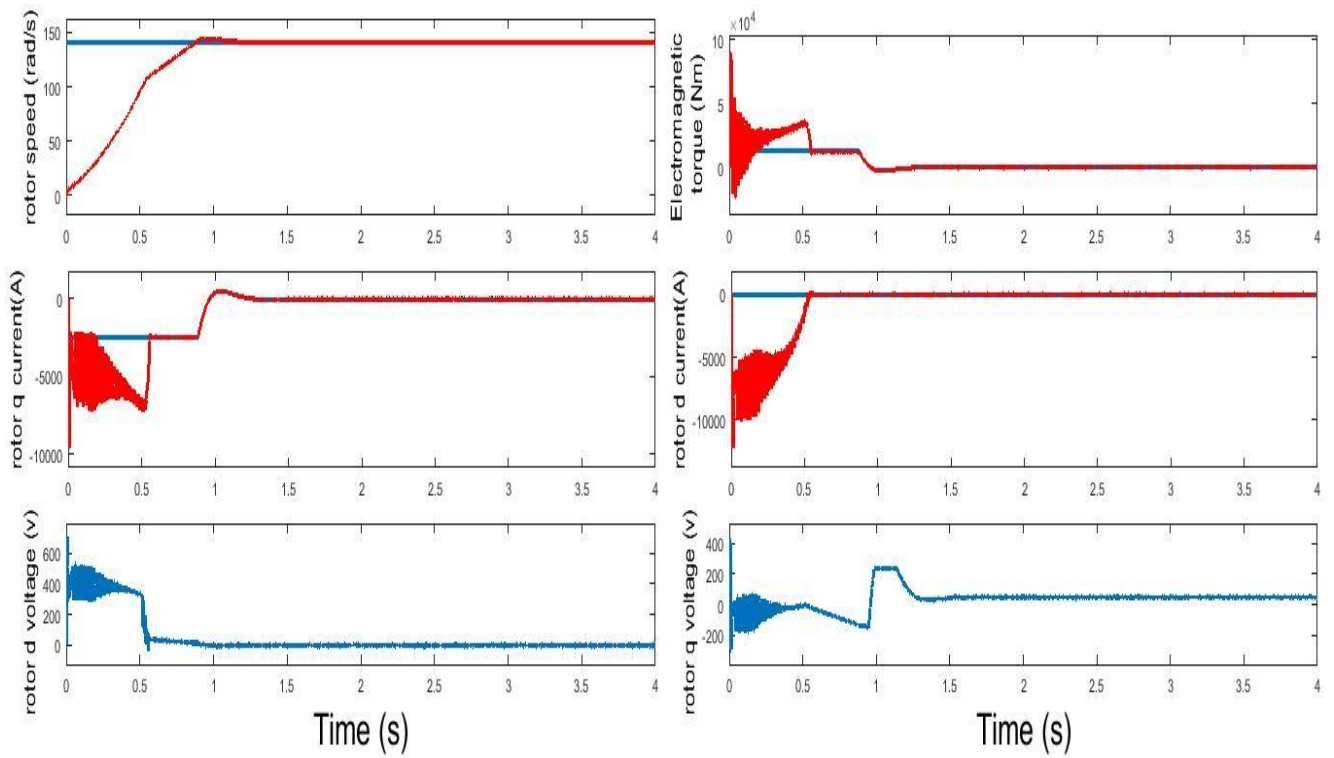
Figure V.13: the Pi vector control simulation results with a one phase to the ground transmission line fault

V.3.4.1.2   Rst controller

The figure bellow shows the RST vector control simulation results with a one phase to the ground transmission line fault.
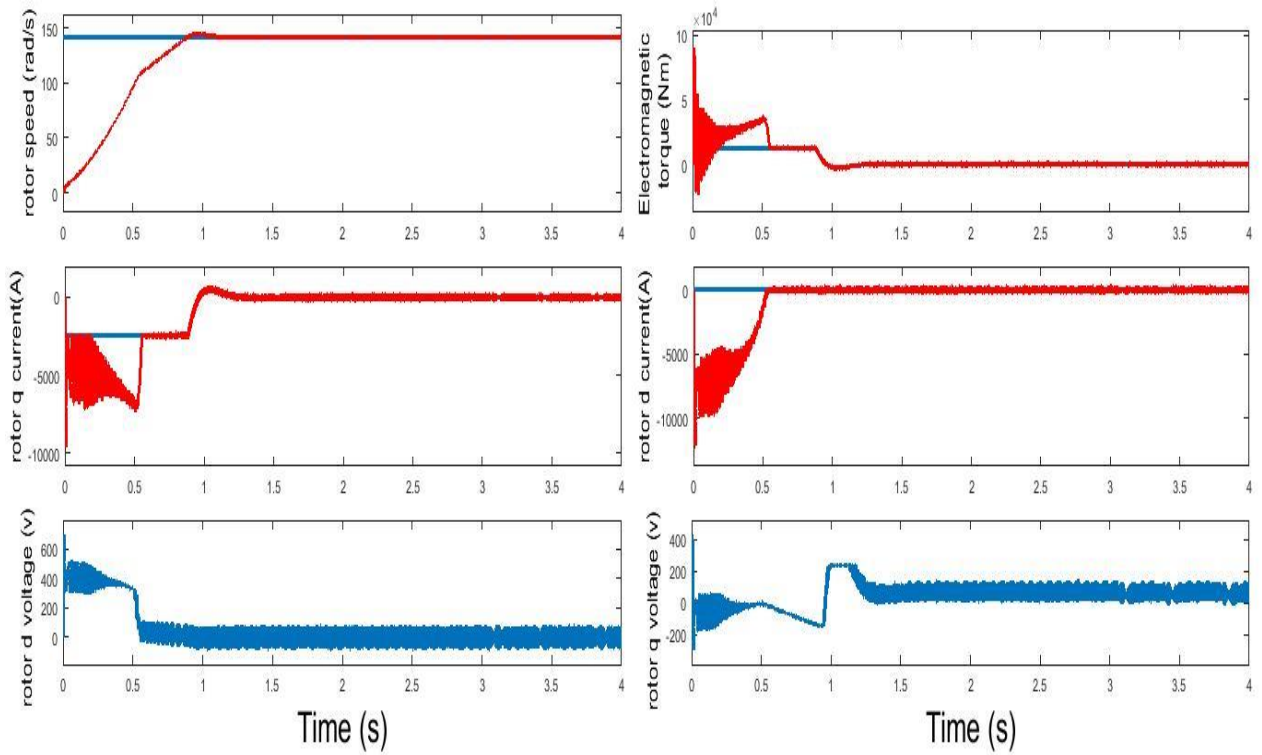
Figure V.14: the RST vector control simulation results with a one phase to the ground transmission line fault

V.3.4.1.3 Lmi based lqr controller

The figure bellow shows the LMI based LQR vector control simulation results with a one phase to the ground transmission line fault.
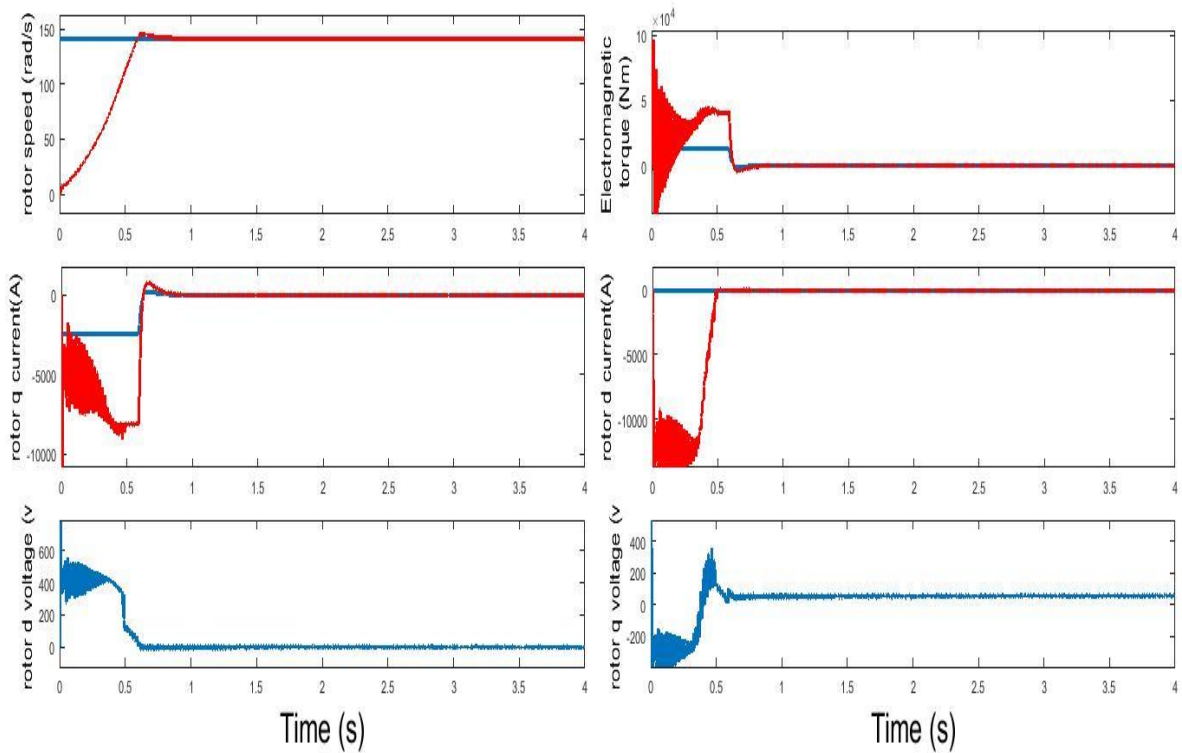
Figure V.15: the LMI based LQR vector control simulation results with a one phase to the ground transmission line fault.

V.3.4.1.4 Comparison

In comparison with the PI and RST controllers, figures above show the superiority and the good regularity of power signals of the LQR regulator in the case of one phase to the ground transmission line fault which is barely noticeable.

V.3.4.2 Two Phases to Ground (L-L-G) Fault

The faulty phases of the transmission line block parameters, has been selected as phases A and B to the ground. With a fault resistance of 0.001Ohm,a ground resistance of 0.01Ohm, a snubber resistance of 1e6Ohm and an infinite snubber capacitance.

V.3.4.2.1 Pi controller

The figure bellow shows the Pi vector control simulation results with two phases to the ground transmission line fault.
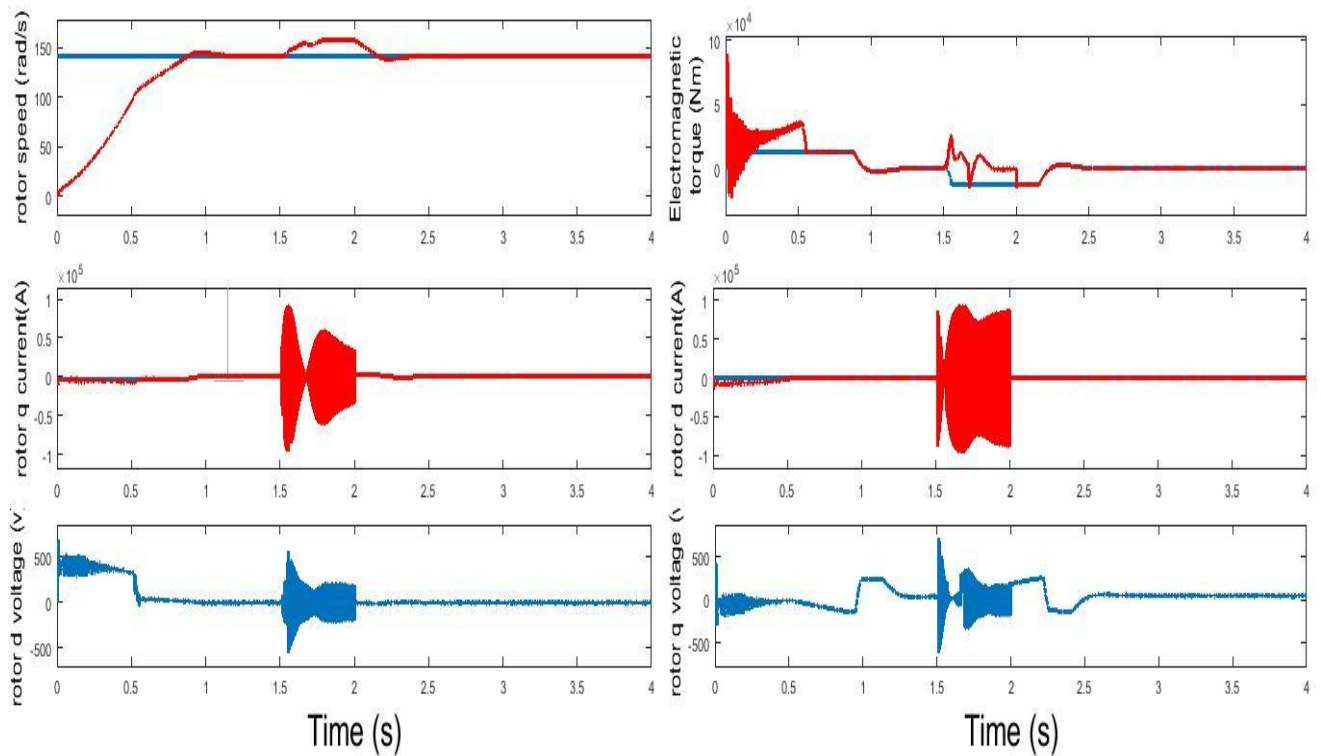
Figure V.16: the Pi vector control simulation results with two phases to the ground transmission line fault

V.3.4.2.2 Rst controller

The figure bellow shows the RST vector control simulation results with two phases to the ground transmission line fault.
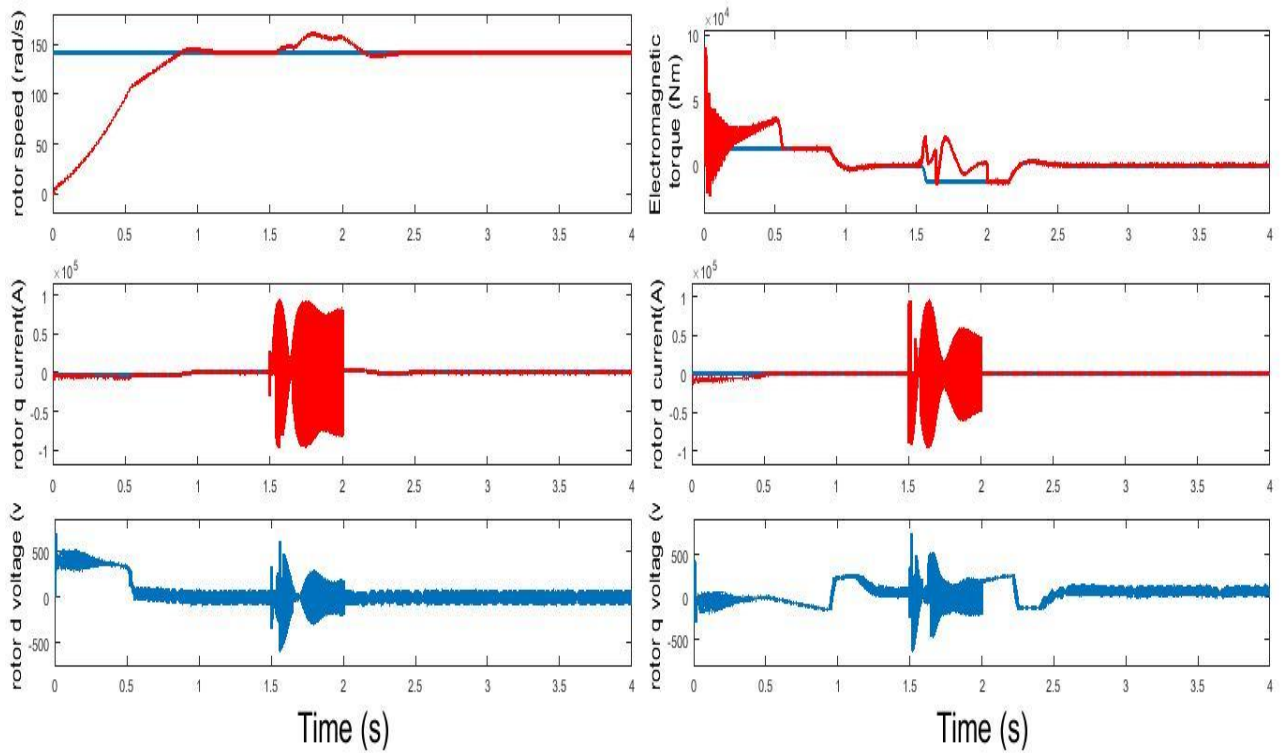
Figure V.17: the RST vector control simulation results with two phases to the ground transmission line fault

V.3.4.2.3   LMI based LQR controller

The figure bellow shows the LMI based LQR vector control simulation results with two phases to the ground transmission line fault.
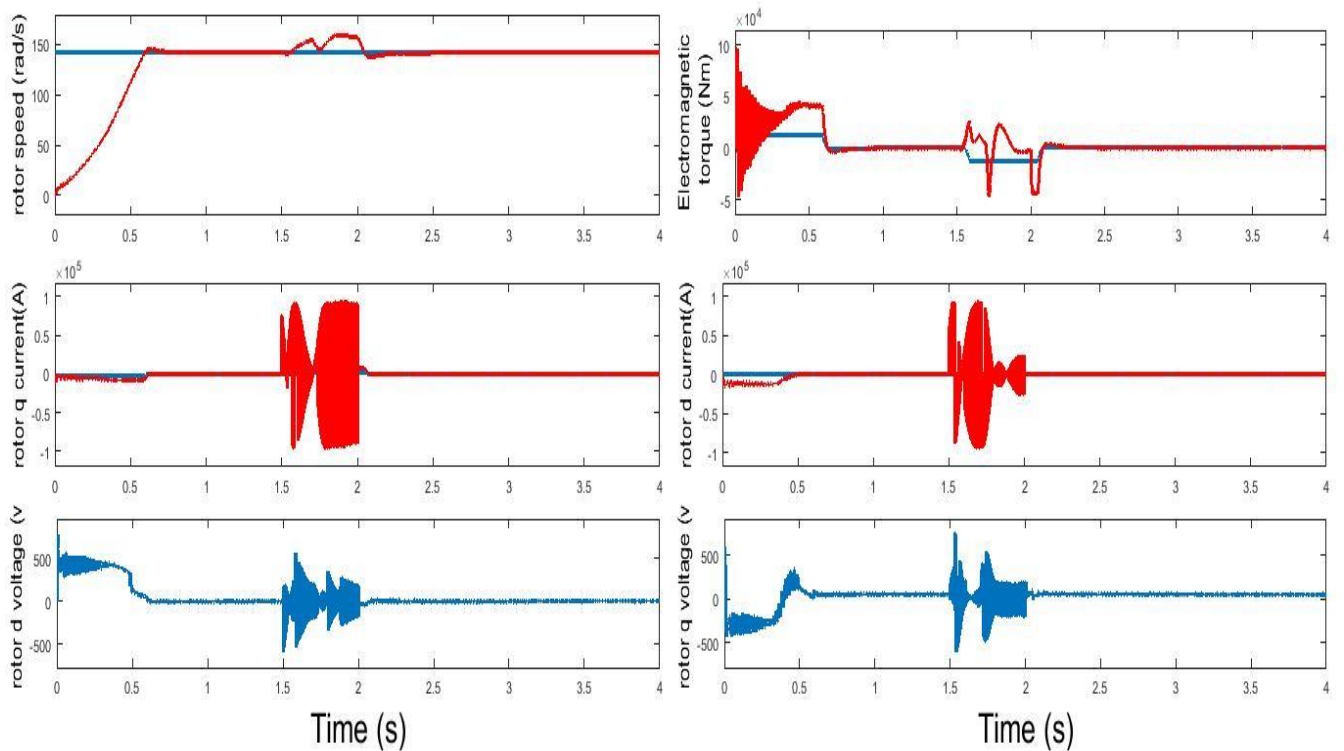
Figure V.18: the LMI based LQR vector control simulation results with two phases to the ground transmission line fault.

In comparison with the LQR and RST controllers, figures above show the superiority and the good regularity of power signals of the PI regulator in the case of two phases to the ground transmission line fault which minimizes the amplitude of the oscillations.

V.3.4.3 Three-Phase (L-L-L) Fault.

The faulty phases of the transmission line block parameters, has been selected as phases A, B and C to the ground. With a fault resistance of 0.001Ohm,a ground resistance of 0.01Ohm, a snubber resistance of 1e6Ohm and an infinite snubber capacitance.

V.3.4.3.1 Pi controller

The figure bellow shows the Pi vector control simulation results with three phases to the ground transmission line fault.
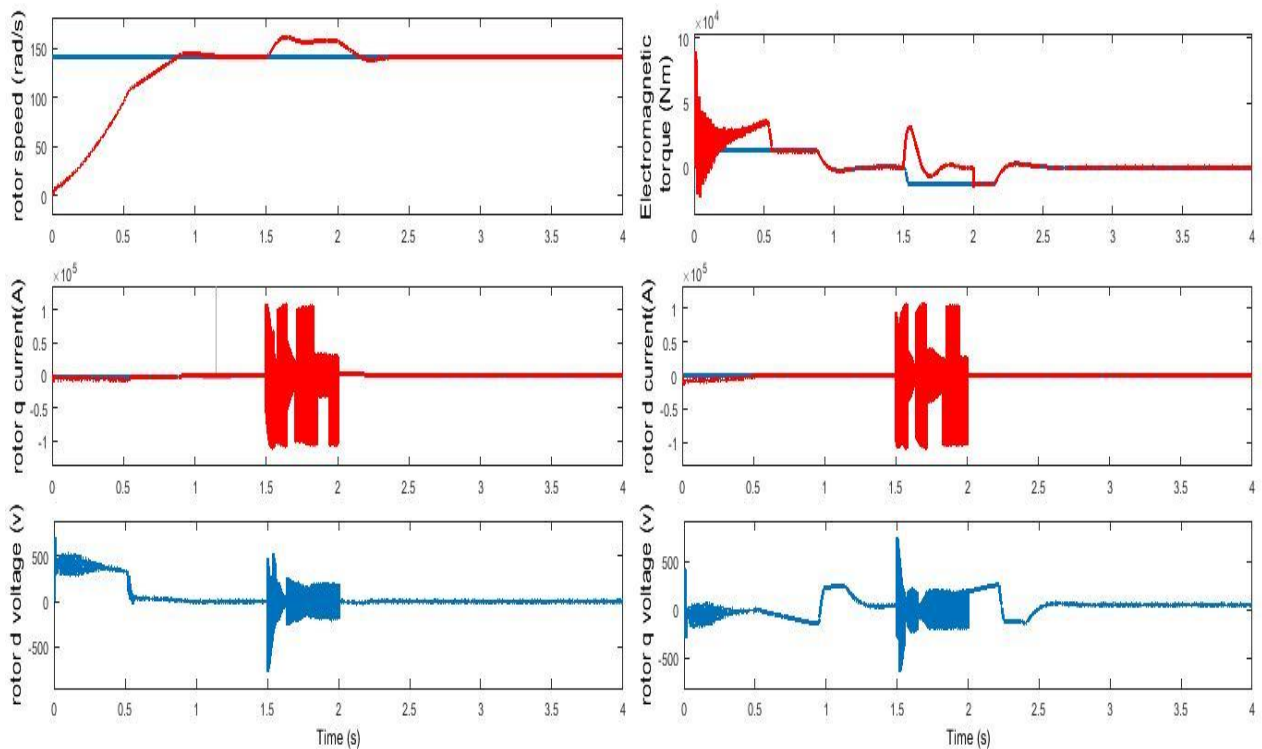
Figure V.19: the Pi vector control simulation results with three phases to the ground transmission line fault.

V.3.4.3.2 RST controller

The figure bellow shows the RST vector control simulation results with three phases to the ground transmission line fault.
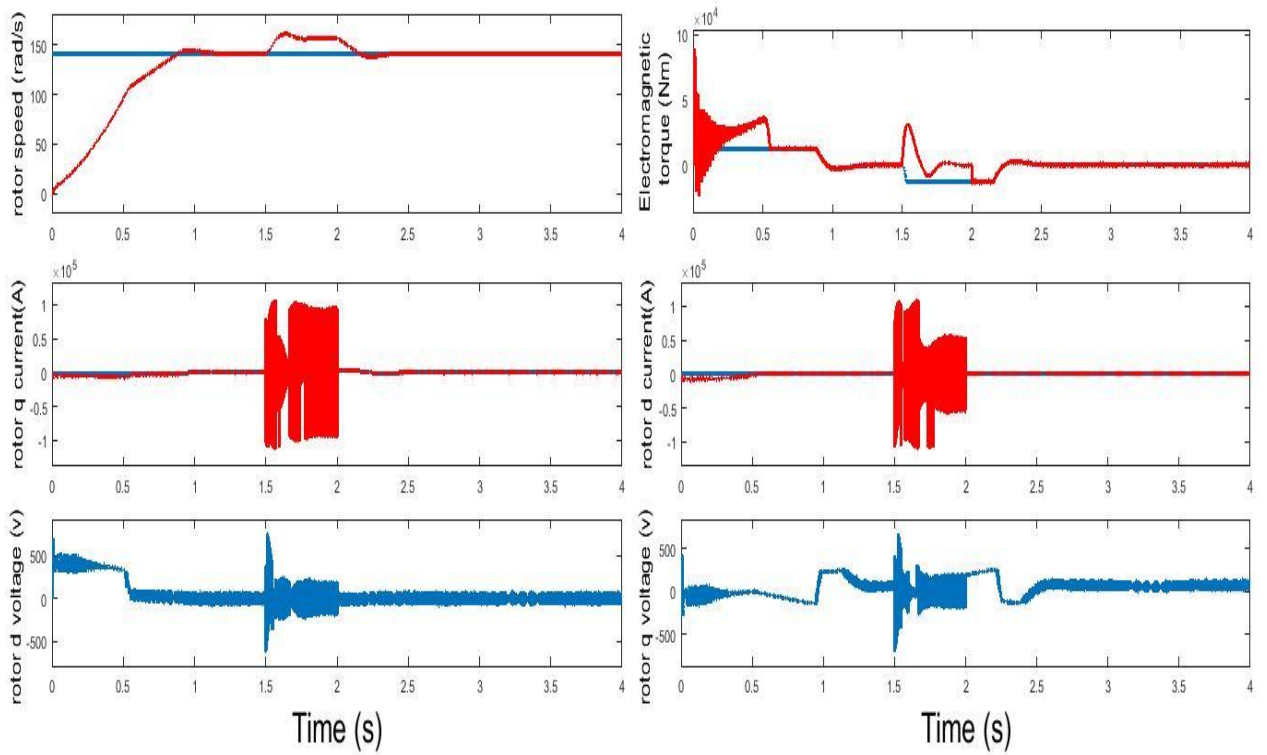
Figure V.20: the RST vector control simulation results with three phases to the ground transmission line fault

V.3.4.3.3   LMI based LQR controller

The figure bellow shows the LMI based LQR vector control simulation results with three phases to the ground transmission line fault.
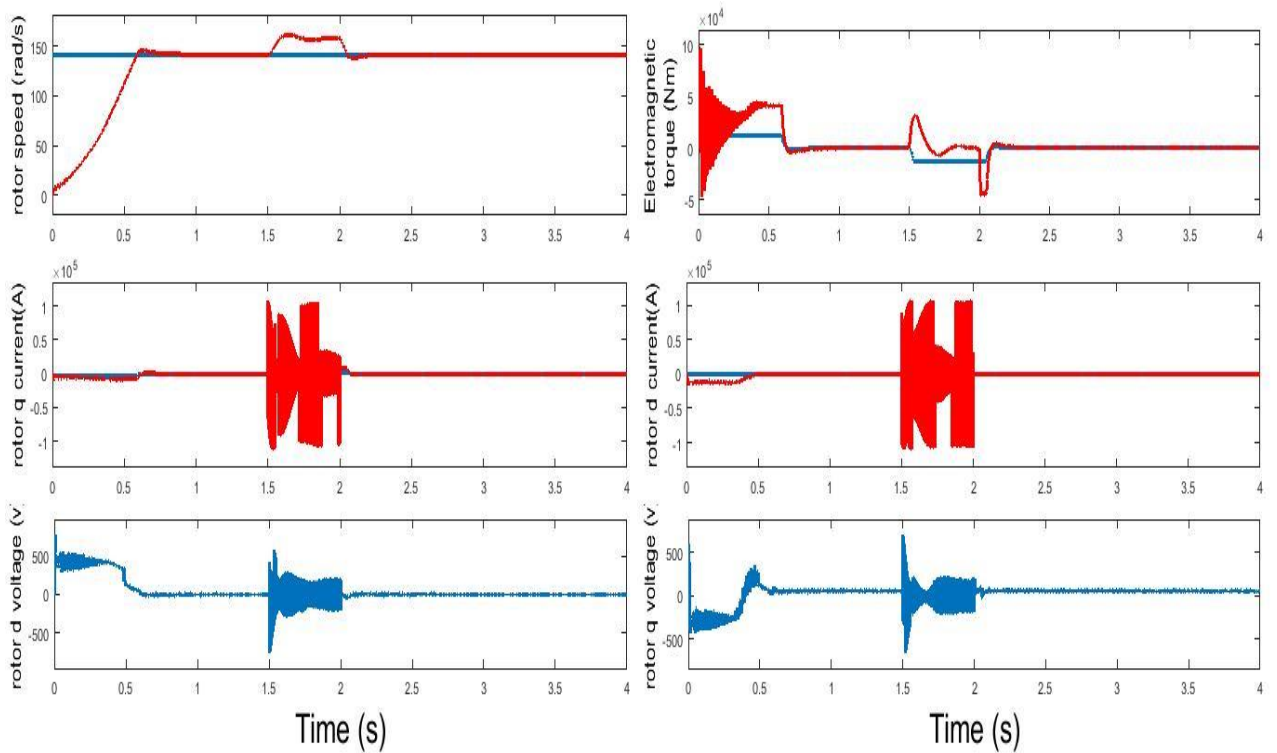
Figure V.21: the LMI based LQR vector control simulation results with three phases to the ground transmission line fault.

V.3.4.3.4 Comparison

In comparison with the RST and PI controllers, figures above show the superiority and the good regularity of power signals of the LQR regulator in the case of three phases to the ground transmission line fault which minimizes the amplitude of the oscillations.

V.3.5 Fault tolerant control of solar system

This part presents the performance of the solar system model and its dynamic response in the occurring of a fault in the boost converter where different open and short circuit faults are tested on the converters and results were obtained based on the converters performance. The faults studied in this suction occur on diode, inductor, capacitor and the switch. Simulation results are shown for these faults next. All faults are applied between 0.5 to 1 sec in Mat-lab/Simulink and simulation runs for total of 1.5 sec.

V.3.5.1 Inductor short circuit fault

The figure bellow shows the faulty boost converter model, where the fault has been selected as a short circuit fault across the inductor. . With a breaker resistance of 0.01Ohm,a snubber resistance of 1e6Ohm and an infinite snubber capacitance.
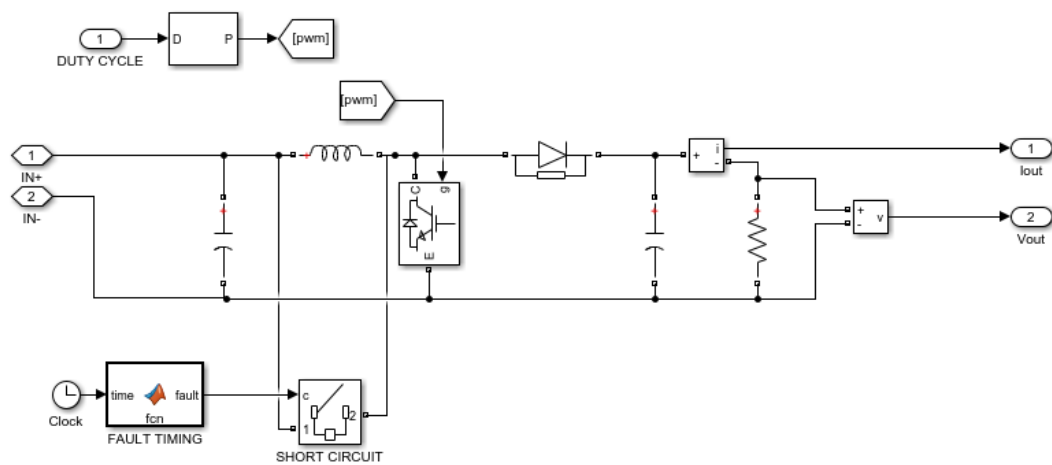
FigureV.22: short circuit fault across the inductor

V.3.5.1.1 P & O controller

The figure bellow shows the P & O control simulation results with a short circuit fault across the inductor.
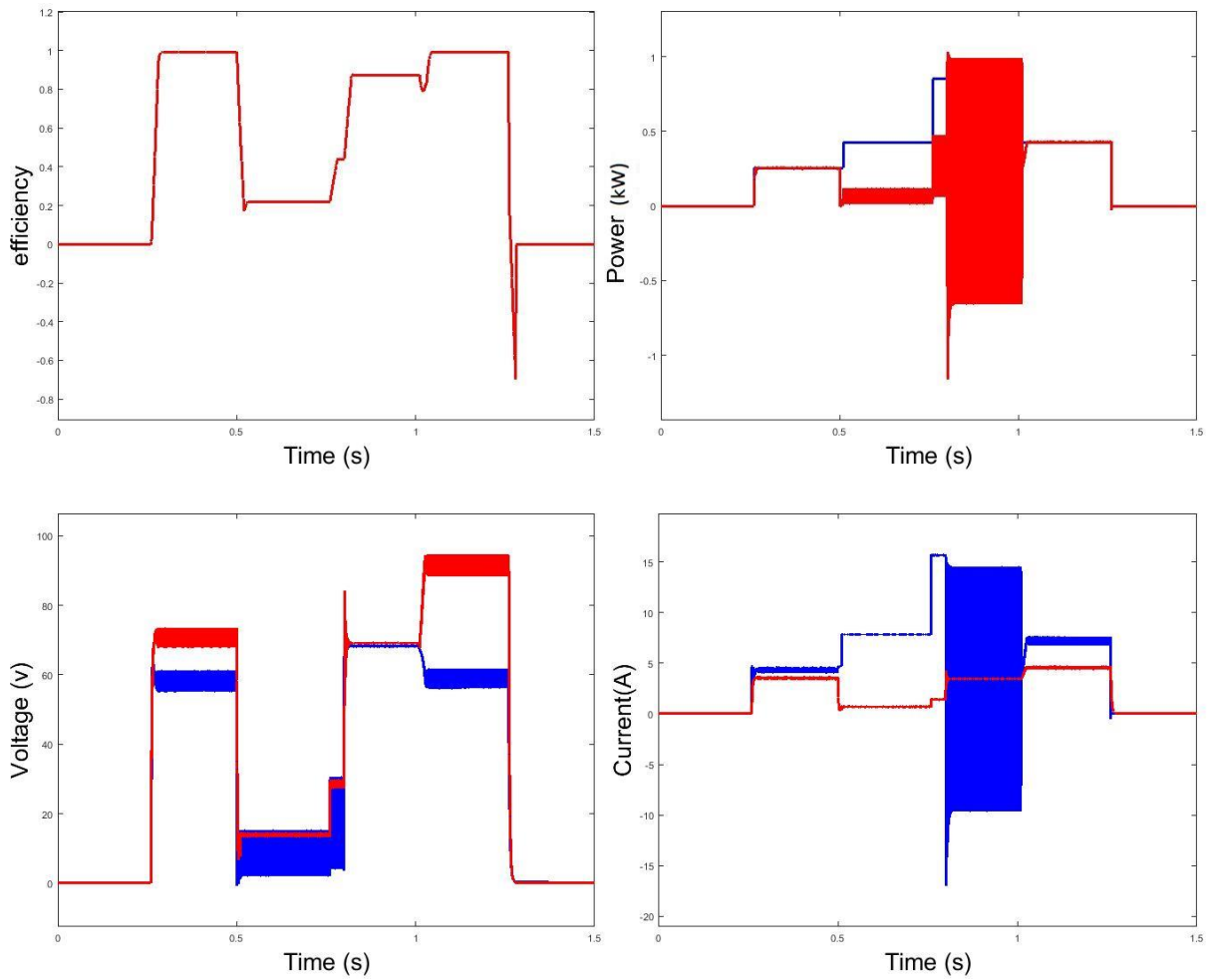
Figure V.23: the P & O control simulation results with a short circuit fault across the inductor

V.3.5.1.2 *Fuzzy logic controller*

The figure bellow shows the FUZZY logic control simulation results with a short circuit fault across the inductor.
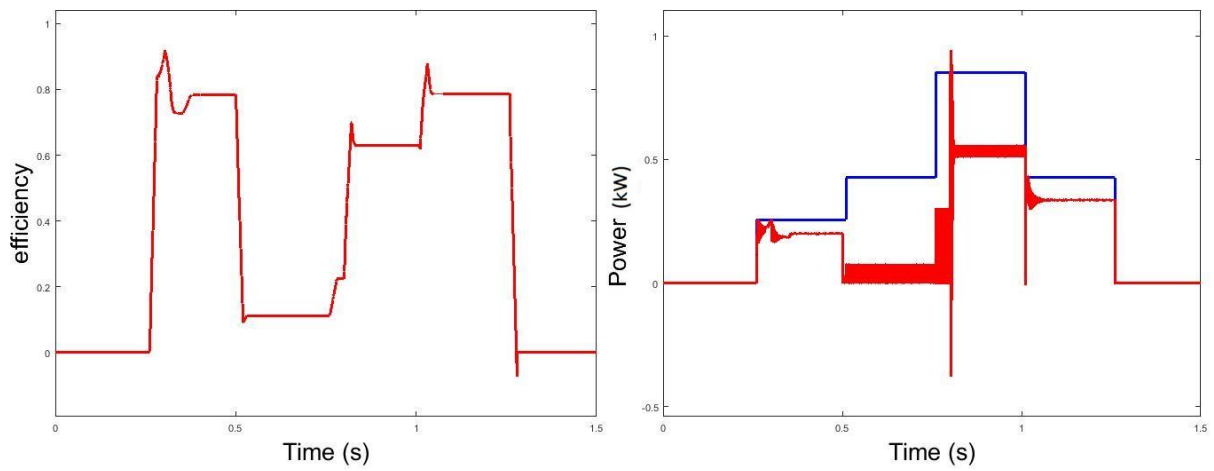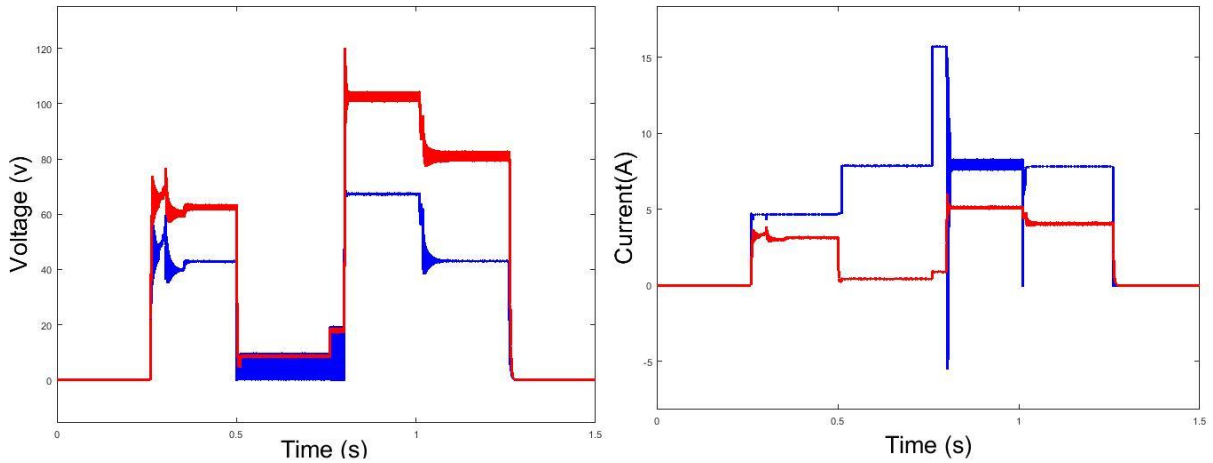
Figure V.24: the FUZZY logic control simulation results with a short circuit fault across the inductor

V.3.5.2   Diode Open circuit

The figure bellow shows the faulty boost converter model, where the fault has been selected as an open circuit fault across the diode.
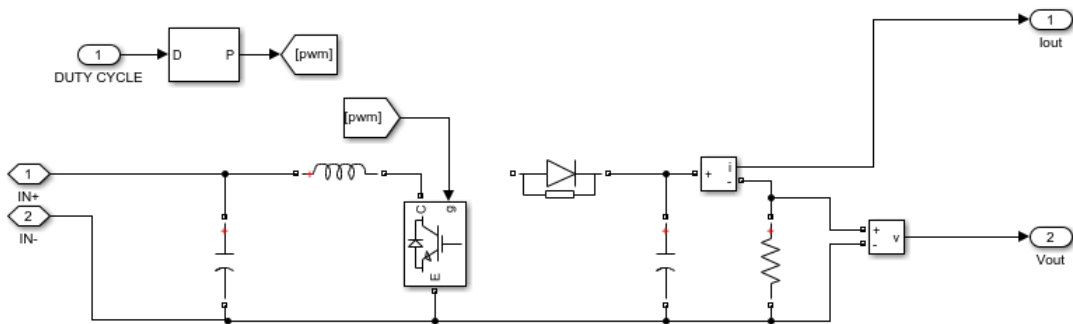
Figure V.25: open circuit fault across the diode.

V.3.5.2.1   P & O controller

The figure bellow shows the P & O control simulation results with an open circuit fault across the diode.
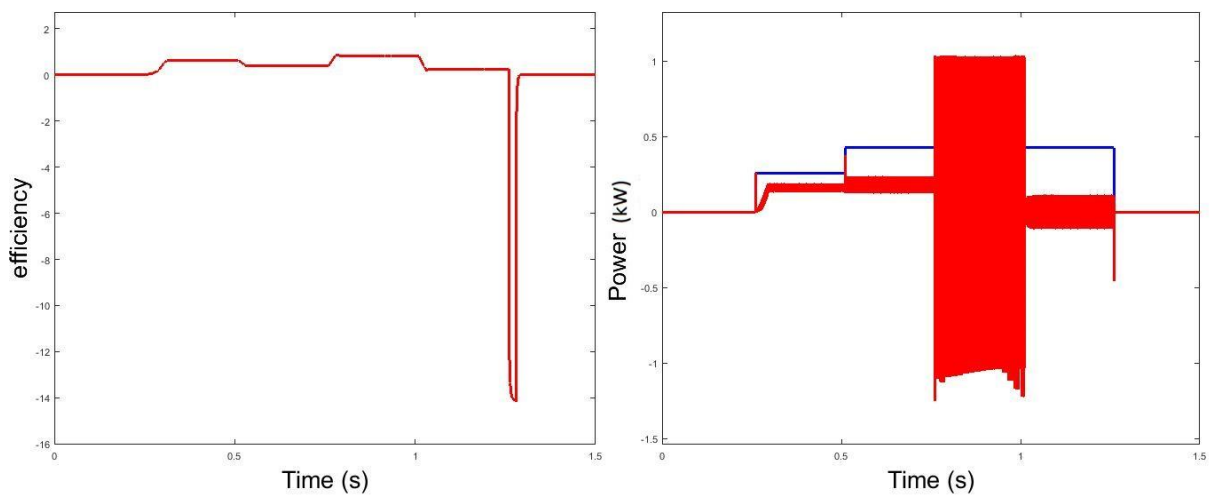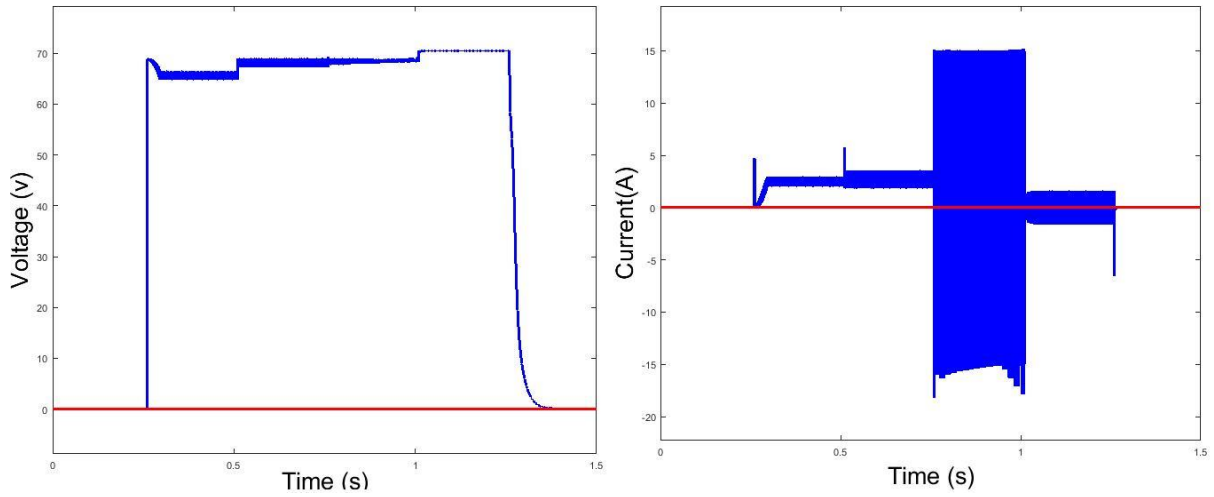
Figure V.26: the P & O control simulation results with an open circuit fault across the diode.

V.3.5.2.2   *Fuzzy logic controller*

The figure bellow shows the FUZZY logic control simulation results with an open circuit fault across the diode.
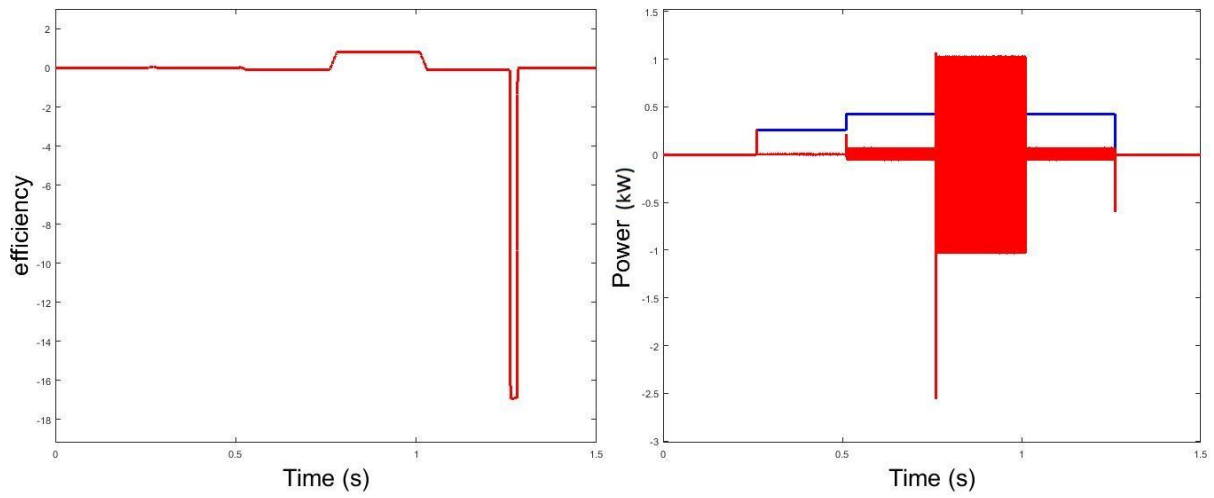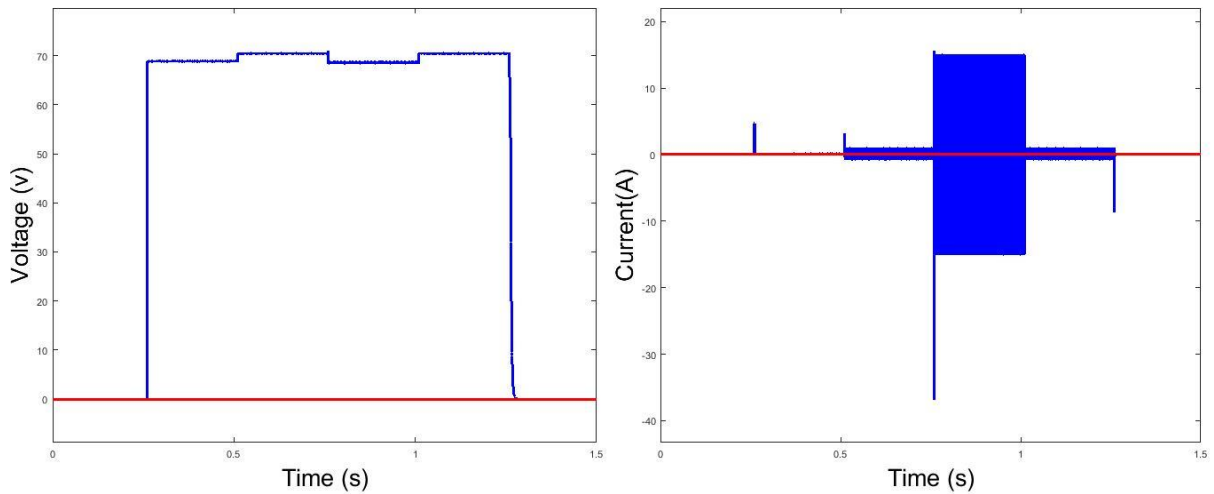
Figure V.27: the FUZZY logic control simulation results with an open circuit fault across the diode

V.3.5.3   Switch Open Circuit

The figure bellow shows the faulty boost converter model, where the fault has been selected as an open circuit fault across the switch.
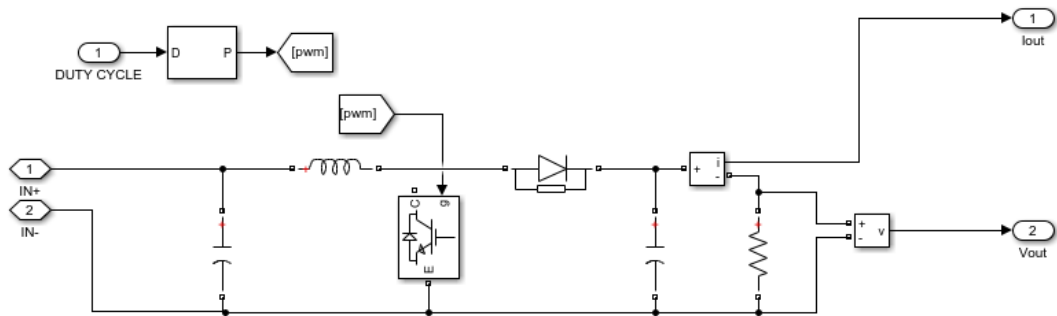
Figure V.28: open circuit fault across the switch.

V.3.5.3.1   P & O controller

The figure bellow shows the P & O control simulation results with   an   open circuit fault across the switch.
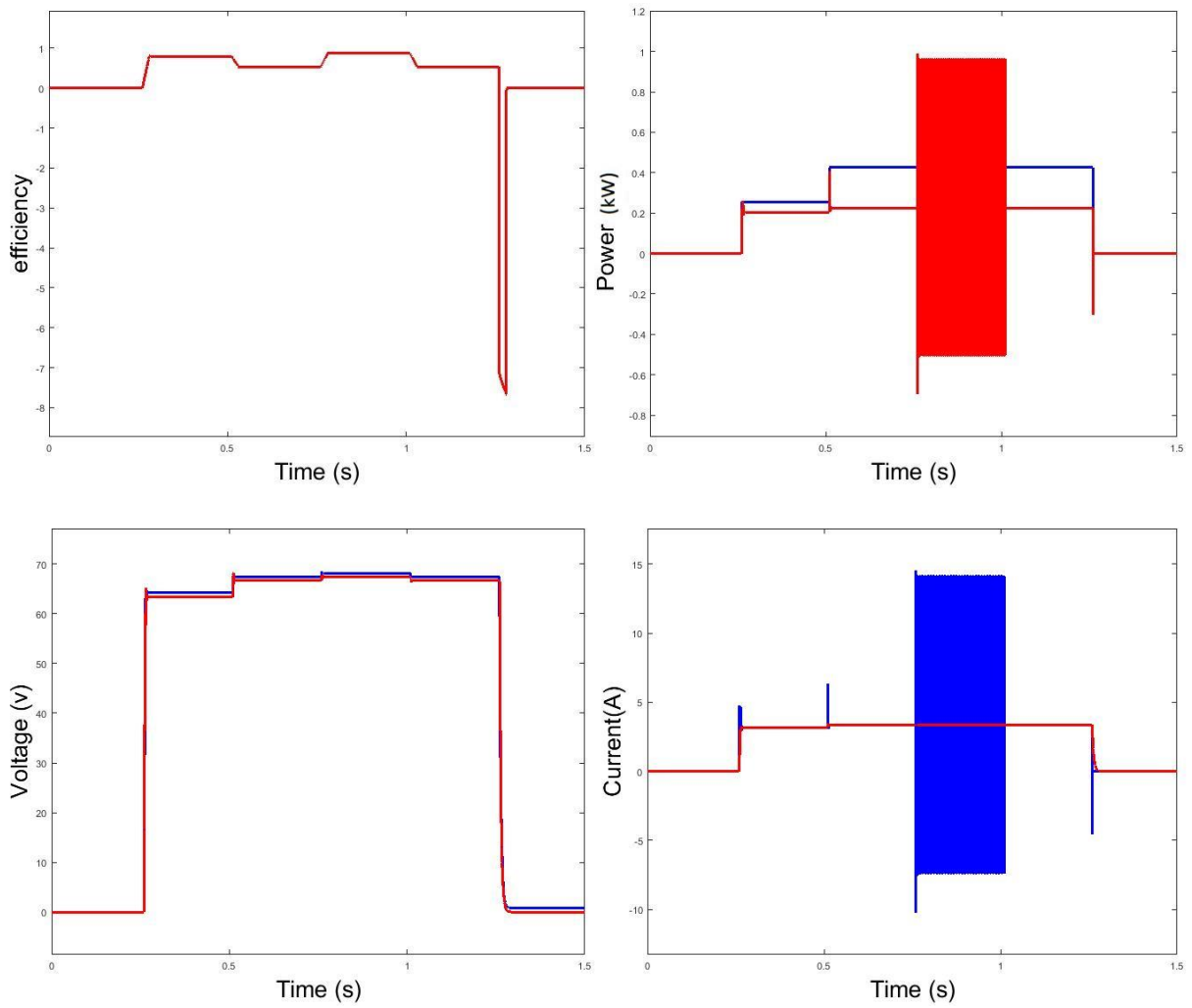
Figure V.29: the P & O control simulation results with an open circuit fault across the switch

V.3.5.3.2   Fuzzy logic controller

The figure bellow shows the FUZZY logic control simulation results with   an open circuit fault across the switch.
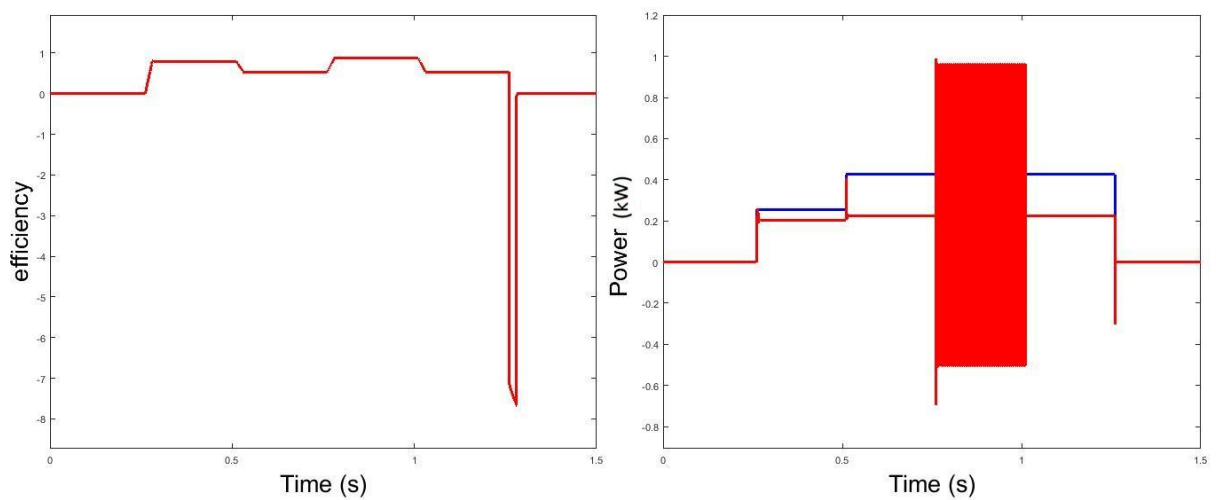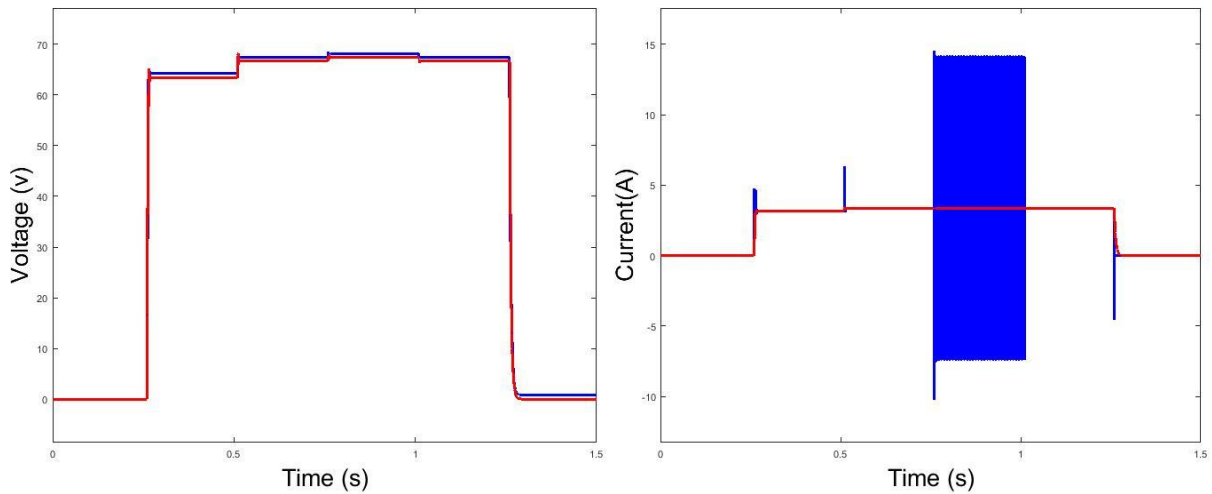
Figure V.30: the FUZZY logic control simulation results with an open circuit fault across the switch

V.3.5.4   Switch Short Circuit Fault

The figure bellow shows the faulty boost converter model, where the fault has been selected as a short circuit fault across the switch. . With a breaker resistance of 0.01Ohm,a snubber resistance of 1e6Ohm and an infinite snubber capacitance.
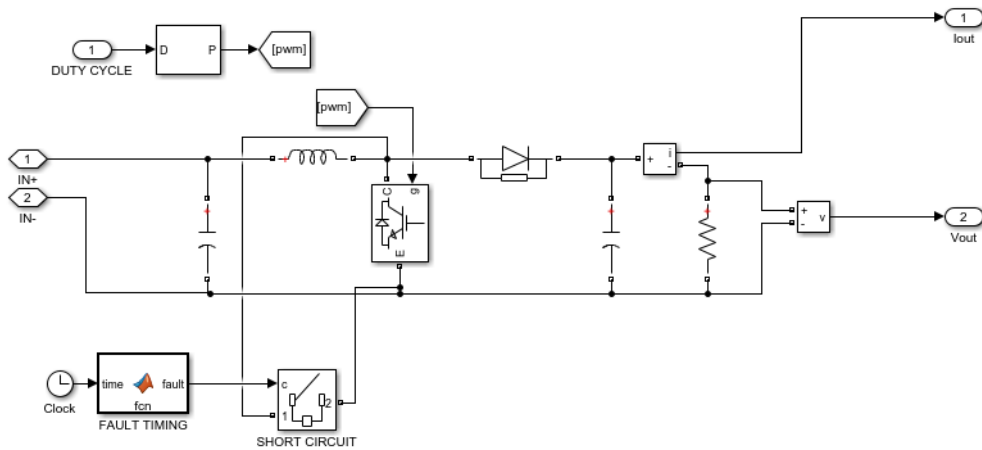
Figure V.31: short circuit fault across the switch

V.3.5.4.1   P & O controller

The figure bellow shows the P & O control simulation results with a short circuit fault across the switch.
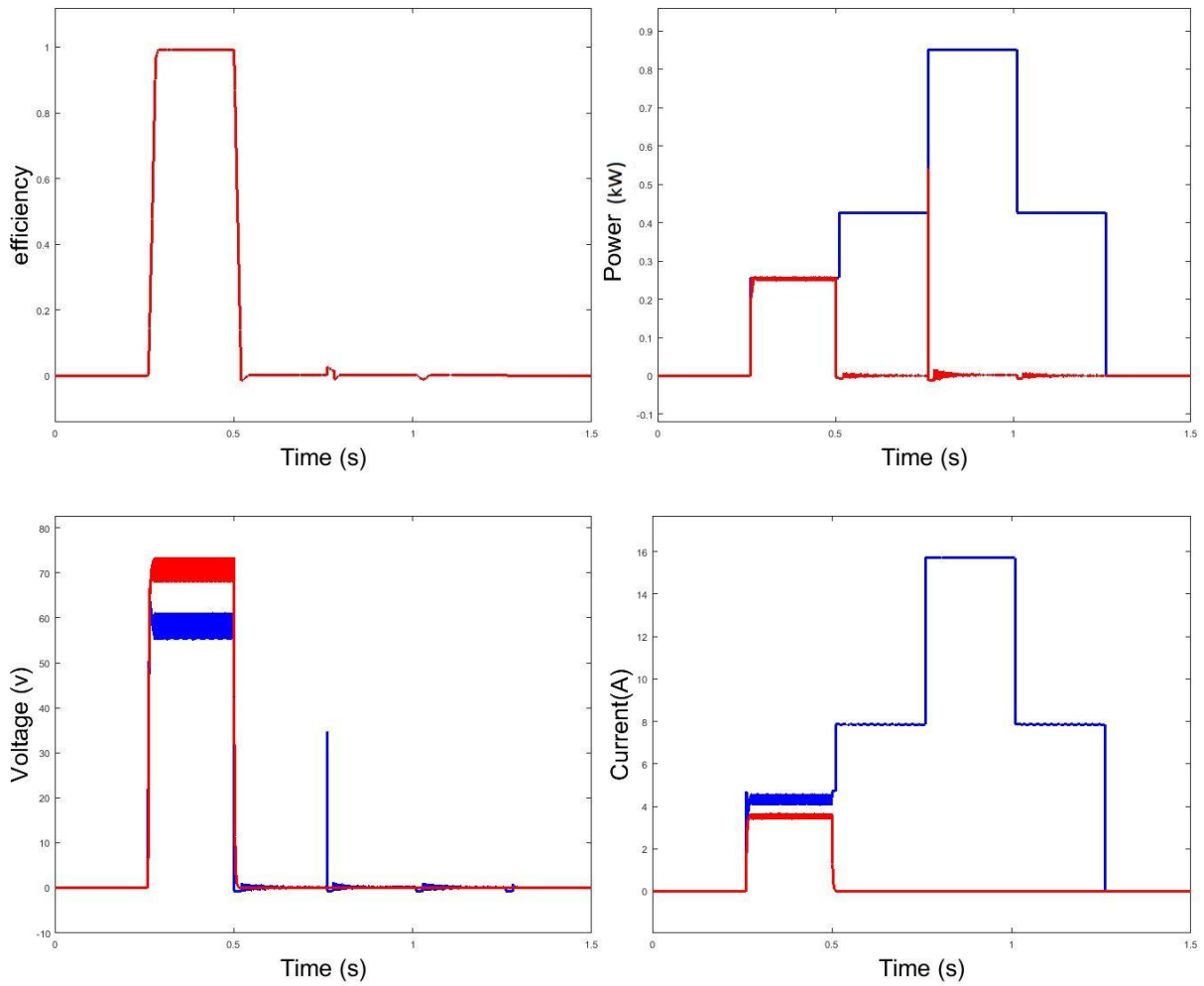
Figure V.32: the P & O control simulation results with a short circuit fault across the switch

V.3.5.4.2 *Fuzzy logic controller*

The figure bellow shows the FUZZY logic control simulation results with a short circuit fault across the switch.
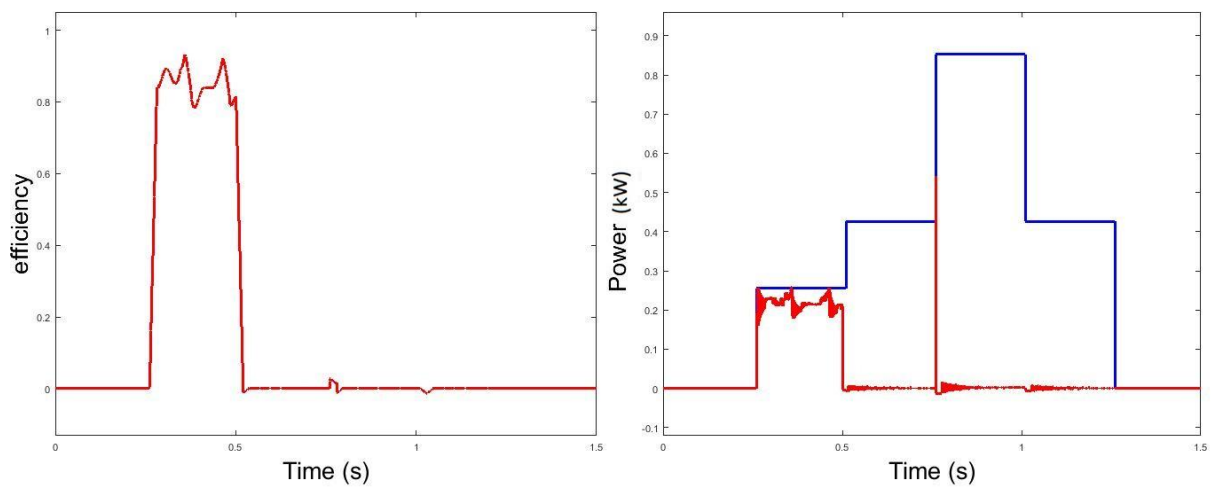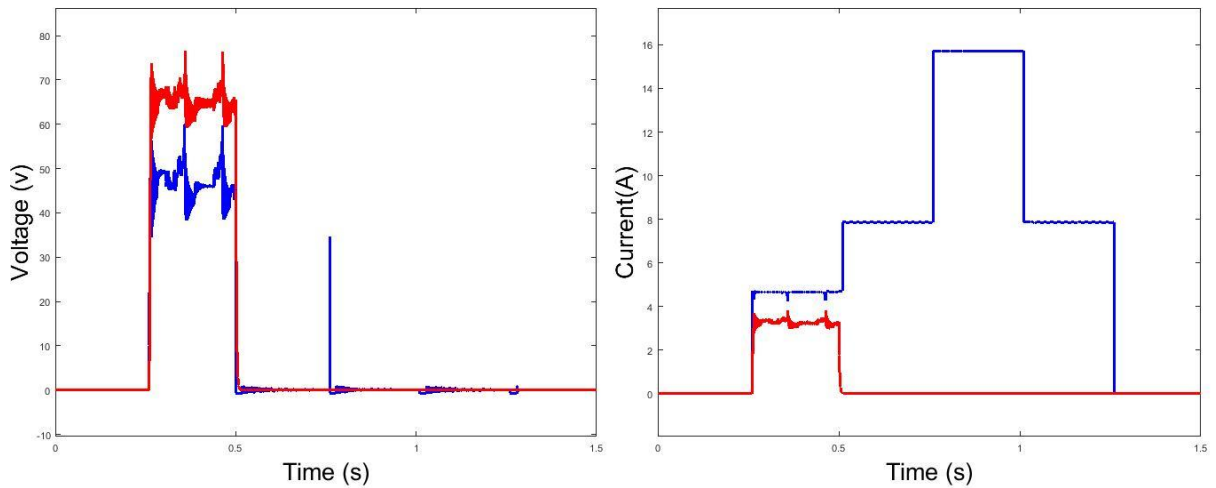
Figure V.33: the FUZZY logic control simulation results with a short circuit fault across the switch

V.3.5.5 Capacitor Open Circuit Fault

The figure bellow shows the faulty boost converter model, where the fault has been selected as an open circuit fault across the capacitor.
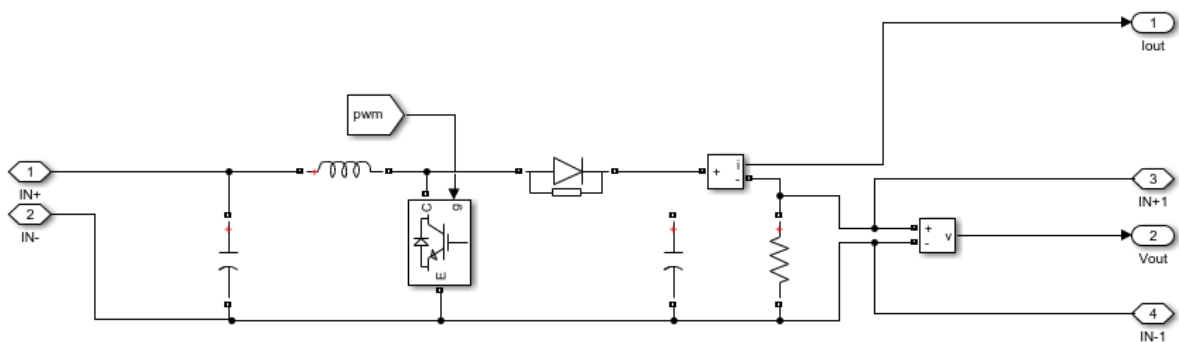
Figure V.34: open circuit fault across the capacitor

V.3.5.5.1 P & O controller

The figure bellow shows the P & O logic control simulation results with an open circuit fault across the capacitor.
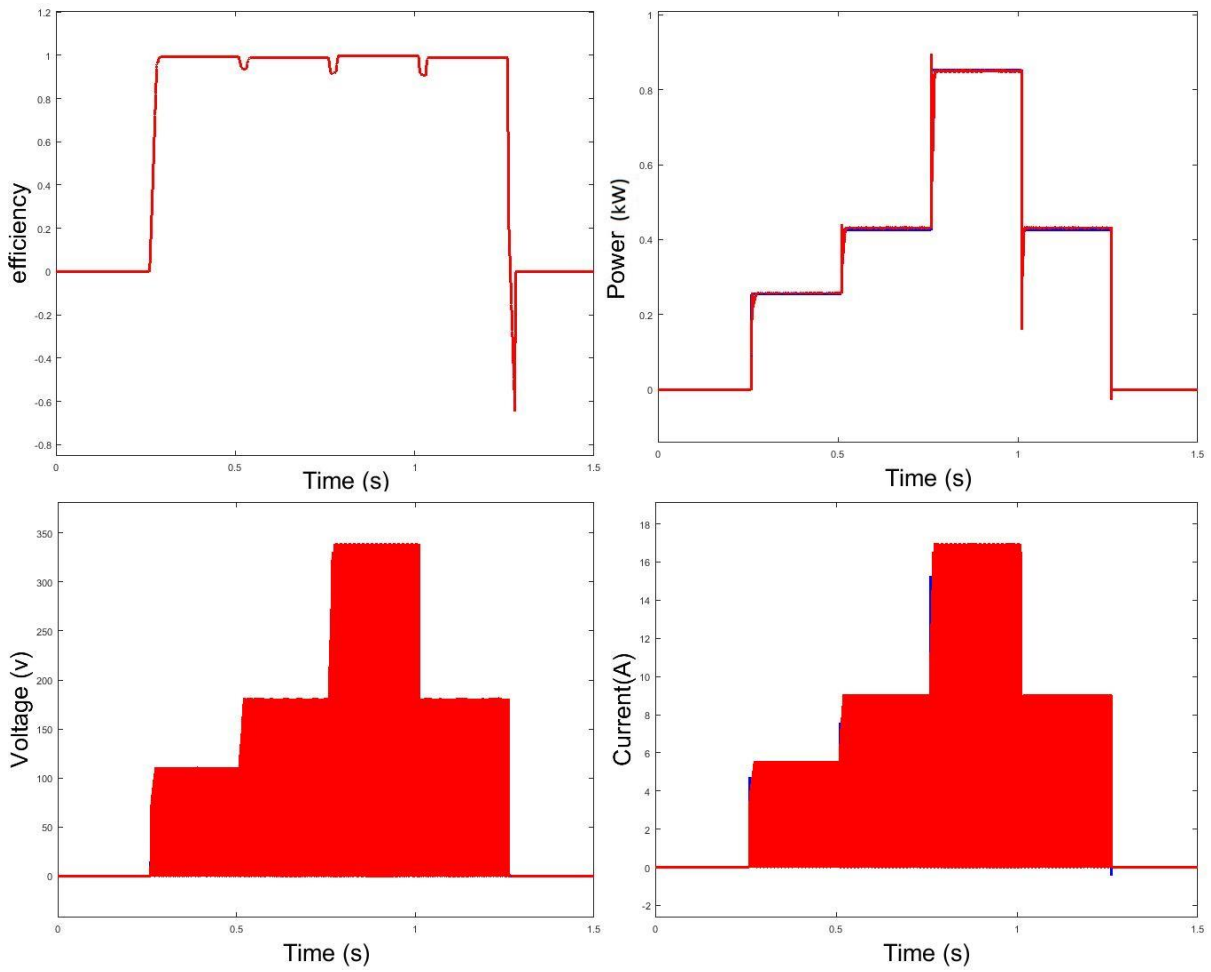
Figure V.35: the P & O logic control simulation results with an open circuit fault across the capacitor.

V.3.5.5.2 *Fuzzy logic controller*
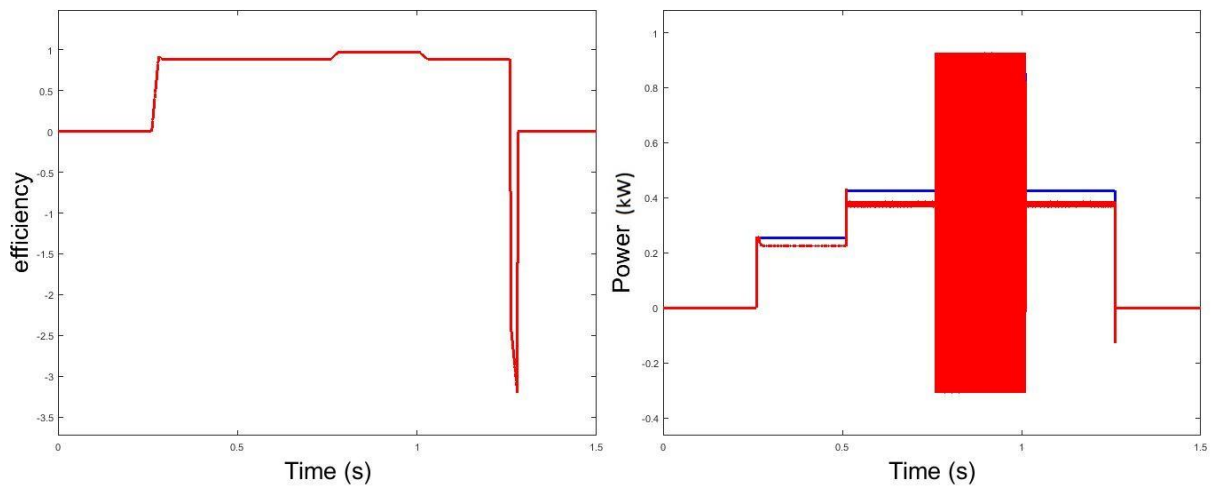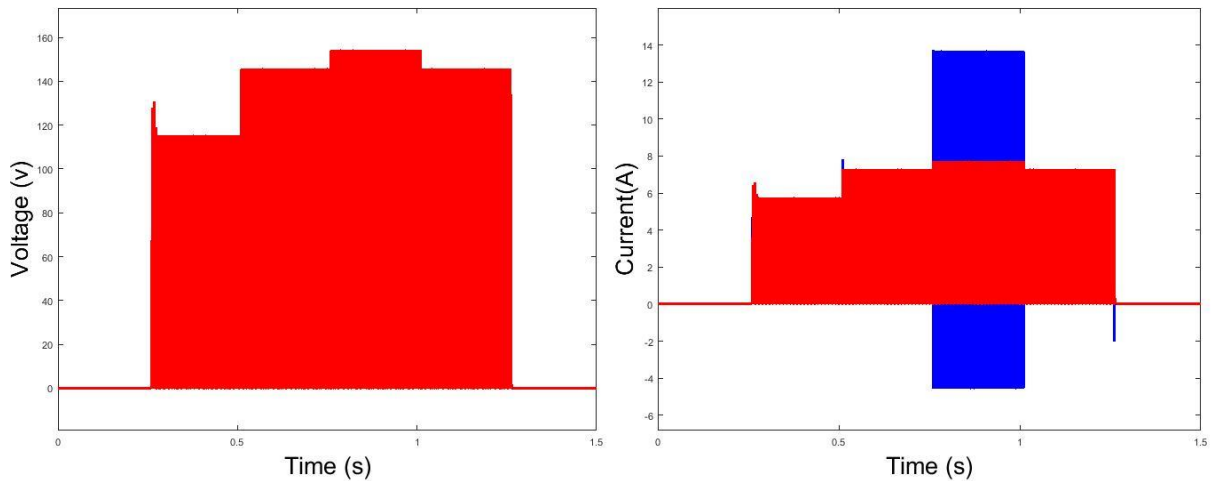
The figure bellow shows the FUZZY logic control simulation results with an open circuit fault across the capacitor.

V.3.5.5.3   Comparison

By comparing Fuzzy Logic based MPPT and conventional P&O MPPT when all kind of faults (short or open circuit) occurs on the boost converter. It has been clearly noticed continues oscillation of operation point for the FL technique. Whereas the oscillation is not observed in P&O based MPPT technique, where signals of power, voltage, current, and efficiency remain almost constant. The P&O Controller provided a better response than a conventional FL controller in terms of the maximum power tracking performance.

V.3.6   Conclusion

In this chapter, first for the wind system part ,three regulators (PI, RST and LQR) have been developed   and compared. The differences sensitive between the regulators are not very explicit but measurements are more regular in the case of the LQR regulator and have smaller overshoots.

Then for the solar system part, Fuzzy logic (FL) and P&O based maximum power point tracking (MPPT) controllers have been developed , presented and implemented in Matlab-Simulink environment to identify the MPP, subsequently regulate the PV array to operate at that particular operating voltage. The P&O Controller provided a better response than a conventional FL controller in terms of the maximum power tracking performance.

General conclusion

The issues addressed in this thesis have enabled us to deeply study the hybrid wind solar systems and briefly the fault tolerant as well as the simulation which was the closest to the reality.

The first chapter presented the fundamental concepts of hybrid energy systems, where it has been concluded that they are the most efficient way for electrical power generation, more specifically hybrid wind-solar energy system, because they are both highly predictable and follow recognizable patterns which make it easy to control power output ;when they are combined together they provide more electricity during more hours, as well as ensure production during both summer and winter hours of peak electricity usage.

The second chapter presented a detailed modeling of a hybrid system based on PV and Wind energy. The chapter systematically outlined an electrical characteristic modeling of a DFIG unit for wind turbine designing. And an electrical characteristic of a solar cell for Solar Photovoltaic System design. It was also an introduction to the third chapter where it has allowed us to develop the hybrid wind solar system controller .first the synthesis of three linear regulators for the control of the DFIM has been studied. A Proportional-Integral regulator which served as a reference for comparison, a polynomial RST regulator based on the theory of robust pole placement and an LQR regulator based on the LMI method. Then two controllers are developed for the MPP tracking and minimizing the error between the operating power and the reference maximum power which is variable according to the load and of the weather conditions. An intelligent method of maximum power point tracking (MPPT) using fuzzy logic control for stand-alone was used then a conventional perturbation and observation (P&O) technique.

The fourth chapter has presented a brief introduction to the fields of the fault tolerant control. It has included basic definitions and classifications of terms mostly used in fault tolerant control such as faults and failures. The importance of redundancy to the fault tolerant control has been also discussed.

In the last chapter three regulators (PI, RST and LQR) have been developed   and compared for the wind system part. The LQR controller provided a better response where the differences sensitive between the regulators are not very explicit but measurements are more regular in the case of the LQR regulator and have smaller overshoots. Then for the solar

system part, Fuzzy logic (FL) and P&O based maximum power point tracking (MPPT) controllers have been developed to identify the MPP, subsequently regulate the PV array to operate at that particular operating voltage. The P&O Controller provided a better response than a conventional FL controller in terms of the maximum power tracking performance.

Appendix

VI DFIG parameters

Rotor parameters side

- Stator frequency 50 (Hz)
- Rated stator power 2e6 (W)
- Rated rotational speed 1500 (rev/min)
- Rated stator voltage 690 (V)
- Rated stator current 1760 (A)
- Rated torque 12732 (N.m)
- Pole pair 2
- Stator/rotor turns ratio 1/3
- Rated rotor voltage (non-reached) 2070 (V)
- Maximum slip 1/3
- Stator resistance 2.6e-3 (ohm)
- Leakage inductance (stator and rotor) 0.087e-3 (H)
- Magnetizing / Mutual inductance 2.5e-3 (H)
- Rotor resistance refered to stator 2.9e-3 (ohm)

Mechanical Parameters

- Inertia force 127 kg m2
- Friction Pair 1e-2

Grid parameters side

- Bus capacitor 80e-3(C)
- Grid resistance 20e-6(ohm)
- Grid inductance 400e-6 (H)

VII Wind turbine parameters

- Nominal mechanical output power 1.5e6 (W)
- Base power of the electrical generator 1.5e6/0.9 (VA)
- Base wind speed 12 (m/s)
- Maximum power at base wind speed (pu of nominal mechanical power) 0.73
- Base rotational speed (p.u. of base generator speed) 1.2

VIII Boost converter parameters

- Converter inductance 2e-3 (H)
- Converter capacitor 100e-6 (C)
- Load resistance 20 (Ohms)

IX   Boost converter switch parameters

- Device on-state resistance (Ohms) 0.001
- Snubber resistance 500 (Ohms)
- Snubber capacitance 250e-9 (F)
- Forward voltages 0.8 (V)

Bibliography

[1]   G. Petrecca, Energy Conversion and Management. Cham: Springer International Publishing, 2014.

[2]   S. C. Ameta and R. Ameta, Solar energy conversion and storage: photochemical modes. Boca Raton: CRC Press, Taylor & Francis Group, 2016.

[3]   J. F. Manwell, « Wind Energy Explained: Theory, Design and Application », p. 705.

[4]   G. Petrecca, Energy Conversion and Management. Cham: Springer International Publishing, 2014..

[5]   H. Abu-Rub, M. Malinowski, et K. Al-Haddad, « Power Electronics for Renewable Energy Systems, Transportation », p. 827.

[6]   Y. Fernando et S. Yahya, « Challenges in Implementing Renewable Energy Supply Chain in Service Economy Era », Procedia Manufacturing, vol. 4, p. 454-460, 2015, doi: 10.1016/j.promfg.2015.11.062..

[7]   S. White, Solar Photovoltaic Basics: A Study Guide for the NABCEP Entry Level Exam, 1re éd. Routledge, 2014.

[8]   M. R. Patel, Wind and solar power systems design, analysis, and operation. Londres: Taylor, 2005.

[9]   "Free solar savings report," SolarHomeReport. [Online]. Available: https://solarhomereport.com/?gclid=CjwKCAjwz6_8BRBkEiwA3p02VcInv9f-LZKYuPxfug0ZFGemK2KZTCgO-QlDUtKyCjDE-qJDmt0XrxoCjnAQAvD_BwE. [Accessed: 18-Oct-2020].

[10]   pdf4pro.com, "Solar Electric System Design, Operation and Installation download / solar-electric-system-design-operation-and-installation.pdf / PDF4PRO," PDF4PRO, 22-Mar-2019. [Online]. Available: https://pdf4pro.com/download/solar-electric-system-design-operation-and-installation-59f253.html. [Accessed: 18-Oct-2020].

[11]   "a reservoir of Indian theses @ INFLIBNET," Shodhganga. [Online]. Available: https://shodhganga.inflibnet.ac.in:8443/jspui/pdfToThesis.jsp?toHandle=https%3A%2F%2Fshodhganga.inflibnet.ac.in%2Fhandle%2F10603%2F173729. [Accessed: 18-Oct-2020].

[12]   "Wiring Parallel And Series," Wiring Database - Installation Manuals and Wiring Diagram Library. [Online]. Available: http://lence.noneq.cloud.manonellamano.org/wiring-parallel-and-series.html. [Accessed: 18-Oct-2020].

[13]   "File:Solar PV & Thermal Applications for Hotel Sector ..." [Online]. Available: https://energypedia.info/wiki/File:Solar_PV_%26_Thermal_Applications_for_Hotel_Sector-Technical_Manual_for_the_MENA_Region.pdf. [Accessed: 18-Oct-2020].

[14]   J. Haney et A. Burstein, « PV System Operations and Maintenance Fundamentals », p. 46.

[15]   M. D. Platzer, « U.S. Solar Photovoltaic Manufacturing: Industry Trends, Global Competition, Federal Support », Global Competition, p. 31.

[16]   "Global Market Outlook 2018-2022," Solar Power Europe, 27-Jun-2018. [Online]. Available: https://www.solarpowereurope.org/global-market-outlook-2018-2022/. [Accessed: 18-Oct-2020].

[17]   "TRAINING MANUAL FOR DOMESTIC SOLAR ELECTRICITY TRAINERS." [Online]. Available: https://www.pseau.org/outils/ouvrages/alliance_soleil_etc_foundation_training_manual_for_domestic_solar_electricity_trainers_2009.pdf. [Accessed: 18-Oct-2020]..

[18]   "FUTURE OF SOLAR PHOTOVOLTAIC Deployment, investment, technology, grid integration and socio-economic aspects," United Arab Emirates, november 2019.

[19]   M. M. | O. 15, Bio   Posted by Marta Moses Posts Posts by Marta Moses Electric cars of the future Three EV-friendly rural and city road trips, P. by M. Moses, and Posts by Marta Moses
Electric cars of the future Three EV-friendly rural and city road trips   Top 6 Electric Car Questions Answered, "All you need to know about wind power," EDF. [Online]. Available: https://www.edfenergy.com/for-home/energywise/all-you-need-to-know-about-wind-power. [Accessed: 18-Oct-2020].

[20]   "Everything You Need to Know About Wind Power," PartSelect.com. [Online]. Available: https://www.fix.com/blog/everything-you-need-to-know-about-wind-power. [Accessed: 18-Oct-2020].

[21]   Bahman Zohuri, Hybrid Energy Systems: Driving Reliable Renewable Sources of Energy Storage. USA: Galaxy Advanced Engineering Inc., Department of Electrical and Computer EngineeringUniversity of New MexicoAlbuquerque, November 25, 2017.

[22]   Anant Pise2 , Ajit Shinde3 , Pritesh P. Shirsath1, "Solar-Wind Hybrid Energy Generation System," vol. Volume 4, no. Issue 2, March-April, 2016.

[23]   Md Umar Hashmi, COMPONENTS SOLAR PV STAND-ALONE SYSTEM., March 2011.

[24]   Chandani Sharma et al Int, "Solar Panel Mathematical Modeling Using Simulink," vol. Vol. 4, no. Issue 5(

Version 4, May 2014.

[25] A. Scott, "Basic Solar Panel Model," 2N3904Blog, 17-Feb-2018. [Online]. Available: https://2n3904blog.com/basic-solar-panel-model/. [Accessed: 18-Oct-2020].

[26] "Chapter 9 – Photovoltaic Systems." [Online]. Available: https://academics.uccs.edu/rtirado/PES_1600_SolarEnergy/Text_2e/ch_9.pdf. [Accessed: 18-Oct-2020].

[27] "Short-Circuit Current," PVEducation. [Online]. Available: https://www.pveducation.org/pvcdrom/solar-cell-operation/short-circuit-current. [Accessed: 18-Oct-2020].

[28] H. Yatimi, E. Aroudam, et M. Louazni, « Modeling and Simulation of photovoltaic Module using MATLAB/SIMULINK », MATEC Web of Conferences, vol. 11, p. 03018, 2014, doi: 10.1051/matecconf/20141103018.

[29] V. Tamrakar, G. S.C, et Y. Sawle, « Single-Diode Pv Cell Modeling And Study Of Characteristics Of Single And Two-Diode Equivalent Circuit », ELELIJ, vol. 4, n° 3, p. 13-24, août 2015, doi: 10.14810/elelij.2015.4302.

[30] CHANDANI SHARMA, « Solar Cells, Present State and Future Challanges », 2014, doi: 10.13140/RG.2.1.2316.4966.

[31] C. Sharma et A. Jain, « Solar Panel Mathematical Modeling Using Simulink », vol. 4, n° 5, p. 7, 2014.

[32] R. Szabo et A. Gontean, « Photovoltaic Cell and Module I-V Characteristic Approximation Using Bézier Curves », p. 23, 2018.

[33] W. K. Ahmed, « Mechanical Modelling of Wind Turbine: Comparative Study », p. 5, 2013.

[34] "Modeling of Type 1 Wind Turbine Generators," ESIG. [Online]. Available: https://www.esig.energy/wiki-main-page/modeling-of-type-1-wind-turbine-generators/. [Accessed: 18-Oct-2020].

[35] "Dynamic Models for Wind Turbines and Wind Power Plants." [Online]. Available: https://www.nrel.gov/docs/fy12osti/52780.pdf. [Accessed: 18-Oct-2020].

[36] « Tip Speed Ratio: How to Calculate and Apply TSR to Blade Selection », p. 3, 2010.

[37] parteeksmagh007, "betz_limit_0.pdf - kidwind science snack betz limit Understanding Coefficient of Power(Cp and Betz Limit The coefficient of power of a wind turbine is a: Course Hero," betz_limit_0.pdf - kidwind science snack betz limit Understanding Coefficient of Power(Cp and Betz Limit The coefficient of power of a wind turbine is a | Course Hero. [Online]. Available: https://www.coursehero.com/file/41496000/betz-limit-0pdf/. [Accessed: 18-Oct-2020].

[38] C. I. Martínez-Márquez, J. D. Twizere-Bakunda, D. Lundback-Mompó, S. Orts-Grau, F. J. Gimeno-Sales, et S. Seguí-Chilet, « Small Wind Turbine Emulator Based on Lambda-Cp Curves Obtained under Real Operating Conditions », Energies, vol. 12, n° 13, p. 2456, juin 2019, doi: 10.3390/en12132456.

[39] A. Kalmikov, « Wind Power Fundamentals », in Wind Energy Engineering, Elsevier, 2017, p. 17-24.

[40] "How to draw wind turbine power curve," Quora. [Online]. Available: https://www.quora.com/How-do-I-draw-wind-turbine-power-curve. [Accessed: 18-Oct-2020].

[41] G. S. Stavrakakis, « Electrical Parts of Wind Turbines », in Comprehensive Renewable Energy, Elsevier, 2012, p. 269-328.

[42] J. Mwaniki, H. Lin, et Z. Dai, « A Condensed Introduction to the Doubly Fed Induction Generator Wind Energy Conversion Systems », Journal of Engineering, vol. 2017, p. 1-18, 2017, doi: 10.1155/2017/2918281.

[43] S. Karim, T. Mohamed, et A. Tayeb, « Fault Detection and Control Reconfiguration of Wind Power Plants », in 2019 6th International Conference on Electrical and Electronics Engineering (ICEEE), Istanbul, Turkey, avr. 2019, p. 38-44, doi: 10.1109/ICEEE2019.2019.00015.

[44] E. J. Novaes Menezes, A. M. Araújo, et N. S. Bouchonneau da Silva, « A review on wind turbine control and its associated methods », Journal of Cleaner Production, vol. 174, p. 945-953, févr. 2018, doi: 10.1016/j.jclepro.2017.10.297.

[45] A. Hwas et R. Katebi, « Wind Turbine Control Using PI Pitch Angle Controller », IFAC Proceedings Volumes, vol. 45, n° 3, p. 241-246, 2012, doi: 10.3182/20120328-3-IT-3014.00041.

[46] L. Baghli1,2 IEEE SM, A. Boumediene 1, M. Djemai 3 Z. Dekali1, "Control of a Grid Connected DFIG Based Wind Turbine Emulator," September 2018.

[47] L. Queval et H. Ohsaki, « Back-to-back converter design and control for synchronous generator-based wind turbines », in 2012 International Conference on Renewable Energy Research and Applications (ICRERA), Nagasaki, Japan, nov. 2012, p. 1-6, doi: 10.1109/ICRERA.2012.6477300.

[48] Poitiers Frédéric, Doeuff René Le, and M. Machmoum, "Étude et commande de génératrices asynchrones pour l'utilisation de l'énergie éolienne: machine asynchrone à cage autonome: machine asynchrone à double alimentation reliée au réseau," thesis.

[49] Barotto Béatrice and J.-P. Raymond, Introduction de paramètres stochastiques pour améliorer l'estimation des trajectoires d'un système dynamique par une méthode de moindres carrés: application à la détermination de l'orbite d'un satellite avec une précision centimétrique. S.l.: s.n., 1995.

[50] O. A. Dhewa, A. Dharmawan, et T. K. Priyambodo, « Model of Linear Quadratic Regulator (LQR) Control Method in Hovering State of Quadrotor », vol. 9, n° 3, p. 10.

[51] Robust observer-based fault diagnosis for nonlinear systems using MATLAB. , Switzerland: Springer, 2016.

[52] H. Elaimani, A. Essadki, N. Elmouhi, et R. Chakib, « Comparative Study of the Grid Side Converter's Control during a Voltage Dip », Journal of Energy, vol. 2020, p. 1-11, févr. 2020, doi: 10.1155/2020/7892680.

[53] B. Abdessamad, "Design and Modeling of DC/ DC Boost Converter for Mobile Device Applications," Academia.edu - Share research. [Online]. Available: https://www.academia.edu/33936969/Design_and_Modeling_of_DC_DC_Boost_Converter_for_Mobile_Device_Applications. [Accessed: 18-Oct-2020].

[54] A. M. Noman, K. E. Addoweesh, et H. M. Mashaly, « A fuzzy logic control method for MPPT of PV systems », in IECON 2012 - 38th Annual Conference on IEEE Industrial Electronics Society, Montreal, QC, Canada, oct. 2012, p. 874-880, doi: 10.1109/IECON.2012.6389174.

[55] M. S. A. Cheikh, C. Larbes, G. F. T. Kebir, et A. Zerguerras, « Maximum power point tracking using a fuzzy logic control scheme », p. 9.

[56] [1]F. Chekired, C. Larbes, D. Rekioua, et F. Haddad, « Implementation of a MPPT fuzzy controller for photovoltaic systems on FPGA circuit », Energy Procedia, vol. 6, p. 541-549, 2011, doi: 10.1016/j.egypro.2011.05.062.

[57] A. S. Mubarak, A. S. Hassan, N. H. Umar, et M. Nasiru, « An Analytical Study of Power System under the Foult Conditons using different Methods of Fault Analysis », vol. 2, n° 10, p. 8, 2015.

[58] H. Says: 135276 says: and A. says: "▷ Faults in Electrical Systems (back to basics)," Electrical Equipment, 04-May-2013. [Online]. Available: http://engineering.electrical-equipment.org/electrical-distribution/faults-in-electrical-systems-back-to-basics.html. [Accessed: 18-Oct-2020].

[59] "Introduction to Short Circuit Analysis - PDHonline.com." [Online]. Available: https://www.pdhonline.com/courses/e204/e204content.pdf. [Accessed: 18-Oct-2020].

[60] Present Group, "Importance of Short Circuit Fault Analysis: PowerTech," Present Group, 30-Aug-2019. [Online]. Available: https://presentgroup.com.au/short-circuit-fault-analysis/. [Accessed: 18-Oct-2020].

[61] H. Says: 135276 says: and A. says: "▷ Faults in Electrical Systems (back to basics)," Electrical Equipment, 04-May-2013. [Online]. Available: http://engineering.electrical-equipment.org/electrical-distribution/faults-in-electrical-systems-back-to-basics.html. [Accessed: 18-Oct-2020].

[62] "Introduction," Ultimate Electronics Book, 28-Aug-2020. [Online]. Available: https://ultimateelectronicsbook.com/introduction/. [Accessed: 18-Oct-2020].

[63] "Transmission line definition and meaning: Collins English Dictionary," Transmission line definition and meaning | Collins English Dictionary. [Online]. Available: https://www.collinsdictionary.com/dictionary/english/transmission-line. [Accessed: 18-Oct-2020].

[64] S. Gowtham, M. Balaji, S. Harish, M. A. Pinto, and G. Jagadeesh, "Fault Tolerant Single Switch PWM DC-DC Converters for Battery charging Applications," Energy Procedia, vol. 117, pp. 753–760, 2017.

[65] S. Pourmohammad et A. Fekih, « Fault-Tolerant Control of Wind Turbine Systems - A Review », in 2011 IEEE Green Technologies Conference (IEEE-Green), Baton Rouge, LA, USA, avr. 2011, p. 1-6, doi: 10.1109/GREEN.2011.5754880.

[66] R. Stetter, R. Göser, S. Gresser, M. Witczak, et M. Till, « FAULT-TOLERANT DESIGN OF A GEAR SHIFTING SYSTEM FOR AUTONOMOUS DRIVING », Proc. Des. Soc.: Des. Conf., vol. 1, p. 1125-1134, mai 2020, doi: 10.1017/dsd.2020.31.

[67] "What is Fault Tolerance?: Creating a Fault Tolerant System: Imperva," Learning Center, 30-Dec-2019. [Online]. Available: https://www.imperva.com/learn/availability/fault-tolerance/. [Accessed: 18-Oct-2020].

[68] "Securing Your System," Understanding Fault Tolerance. [Online]. Available: https://www.enterprisestorageforum.com/storage-management/fault-tolerance.html. [Accessed: 18-Oct-2020].

[69] V. J. Chin, Z. Salam, et K. Ishaque, « Cell modelling and model parameters estimation techniques for photovoltaic simulator application: A review », Applied Energy, vol. 154, p. 500-519, sept. 2015, doi: 10.1016/j.apenergy.2015.05.035.

[70]   E. M. G. Rodrigues, R. Melício, V. M. F. Mendes, et J. P. S. Catalão, « Simulation of a Solar Cell considering Single-Diode Equivalent Circuit Model », p. 6.

[71]   G. Abad, Doubly fed induction machine: modeling and control for wind energy generation. Hoboken: Wiley, 2011.

[72]   G. He, Y. Pan, et T. Tanaka, « The short-term impacts of COVID-19 lockdown on urban air pollution in China », Nat Sustain, juill. 2020, doi: 10.1038/s41893-020-0581-y.

[73]   « Sources of Greenhouse Gas Emissions ». [En ligne]. Disponible sur: https://www.epa.gov/ghgemissions/sources-greenhouse-gas-emissions.